**EFFECTS OF LEAD CORE HEATING ON THE
SUPERSTRUCTURE RESPONSE OF SEISMIC
ISOLATED BUILDINGS**

Sedar ARGUÇ

Master of Science

Thesis

Civil Engineering Program

October-2015

JÜRİ VE ENSTİTÜ ONAYI

Sedar Arguç'un "**Effects of Lead Core Heating on the Superstructure Response of Seismic Isolated Buildings**" başlıklı **İnşaat Mühendisliği** Anabilim Dalındaki, Yüksek Lisans Tezi 02.10.2015 tarihinde, aşağıdaki jüri tarafından Anadolu Üniversitesi Lisansüstü Eğitim- Öğretim ve Sınav Yönetmeliğinin ilgili maddeleri uyarınca değerlendirilerek kabul edilmiştir.

	Adı-Soyadı	**İmza**
Üye (Tez Danışmanı)	**: Doç. Dr. ÖZGÜR AVŞAR**	………………
Üye	**: Doç. Dr. GÖKHAN ÖZDEMİR**	………………
Üye	**: Doç. Dr. CENK ALHAN**	………………

Anadolu Üniversitesi Fen Bilimleri Enstitüsü Yönetim Kurulu'nun ……………… tarih ve ………… sayılı kararıyla onaylanmıştır.

Enstitü Müdürü

ABSTRACT

Master of Science Thesis

EFFECTS OF LEAD CORE HEATING ON THE SUPERSTRUCTURE "RESPONSE OF SEISMIC ISOLATED BUILDINGS

Sedar ARGUÇ

Anadolu University
Graduate School of Sciences
Civil Engineering Program

Supervisor: Assoc. Prof. Dr. Özgür AVSAR
2015, 84 pages

Temperature of the lead core of the lead rubber bearing (LRB) increases and accordingly strength of the isolator decreases under reverse cyclic motions. However, the widely used analysis methods (bounding analyses) for seismically isolated structures do not consider strength deterioration in the force displacement relationship of the LRB model unlike the actual behavior. The theoretical basis of an analysis (temperature dependent analysis) method that gives acceptably closer results to the actual behavior has been presented in recent years. This analysis method updates the force displacement relationship of LRB instantly with the increasing heat in the lead core. This study focuses on comparison of the bounding analyses that predict the results with approximate calculation methods and temperature dependent analysis, which gives acceptably closer results to the actual behavior in terms of engineering demand parameters of superstructure (peak floor accelerations and peak drift ratios). In other words, the reliability of the widely used analyses methods (bounding analyses) have been controlled with temperature dependent analysis method. Also, the effect of several parameters, which are considered to play an active role in the lead core heating, on the response of the superstructure were investigated. These parameters are the as the isolation period (T), Q/W ratio and peak ground velocity (PGV) of the ground motion. In this study, 5760 nonlinear time history analyses were conducted in OpenSees platform with two different base isolated structural systems, whose superstructures are composed of 23-story reinforced concrete and 3-story steel buildings. Analyses results indicate that the bounding analyses remain on the safe side but do not provide a cost-effective solution compared to temperature dependent analyses for the 3-storey steel building. Especially, for certain isolator types, floor acceleration values obtained by temperature analyses are less than the lower bound analyses. This can lead to overdesign calculations for the equipment in the stories. Because the results of temperature dependent analyses can be less than or very close the lower bound limits, the bounding analyses must be supported with the temperature dependent analyses.

Keywords: Seismic Isolators, Lead Core, Dynamic Analysis, Earthquake, Bounding Analyses

ÖZET

Yüksek Lisans Tezi

SİSMİK İZOLASYONLU BİNALARDA
KURŞUN ÇEKİRDEKTEKİ ISINMANIN
ÜST YAPI DAVRANIŞINA ETKİLERİ

Sedar ARGUÇ

Anadolu Üniversitesi
Fen Bilimleri Enstitüsü
İnşaat Mühendisliği Anabilim Dalı

Danışman: Doç. Dr. Özgür AVŞAR
2015, 84 sayfa

Kurşun çekirdekli kauçuk izolatörlerde (KÇKİ) bulunan kurşun çekirdek kısmı izolatörün tersinir tekrarlanır yükler altında harekete geçmesi ile ısınır ve buna bağlı olarak izolatör dayanım kaybı yaşar. Fakat günümüzde yaygın olarak kullanılan analizlerde (limit analizleri) KÇKİ'ye ait kuvvet yerdeğiştirme ilişkisi gerçek davranışın aksine azalım göstermemektedir. Son zamanlarda KÇKİ'nin gerçek davranışına çok yakın sonuçlar veren bir hesap yönteminin (ısınma anlizi) teorik esasları ortaya koyulmuştur. Bu hesap yönteminde izolatöre ait kuvvet yerdeğiştirme ilişkisi kurşun çekirdeğin ısınması ile kendini anlık olarak güncellemektedir. Bu çalışmanın amacı analizlerde yaklaşık bir hesap yöntemi kullanan limit analizleri yöntemi ile gerçek davranışa çok yakın sonuçlar veren ısınma analizi yöntemini üst yapı istem parametreleri (maksimum kat ivmeleri ve maksimum rölatif yer değiştirme oranı) açısından karşılaştırmaktır. Bir başka deyişle günümüzde yaygın olarak kullanılan limit analizleri yönteminin ne derece güvenilir olduğu ısınma analizleri ile kontrol edilmiştir. Ayrıca kurşun çekirdeğin ısınmasında etkin rol oynadığı düşünülen izolasyon periyodu (T), izolatörün Q/W oranı ve yer hareketinin maksimum hızının (PGV) değişimi ile üst yapı istem parametrelerinin nasıl etkilendiği araştırılmıştır. Bu bağlamda 23-katlı betonarme üst yapı modeli ve 3-katlı çelik yapı modeli üzerinden gerçekleştirilen 5760 adet zaman tanım alanında doğrusal olmayan analizler OpenSees programı ile gerçekleştirilmiştir. Sonuç olarak limit analizleri yönteminin her iki üst yapı modeli için güvenli yönde kaldığı fakat özellikle 3 katlı çelik yapı için ısınma analizleri yöntemine göre ekonomik olmayan sonuçlar doğurduğu tespit edilmiştir. Özellikle bazı tip izolatörlü binalarda, ısınma analizi sonucu elde edilen kat ivmeleri alt limit analiz değerlerinden daha az hesaplanmıştır. Bu durum kattaki ekipmanların, olması gerekenden daha büyük istem değerleri ile tasarlanmasına neden olmaktadır. Isınma analizlerinden elde edilen sonuçların alt limit analizlerinden elde edilen sonuçlara ya çok yakın ya da alt limit değerlerinden daha az olması limit analizleri yönteminin ısınma analizleri yöntemi ile desteklenmesi gerektiği sonucunu doğurmuştur.

This thesis is dedicated to my family and my girlfriend

ACKNOWLEDGEMENT

LIST OF FIGURES

LIST OF TABLES

TABLE OF CONTENTS

1. INTRODUCTION

1.1. Seismic Isolation

Humans have to live with natural events and their destructive results. One of the most frightening and destructive phenomena of nature is severe earthquakes and their terrible aftereffects on the structures and society. Academicians and engineers have developed various techniques in order to protect these structures from destructive earthquakes up to now. These techniques can be classified in two groups according to the concept of protecting a structure. One technique is fixed base (classical) method and the other one is base isolation method. A structure, which is designed with classical method, dissipates the earthquake energy within the structural components while the base isolated structure dissipates the large part of earthquake energy with the seismic isolators.

In the classical method the structure is designed with fixed base technique. In other words, the columns of the structures are fixed to the foundation as shown in Figure 1.1. Therefore, the effects of earthquake ground motions are directly transferred to the structural elements through the foundation without significant dissipation.
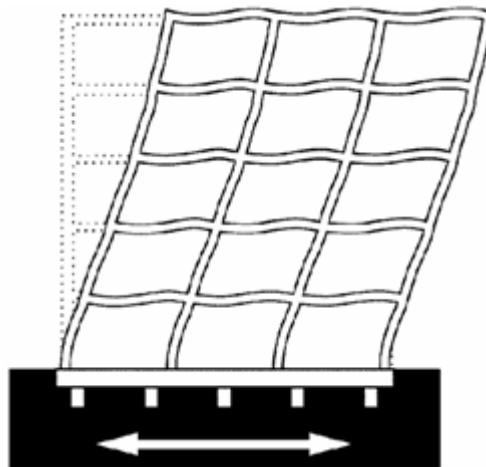
Figure 1.1. Earthquake response of fixed base building [1]

In this method the energy of earthquake which is transferred directly through the foundation to the structure is substantially dissipated with plastic deformations. Besides, internal friction, opening and closing micro cracks of elements, friction between the structure itself and nonstructural elements also dissipate the energy. In this way, a large part of earthquake energy is dissipated within the superstructure of the building through the formation of damage.

Dissipation of that much of energy brings two important problems. One is high drift ratio and the other is high floor acceleration. Designers have to limit these two parameters at the same time. Limiting the drift ratio is necessary for minimizing the effects of earthquake on the structural components between two adjacent stories such as columns and infill walls. Besides that, controlling floor acceleration is important for protecting the sensitive equipment from undesirable vibrations.

Limiting both drift ratio and floor acceleration is the main challenge of the design process of structures because these two parameters are related to each other. Decreasing one of these parameters affects the other parameter negatively. For example, if drift ratio problem exist at the design process, we increase the stiffness of the structure in order to limit the undesirable relative displacements between two adjacent floors. Besides, stiffening the structure brings high floor accelerations. On the other hand, if high floor acceleration problem exist at the story level, we soften the structure in order to limit the undesirable floor acceleration. Softening the structure results in larger displacements causing drift problem. Within the scope of the earthquake engineering, the designer is responsible to balance both drift ratio and floor accelerations at the same time.

Base isolation method is the best way for limiting both drift ratio and floor acceleration. Base isolation of buildings is an innovative seismic protection method that is already implemented in many countries. In this method, the considered building is decoupled from the horizontal components of the earthquake ground motion by placing seismic isolation devices between the superstructure and its foundation. These devices have low stiffness in horizontal direction and high stiffness in vertical direction. Due to insertion of these devices between the superstructure and the foundation, the fundamental period of the

structure shifts to higher value which results low earthquake forces and higher displacement values at the isolation level (Figure 1.2). Therefore, the nonlinear behavior concentrates at the isolation level and the superstructure remains elastic during the earthquake shaking as shown in the Figure 1.3.
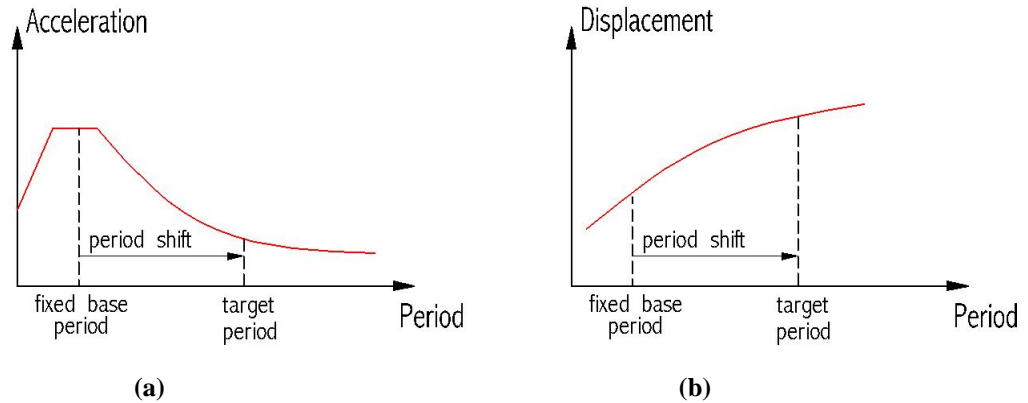
Figure 1.2. Period shifting a) acceleration response spectrum, b) displacement response spectrum
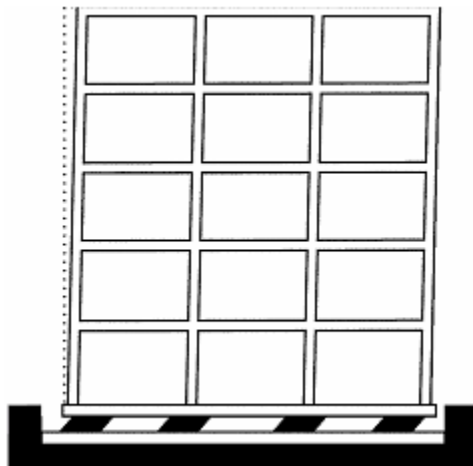
Figure 1.3. Earthquake response of base isolated building [1]

1.2. History of Seismic Isolation

Base isolation method is an innovative earthquake resistant design philosophy that requires expertise at the design process. However, a number of ancient structures had been constructed with base isolation philosophy before

development of the theory of base isolation. Some of these historical structures were given below.

Erechtheion Temple that was built up with interesting construction technique was applied in Greece between 421 and 407 BC (Figure 1.4). At the construction process, the crumbled stones were laid under the foundation as first layer to absorb the primary shock of earthquake and big stones were formed above that first layer without any bounding material. Then, foundation was constructed after that layer. The stones were allowed to slide over each other. This sliding action was the main idea that related to base isolation technique.

Figure 1.4. Erechtheion Temple, Greece [2]

The historical structures get too much damage when they are subjected to severe earthquakes because they are generally designed under only vertical (dead) loads. Structural members can be easily damaged under any earthquake due to absence of reinforcement. Therefore, destructive effect of earthquakes must be reduced. For this reason, the cylindrical shaped woods were placed under the arches like isolation system that is used for reducing the potential earthquake forces as shown in Figure 1.5.

Figure 1.5. Historical structure, Medina [3]

The historical structure Parthenon was constructed in Greece in 440 BC. The columns of the structure were made up with marbles that were connected to each other with lead and dowel pieces as given in the Figure 1.6. The system had a gap between marbles and dowels. So, when the earthquake hit the structure the marbles were able to move freely and the large part of seismic energy was dissipated by this mechanism.
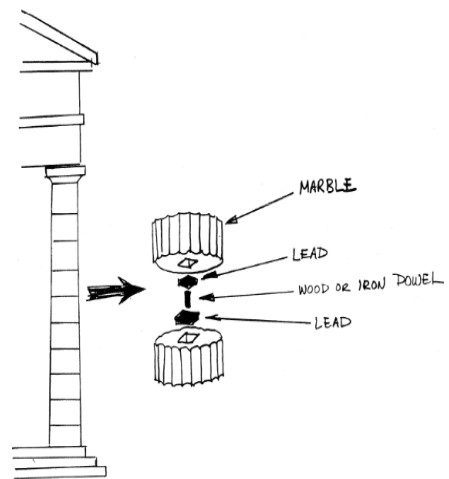
Figure 1.6. Parthenon, Greece [4]

The wood pieces were used to decouple the structures from the ground in North of Iran, Lahijan. They were placed to reduce the earthquake forces in X and Y direction (Figure 1.7).

Figure 1.7. Decoupling the structure from the ground, Iran [5]

The examples of historical structures that were designed with the philosophy of base isolation were presented above and the historical development of base isolation was given in Table 1.1.

Table 1.1. Historical development of base isolation [6]

Date	Location	Explanation
440 BC	Ancient Greece	Parthenon (did they know?)
1320	Kunya-Urgency, Turkmenistan	Minaret with reed mat foundation
1870	US	Touaillon of San Francisco obtains US Patent
1907	US	J. Bechtold of Germany obtains US Patent

Table 1.1. (Continue) Historical development of base isolation [6]

1909	US	Dr. Calantarients of England applies for US Patent
1909	Italy	Messina-Reggio Commission considers seismic isolation
1921	Japan	Imperial Hotel, Tokyo designed by Frank Lloyd Wright
1929	US	Flexible first story (Mantel)
1930	New Zealand	de Montalk applies for Patent
1959	USSR	First engineered seismic-isolated building (cable suspended) in Ashkabad, Turkmenistan
1963	USSR	Ellipsoid-shaped roller bearings Sevastopol
1969	Yugoslavia	Robber isolation system, Skopje
1970s	France New Zeland US	EDF system, GAPEC isolators Lead/rubber bearings Prof. Kelly starts testing at UCB
1980s	US, Japan	Research, applications

1.3. Seismically Isolated Buildings

The seismic isolation devices reduce the earthquake forces with high deformation capacity at the isolation level. Therefore, the superstructure, which decouples from the horizontal component of the earthquakes, remains elastic during the shaking. For this reason, the damage of the structural and non-structural components of the structure is minimized. This feature means that the

mission critical structures must keep their functionality after severe earthquakes without any damage. For that purpose, it is desired to design hospitals, fire stations, municipal buildings, operation centers by using seismic base isolation method. The examples of seismically isolated buildings were given below.

Foothill Communities Law & Justice Center was constructed in San Bernardino, California in 1985. The front view of the building was given in Figure 1.8. Since the building was located 21 km from the San Andreas Fault, it was designed with seismic isolators. High damping rubber bearings were decided to use for this building. It was the first use of high damping rubber bearing all over the world. Also the building was the first in United States to have a base isolation system. Producer developed four high damping natural rubber compound for this building.

Figure 1.8. Foothill Communities Law & Justice Center, San Bernardino, California [7]

Los Angeles County Fire Command & Control Facility was built in California in 1990 (Figure 1.9). The building is used as a fire department and serves to 58 cities. The base isolation system is necessary for this building to protect the sensitive computer and communication systems located in the building. In addition, the structure must still keep its serviceability after the earthquakes. The high damping rubber bearings were used for this structure. The cost of the isolated structure was 5% higher than the fixed base structure.

Figure 1.9. Los Angeles County Fire Command & Control Facility, California [8]

Los Angeles County Emergency Operations Center is responsible for emergency and disaster management of Los Angeles. Such kinds of mission critical structures are required not to get any damage during the earthquake. For that reason, the structure constructed with 28 high damping rubber bearings. The picture of the building was given in Figure 1.10.

Figure 1.10. Los Angeles County Emergency Operations Center, California [9]

Caltrans Traffic Management Center was constructed in Kearney Mesa, California (Figure 1.11). The flow of vehicle traffic and traffic safety are controlled by this center. The reason for the application of base isolation method on this building is to protect the technological equipment from destructive earthquake forces.

Figure 1.11. Caltrans Traffic Management Center, Kearney Mesa, California [10]

Drew Diagnostics Trauma Center was built as a hospital in Willow Brook, California in 1995 (Figure 1.12). Base isolation method was necessarily chosen for this building to keep the hospital in service after an earthquake because the building is located 5km away from Newport Inglewood Fault. The natural rubber and sliding bearings were used together for that project.

Figure 1.12. Drew Diagnostics Trauma Center, California [11]

Another base isolated building is Flight Simulator Manufacturing Facility which has valuable computer system and located near the Wastach Fault which generates 7-7.5 magnitude earthquakes. Therefore, the building was designed with the seismic base isolation method. Lead plug bearings were used to isolate the building. The building was given in Figure 1.13.

After the severe earthquakes many hospitals have heavily damaged and they lost their functionalities. Therefore the ministry of health of Turkey decided to design the hospitals with base isolation technique in earthquake prone regions. Erzurum health campus and Kocaeli hospitals are the examples of this decision (Figure 1.14-Figure 1.15).

Figure 1.13. Flight simulator manufacturing facility [12]

Figure 1.14. Erzurum health campus [13]

Figure 1.15. Van maternity hospital [14]

Oakland City Hall was established in Oakland, California in 1914 (Figure 1.16). It was constructed as a fixed base structure. The structural system of the building was damaged during the Loma Prieta Earthquake. After that earthquake,

the building was immediately closed to service. The city leaders decided to retrofit the structure with isolation technique instead of tearing it down. The columns of the structure were cut and the rubber isolators were placed under the columns one by one. The total cost of the retrofitting of the structure with seismic isolators was $85 million.

Figure 1.16. Oakland City Hall was established in Oakland, California [15]

San Francisco City Hall was constructed in San Francisco, California in 1800s (Figure 1.17). The structure was heavily damaged during the severe earthquake. Each structural member lost its functionality except the dome located at the top. The building was rebuilt in 1915. But unfortunately Loma Prieta Earthquake hit the building in 1989. It was decided to isolate the structure in order to protect the historical value of the structure.

Figure 1.17. San Francisco City Hall, San Francisco, California [16]

Los Angles City Hall was completed in 1928 (Figure 1.18). The height of the building is 138m. The earthquake resistant method was selected as classical method with the steel cross bracing, reinforced concrete walls and masonry infill perimeter walls. The Northridge earthquake damaged the building in 1994. The base isolation method was selected as a design strategy in order to protect the structure from the severe earthquakes because the historical importance of the building was desired to preserve. High damping rubber bearings and sliding type isolators were used together. And also lots of viscous dampers were used for providing additional damping as well as dissipating the energy of that high-rise building. 12 viscous dampers were installed between the twenty-fourth and twenty-sixth floors to control the inter-story drifts at the soft story level.

Figure 1.18. Los Angles City Hall [17]

The examples of isolated structures were given with their isolation technique in Table 1.2.

Table 1.2. Examples of isolated structures [18]

Building	Location	Stories	Total Floor Area (m^2)	Isolation System	Date Complated
William Claston Building	N. Zeland	4	17000	LRB	1981
Union House	N. Zeland	12	7400	Flex. pile	1983
Wellington Central Pollice Station	N. Zeland	10	11000	Flex. pile	1990
Press Hall, Press Hause	N. Zeland	4	950	LRB	1991
Parliament Hause	N. Zeland	5	26500	LRB	1921
Parliament Library	N. Zeland	5	6500	LRB	1899
Yachiyodai, Dwelling	Japan	2	114	EB+F	1982
Research Lab, Institute	Japan	4	1330	EB+S	1985
High Tech Research Lab, Institute	Japan	5	1623	EB+S	1986
Oiles Tech Centre, Laboratory	Japan	5	4765	LRB+E	1986
Tikuyu-Ryo, Dormitory	Japan	3	1530	EB+V	1986

Table 1.2. (Continue) Examples of isolated structures [18]

Acoustc Lab, Institute	Japan	2	656	EB+S	1986
Elizabeth Sanders, Museum	Japan	2	293	EB+S	1986
Tohoku University, Test Model	Japan	3	208	EB	1986
Hukumiya, Apartment	Japan	4	681	EB+S	1986
Sibuya Simuzu Building, Office	Japan	5	3385	EB+S	1987
Research Lab No. 6, Institute	Japan	3	306	LRB	1987
Tsukuba Muki Zaiken, Institude	Japan	1	616	EB+S	1987
Tsuchiura branch, Office	Japan	4	639	LRB	1987
Lab. J Building, Institute	Japan	4	1173	SL+R	1987
Kousinzuka, Apartment	Japan	3	476	EB+S	1987
Toranomon Building, Office	Japan	8	3373	EB+S	1987
Itoh Mansion, Apartment	Japan	10	3583	LRB	1988
Itinoe Dormitory	Japan	3	770	EB+S	1988
Clean Room Lab, Institude	Japan	2	405	EB+V	1988
Atagawa Hoyojo, Rest House	Japan	1	140	SL+S	1988
Ogawa Mansion, Apartment	Japan	4	1186	HDR	1988
Asano Building, Office	Japan	7	3255	LRB	1988
Ksuda Building, Store	Japan	4	1047	HDR	1988
Ichikawa Residance, Dwelling	Japan	2	297	EB	1988

Table 1.2. (Continue) Examples of isolated structures [18]

Computer Center	Japan	6	10032	HDR	1988
Sagamihara Center, Office	Japan	3	255	HDR	1988
Gerontology Res. Lab., Clinic	Japan	2	1615	EB+S	1988
M-300 Hoyosyo, Dwelling	Japan	2	309	LRB	1989
Harvest Hills, Apartment	Japan	6	2065	EB+S	1989
Acustc Lab, Institude	Japan	2	656	EB+S	1989
Toshin Building, Office	Japan	9	7573	EB+S	1989
Dwell. Test Lab, Laboratory	Japan	3	680	EB+S	1989
MSB-21 Ooluka, Office	Japan	12	5962	LRB	1989
Wind Laboratory, Institute	Japan	3	555	HDR	1989
CP Fukuzimi, Office	Japan	5	4406	EB+F	1989
Employes Building, Apartment	Japan	4	652	LRB+HDR	1989
Toho-Gas Centre, Office	Japan	3	1799	SL+RS	1989
Tudanuma Dormitory	Japan	2	202	EB+S	1989
M-300 Yamadas, Dwelling	Japan	2	214	LRB	1989
Koganei Apartment	Japan	3	741	LRB+EB	1989
Operation Center, Comp.	Japan	2	10463	LRB	1989
Urawa Kogyo	Japan	5	1525	HDR	1989
Kanritou	Japan	3	955	EB+V	1990
Noukyou Center, Computer	Japan	3	5423	LRB	1990

Table 1.2. (Continue) Examples of isolated structures [18]

C-1 Building, Office	Japan	7	37849	LRB	1990
Keisan Kenkyusyo, Off.	Japan	3	627	EB+V	1990
Kasiwa Kojyo, Office	Japan	4	2186	HDR	1990
Acoustic Laboratory, Institude	Japan	2	908	EB+F	1990
Yamato-ryo, Dormitory	Japan	8	1921	EB+S	1990
Kawaguchi-ryo, Dormitory	Japan	4	659	LRB	1990
Dounem Computer Center	Japan	4	3310	EB+LD	1991
Andou Tech Centre, Laboratory	Japan	3	545	LRB	1991
Toyo Rubber, Dormitory	Japan	7	3520	EB+S+oil	1991
Aoki Tech. Center, Office	Japan	4	4400	LRB	1991
Dai Nippon Daboku, Dormitory	Japan	4	1186	EB+LD	1991
Domani Musashino, Apartment	Japan	3	742	EB+S	1991
Foothill Comminities L. and J. Centre	USA	4	17000	EB	1986
Salt Lake City and C. B. (Retrofit)	USA	5	16000	HDR+LRB	1988
Salt Lake City Manufactoring Facility	USA	4	9300	LRB	1988
USC University Hospital	USA	8	33000	HDR+LRB	1989
Fire Command and Control Facility	USA	2	3000	HDR	1989
Rockwell Building (Retr.)	USA	8	28000	LRB	1989

Table 1.2. (Continue) Examples of isolated structures [18]

Kaiser Computer Center	USA	2	10900	LRB	1991
Mackay School of Mines (Retrofi)	USA	3	4700	HDR	1991
Hawley Apartment (Retrofit)	USA	4	1900	SL+RS	1991
Changing Hause R. H. (Retrofit)	USA	11	19600	LRB	1991
Long Beach VA Hospital (Retrofit)	USA	12	33000	LRB	1991

1.4. Research Objectives and Scope

The results of conducted experimental studies [19] showed that the lateral strength of the lead rubber bearings decreases when they are subjected to the reversed cyclic motions such as earthquakes. Aging, contamination of the rubber, heating and load history on the isolator were some of the main causes for this deterioration. In order to reflect the strength deterioration in the calculations, upper and lower bound analyses were developed from the results of the experimental observations. The lower bound value is taken from the yield stress of the lead that was related to the first cycle of the bi-linear force deformation relation. And, the upper bound value was taken from the average yield stress of the lead that was related to the first three cycle of the bi-linear force deformation relation. However, the recent experimental and analytical studies showed that strength deterioration of lead rubber bearings are highly dependent on heat increase in the lead core of the isolator [20, 21]. A result of these experimental and analytical studies, the mathematical model of lead rubber bearings that was able to calculate the strength deterioration due to heat increase were developed and the results of the experimental studies and analytical studies done with that mathematical model were acceptably close to each other.

The first objective of this study is to compare the results of bounding analyses and the analyses that consider the strength deterioration of an isolator on the building type structures in terms of superstructure response such as peak floor accelerations and peak relative story displacements. For this purpose, a series of nonlinear response history analyses (RHA) were performed with near field ground motions.

The second objective is to investigate the effect of earthquake characteristics on the superstructure response of the structures isolated with lead rubber bearings. The experimental results showed that the heat increase in the lead core of the isolator is highly dependent on the speed of the cyclic motion. Therefore, the selected ground motions were clustered with their peak ground velocity (PGV) values in order to observe the variation of temperature dependent behavior clearly.

The third objective is to investigate the effect of isolator characteristics on the superstructure response of the isolated structures with lead rubber bearings. For this reason, Q/W ratio and isolation period that can change the response of the isolated structures were considered as variable parameters to identify the effect of these parameters on the structural response. Therefore, a number of Q/W ratios and isolation periods were selected for the same superstructure models.

This study is believed to provide significant contribution to the existing knowledge of lead rubber bearings with the material model considering strength deterioration specifically on the superstructure response. The reliability of the bounding analysis approach will be examined in detail by comparing the analyses results of the deteriorating model and the commonly used bounding analysis approach especially in terms of superstructure seismic response. Finally, the information provided in this study will help the practicing engineers to design safer and cost-effective base isolated structures with lead rubber bearings.

1.5. Organization of the Dissertation

This dissertation is composed of eight chapters with the brief contents given below:

Chapter 1:   General concept of the fixed base and base isolated structures are introduced. Historical development and recent examples of base isolated structures are presented.

Chapter 2:   Past studies on base isolation systems mentioned briefly. The temperature dependent behavior and previous studies are the issues mainly represented in this chapter.

Chapter 3:   The theoretical basis of the temperature dependent model is presented.

Chapter 4:   Structural and mathematical models of the considered concrete and steel structures are defined. Implemented isolators are given in terms of their Q/W ratios and periods.

Chapter 5:   Selection of ground motions was discussed. 60 selected ground motions were classified with their PGV values.

Chapter 6:   Results of nonlinear time history analyses for the considered structure models subjected to 60 ground motions were presented with respect to PGV, Q/W ratios and isolation period. The results were given in terms of peak relative story displacement and peak floor accelerations.

Chapter 7:   In the light of Chapter 7 the results were discussed.

Chapter 8:   Essential points of the dissertation, conclusion and recommendations for future studies were given.

2. LITERATURE SURVEY

Seismic base isolation technique which is one of the innovative earthquake resistant design methods in the area of earthquake engineering has become more and more popular all over the world in the recent years. The purpose of this method is to reduce the seismic demand instead of making a rigid structure in order to withstand the destructive earthquake forces. The isolation devices are placed to the proper points generally between the base columns and foundation of the structure to provide much more lateral flexibility to the structural system. In this way, the large portion of the seismic energy is dissipated at the isolation level and the superstructure remains elastic during the earthquake shaking.

The seismic base isolation philosophy has been used on many structures at the ancient ages. The designers of these structures did not know the mathematical basis of the seismic base isolation technique at that time. At first, seismic isolation of structures was installed with soil layers that allowed the surfaces slide over each other. Afterwards, many techniques have been created to reduce the severe earthquake forces with the help of balls, rollers, rocking columns, cables instead of sliding soil layers. These early techniques have been improved with the conducted experimental and analytical studies and observed damage on the structures after the severe earthquakes. And now, the theoretical basis of the seismic base isolation method has been understood more clearly and has been supported by many academic studies. After the development of seismic isolation method, it is accepted and used in seismically active regions.

Natural rubber bearings, lead rubber bearings and frictional isolators are widely used seismic devices nowadays (Figure 2.1). Frictional type isolators are the simplest one in that group. However, they need extra damping devices to withstand the small earthquake vibrations and wind loads. Also, the curved surface of the isolation system may cause high frequency vibrations during the earthquake shaking [22]. Natural rubber bearings are composed of steel and rubber layers that are vulcanized to each other. The conducted experimental studies showed that the force-deformation relationship of natural rubber bearings is almost linear to the reasonable deformation point [23]. Therefore, these

isolation devices must be used with additional damping devices as well as sliding isolators. Additional damping devices require much more complex dynamic analyses. Also, they might increase the contribution of higher modes and accordingly they might reduce the effectiveness of base isolation [22]. Besides, lead rubber bearing that is very similar to natural rubber bearings is another widely used isolation device. It was produced in New Zeeland in 1982. The substantial difference of lead rubber bearing compared to the natural rubber bearing is the lead plug insertion that is located in the middle of the isolation devices. The lead plug insertion is an energy dissipation mechanism. Therefore, there is no need to use additional damping devices because it provides enough damping to the structure. Low lateral stiffness, high vertical stiffness and damping mechanism which are combined in a single unit bring economical isolated structures. The lead rubber bearing has become the most widely used isolation device all over the world with the help of these features.

Seismic base isolation took its place in the structural design methods and it is strengthening its position day by day. Therefore, in this study seismic base isolation method was chosen for taking forward to existing seismic base isolation knowledge one step further. Due to the given reasons that mentioned above about the isolation devices (natural rubber bearing, lead rubber bearing, frictional isolator), the study area of this dissertation was restricted with the lead rubber bearings.

(a)   (b)   (c)
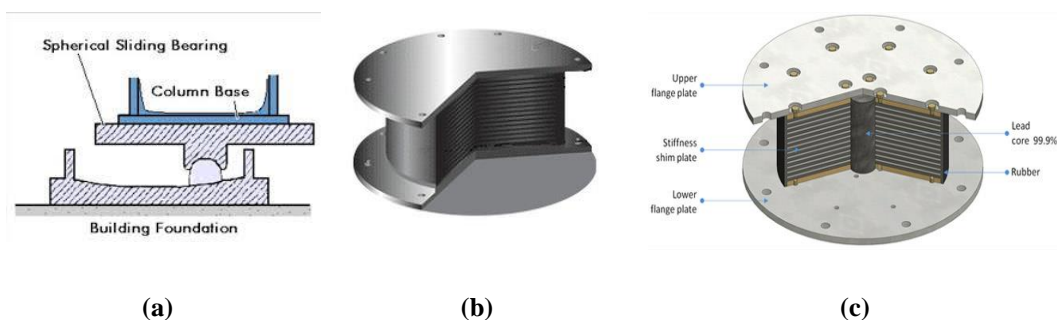
Figure 2.1. Seismic isolation devices: a) frictional isolator, b) natural rubber bearing, c) lead rubber bearing

The force-deformation relationship of lead rubber bearings generally represented by idealized non-deteriorating bilinear hysteretic force deformation relation as given in Figure 2.2. The strength of the isolator does not reduce during the motion according to this type of material model. However, the experimental studies conducted by Robinson [19] showed that strength of the lead rubber bearings exhibits deterioration when the isolator subjected to cyclic motion. But the source of the problem (strength deterioration) had not been identified. Aging, contamination of the rubber, heating and load history on the isolator were pointed for the strength deterioration. Therefore, in order to reflect this deterioration in the calculations, upper and lower bound analyses are conducted at the design phase of the isolated structures with lead rubber bearing [24, 25]. The bounding analyses give two extreme envelope results. One is the lower bound and the other is the upper bound result. The actual result is in-between these two end points and the designer have to consider all these values in the calculations. So, the bounding analyses do not give the exact result, it give only the range of probable results.
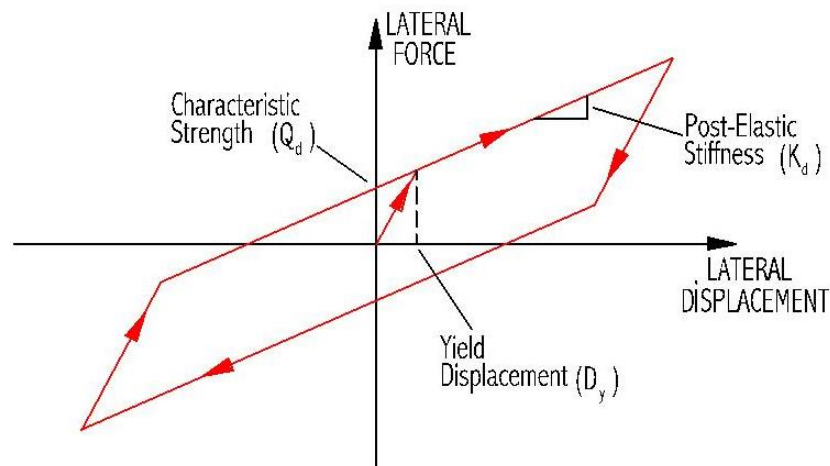
Figure 2.2. Non-deteriorating force displacement loop of lead rubber bearing

After the conducted experimental studies, Constantinou et al. [26] and Kalpakidis and Constantinou [27] showed that the strength deterioration of lead rubber bearing under reverse cyclic motion is primarily caused by the increasing heat in the lead core. The results of these studies are used to establish an effective relation between lead core heating and strength of the isolator. Kalpakidis and Constantinou [20] developed a theory that updates the strength of isolator with

measured heat in the lead core defined in the material model. Thus, the strength of the isolator is calculated instantaneously. The results of the conducted experimental studies and the results of the conducted analytical studies that consider strength deterioration on lead rubber bearings were acceptably close to each other [21]. So, the deteriorating material model gives closer results to the real behavior than the bounding analyses.

There are a few studies that consider the strength deterioration of isolator due to the temperature rise in the lead core because the material model that account the strength deterioration was developed recently in 2009. Most of the studies conducted with lead rubber bearings were performed with the help of bounding analyses. For these reasons, the material model for the lead rubber bearings that accounts the strength deterioration is employed in this study. The studies, which considered the strength deterioration material model for lead rubber bearings, were given below.
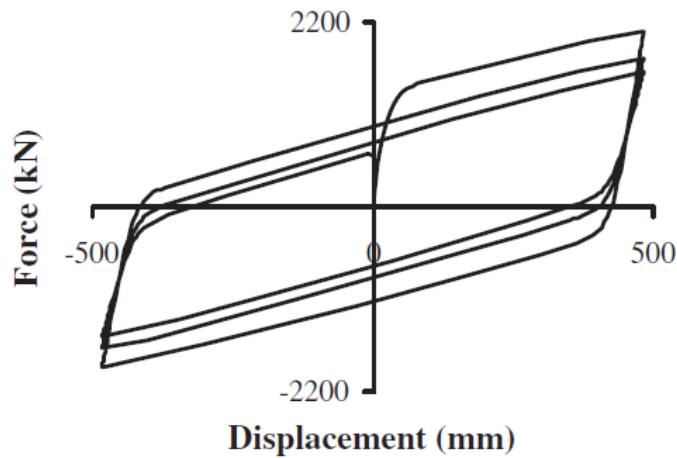
Figure 2.3. Deteriorating force displacement relationship of lead rubber bearing due to the temperature dependent behavior [28]

Kalpakidis and Constantinou [20] developed a bi-linear force deformation relationship, which considers the cycle-to-cycle strength deterioration, because of the heating of the lead core. When a lead rubber bearing is exposed to cyclic motion, heat increases in the lead core vertically and radially. Accordingly the characteristic strength and energy dissipation mechanism of the lead rubber

decreases. The deterioration of the yield strength depends on the geometric characteristics of the lead rubber bearing and the speed of motion. Kalpakidis and Constantinou [20] developed a force deformation relationship model for representing their theory that updates the temperature and accordingly yield stress of the lead core instantaneously.

Kalpakidis and Constantinou [21] verify the results taken from the companion paper that developed theory of cycle-to-cycle deterioration for bi-linear force deformation relation due to the temperature rise in the lead core. Six lead rubber bearings tested for comparison purposes. Both analytical and experimental results are in good agreement.

Kalpakidis et al. [29] investigated the dynamic response of a structure that isolated with lead rubber bearing while the temperature dependent model is of concern. Analyses results of temperature dependent model is compared to upper and lower bound analyses in terms of structural shear, isolator shear force, structural acceleration and structural drift. The results show that the upper and lower bound analyses stated in conservative side.

Ozdemir et al. [30] studied the performance of bridges which are isolated with lead rubber bearings that considers cycle-to-cycle strength deterioration. The main purpose of this study is to investigate the isolator performance affected from heating of the lead core, in terms of maximum isolator displacements and maximum isolator forces. For this reason, two bi-linear force deformation relations were used in the study. One is non-deteriorating model and the other is the model that considers cycle-to-cycle strength deterioration which is shown in Figure 2.3. The analyses of non-deteriorating model divided into two groups. These are upper and lower bound analysis for comparison purposes. The ground motions were selected to be pulse type and near fault. For this study nonlinear response history analysis were performed for determination of maximum isolator displacements and maximum isolator forces. The analyses results showed that lower bound analyses results overestimate the maximum isolator displacement with high velocity pulses ground motion and especially bearings with higher Q/W ratios. And also, the maximum isolator forces obtained by temperature dependent analyses almost coincided with the ones obtained by upper bound analyses.

Ozdemir and Dicleli [31] investigated the effect of lead core heating on the response of seismically isolated bridges with the help of ground motions that were recorded at near fault. The selected ground motions included forward rupture directivity effect. The deteriorating bi-linear force deformation relationship model, which was developed by Kalpakidis and Constantinou [20], was used to perform the temperature dependent analyses. Bounding analyses were also conducted for comparison purposes. A series of nonlinear dynamic analyses were performed for examining the maximum isolator displacements and the maximum isolator forces. The conducted analyses showed that the results of temperature dependent behavior are in-between the results of upper and lower bound analyses.

Ozdemir [32] studied the response of lead rubber bearings subjected to bi-directional earthquake ground motion using temperature dependent hysteretic force deformation relationship. Ground motions were grouped according to their soil types into two groups and nonlinear time history analyses were performed. The maximum isolator displacement and maximum lead core temperature were examined for both bi-directional and unidirectional earthquake excitations. The results showed that maximum temperature obtained with the bi-direction analyses were approximately 50% higher than unidirectional analyses. In order to estimate the maximum isolator displacement, an equivalent lateral load method was proposed. Equivalent lateral load method results close estimations for maximum isolator displacement with some overestimation.

The studies considered the strength deterioration due to lead core heating on the seismic isolators subjected to reverse cyclic motions limited by the examples given above. All these studies concentrated on the response of isolators in terms of forces and displacements.

The strength deterioration material model has not been considered in the analytical studies conducted with lead rubber bearings that deal with response of superstructure up to now. The bounding analyses have been used in order to perform the analyses of these studies. Examples of these studies that related to the response of the superstructure of base isolated buildings were given below.

Benzoni and Casarotti [33] prove that the heat increase in the lead core is directly related to speed of motion and number of hysteretic cycles. For this

reason, the ground motions selected in terms of their peak ground velocity values (PGV) to observe the change in the response of isolated structure.

Matsagar and Jangid [34] studied the effect of isolator characteristics on the response of the superstructures isolated with lead rubber bearings. The material model used in this study does not consider the strength deterioration. Significant variations in the superstructure response were observed for the isolator systems with different force deformation relationships.

Alhan and Gavin [35] investigated the importance of seismic base isolation technique on the protection of vibration sensitive equipment located at the story level with the non-deteriorating material model.

Kelly and Tsai [36] indicated that the high acceleration values that the structures subjected to, can cause damage to structural system as well as the equipment in the buildings. The seismic energy acting on the structural elements and equipment can be dissipated by the high displacement capacity of the seismic isolators. In addition, as a result of conducted studies, it was shown that the lead rubber bearings perfectly dissipate the seismic energy and limit the acceleration and displacements exerted by earthquakes.

Providakis [37, 38] investigated the variation of relative story displacements for the base isolated superstructures with lead rubber bearings, in terms of isolation period and isolator damping. The non-deteriorating force-deformation relationships were used in these studies with the near and far field ground motions.

Yang et al. [39] studied the effect of different type of isolators on the performance of the equipment in the structure. It was emphasized that the rigidity of the superstructure has an important role on protecting the acceleration sensitive equipment.

The studies were given above showed that the response of the superstructures isolated with lead rubber bearings are highly dependent on the force-deformation relationship of the isolators. The non-deteriorating force deformation relationships were used for these studies. Both the deteriorating material model and the response of superstructure have not been discussed in the same study up to now. In this study, it was decided to investigate the effect of lead

core heating on the response of superstructure isolated with lead rubber bearings. It is believed that this study will help both the practicing engineers and the academicians as a guideline for being the first study, which investigates the variation in the superstructure response by considering the strength deterioration in the lead rubber bearings.

3. TEMPERATURE DEPENDENT BEHAVIOUR OF LEAD RUBBER BEARING

The importance and necessity of seismic isolation method have been understood day by day. Among the seismic isolation devices, the lead rubber bearing is the most widely used seismic isolator today. It is mainly composed of rubber and steel layers, lead plug insertion, top and bottom steel plates.

The idealized force-deformation relationship which is used to describe the behavior of lead rubber bearings was given in Figure 3.1. This idealized shape can be easily constructed with Q_d (characteristic strength of the lead) and K_d (post elastic stiffness of the isolator) as given in the ((3.1) and ((3.2). Where, A_L and σ_{YL} are the area and effective yield strength of the lead core respectively, f_L is the non-dimensional parameter that exhibits the effect of lead core on the post elastic stiffness, G is the shear modules of rubber, A_r is the area of the rubber layer, T_r is the total rubber thickness. Because the contribution of rubber is very small, it is neglected in the calculation of elastic stiffness, which is represented with characteristic strength of lead only [27]. There are two stiffness states in this bi-linear hysteresis model. The behavior of the model starts with the elastic stiffness, when the internal resistance of the isolator reaches the characteristic strength of the lead, the system yields and deforms with post elastic stiffness. And also, both unloading and reloading phases occur with the elastic stiffness.
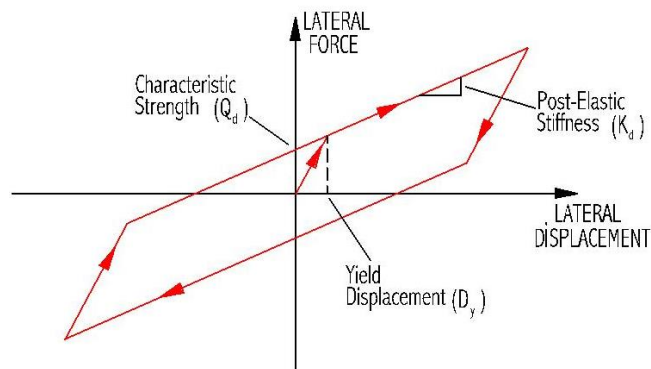

Figure 3.1. Idealized force deformation loop of lead rubber bearing

$$Q_d = A_L \sigma_{YL} \tag{3.1}$$

29

$$K_d = f_L \frac{GA_r}{T_r} \qquad\qquad\qquad \textbf{(3.2)}$$

The force-deformation relationship of lead rubber bearings that was shown in Figure 3.1 is called idealized because in the actual behavior of the the isolator strength reduces under reverse cyclic motion. The reduction of the strength of the lead rubber bearing was first observed with experimental studies by Robinson [19] in 1982. But the theoretical basis of strength deterioration did not described at that time. Therefore, the bounding analyses are used in order to consider the strength reduction to the calculations.

The bounding analyses consist of lower and upper bound analyses. The upper bound analyses are conducted with upper bound values of characteristic strength and post elastic stiffness values that can occur during the lifetime of the isolators. The largest forces demand in the superstructure elements are usually exerted by upper bound analyses [28]. On the other hand, the lower bound analyses are conducted with lower bound values of characteristic strength and post elastic stiffness values that can occur during the lifetime of the isolators. The largest displacement demand of an isolator is usually exerted by lower bound analyses [28]. The bounding analyses do not give the exact results. The obtained results from these analyses give only the range of probable results.

The upper bound value that is used as upper limit of effective yield stress of lead is obtained from the first cycle of the hysteresis loop of the isolator test results. And also, the lower bound value is obtained from average of the first three cycle of the hysteresis loop.

Constantinou et al. [26] showed up the strength deterioration of lead core is primarily results from lead core heating of the isolator under reverse cyclic motion. When a lead rubber bearing is exposed to cyclic motion, heat increases in the lead core vertically and radially. Accordingly the characteristic strength of the lead decreases. Conducted experimental studies showed that the dissipated energy significantly decreases with increasing number of cycles [26]. The amount of dissipated energy is directly related to characteristic strength. Heating also occurs

in the rubber layers but it is very small compared to lead core heating. It can be neglected.
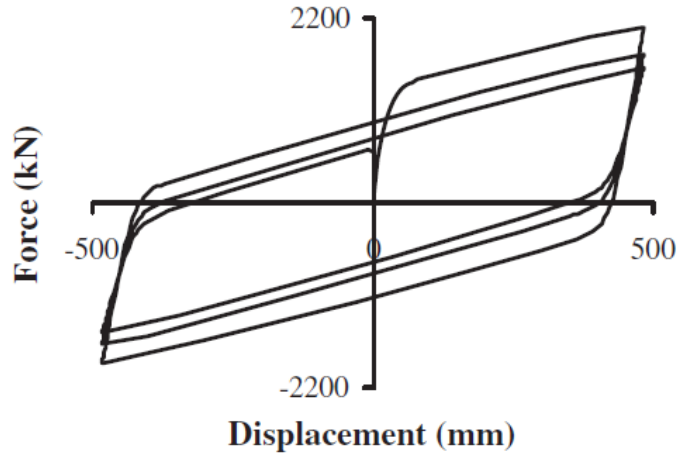

Figure 3.2. Deteriorating force displacement relationship of lead rubber bearing due to the temperature dependent behavior [28]

Kalpakidis and Constantinou [27] developed a force deformation relationship model that updates the temperature and accordingly yield stress of the lead core instantaneously. It is also verified by the experimental results [21]. The Figure 3.1 showed the strength deterioration during the motion. The mentioned companion papers showed that the strength deterioration model of lead rubber bearings proposed by Kalpakidis and Constantinou [27] give acceptably close results to the actual behavior.

The force transmitted to the lead rubber bearing (F_b) with the temperature dependent material model under cyclic motion is calculated as stated in (3.3).

$$F_b = K_d U + \sigma_{YL}(T_L) A_L Z \tag{3.3}$$

K_d is the post elastic stiffness of the isolator, U is the displacement of the lead rubber bearing. The yield stress of the lead core which is updated with the instantaneous temperature is denoted by $\sigma_{YL}(T_L)$. The cross-sectional area of the lead core is represented with A_L, Z is the hysteretic dimensionless quantity satisfies the first order differential equation given in (3.4).

$$U_y \cdot \dot{Z} = \left(A - |Z|^2 B \cdot \left(1 + sgn(\dot{U} \cdot Z)\right)\right) \cdot \dot{U} \tag{3.4}$$

A and B are dimensionless quantities form the hysteresis loop of the isolator in terms of shape and size. Relative velocity of the bearing represented by $\dot{U}$.

The temperature dependent behavior developed by Kalpakidis and Constantinou [20] calculate the yield strength with the help of instantaneous temperature ($\dot{T}_L$) of the lead core as stated before. $\dot{T}_L$ is given in (3.5).

$$\dot{T}_L = \frac{\sigma_{YL}(T_L) \cdot |Z \cdot \dot{U}|}{\rho_L . c_L \cdot h_L} - \frac{k_s \cdot T_L}{r \cdot \rho_L \cdot c_L \cdot h_L} \cdot \left(\frac{1}{F} + 1.274 \cdot \left(\frac{t_s}{r}\right) \cdot (t^+)^{-1/3}\right) \tag{3.5}$$

$$F = \begin{cases} 2 \cdot \left(\frac{t^+}{\pi}\right)^{1/2} - \frac{t^+}{\pi}\left[2 - \left(\frac{t^+}{4}\right) - \left(\frac{t^+}{4}\right)^2 - \frac{15}{4}\left(\frac{t^+}{4}\right)^3\right], & t^+ < 0.6 \\ \frac{8}{3 \cdot \pi} - \frac{1}{2(\pi \cdot t^+)^{1/2}} \cdot \left[1 - \frac{1}{3 \cdot (4 \cdot t^+)} + \frac{1}{6 \cdot (4 \cdot t^+)^2} - \frac{1}{12 \cdot (4 \cdot t^+)^3}\right], & t^+ > 0.6 \end{cases} \tag{3.6}$$

$$t^+ = \frac{\alpha_s t}{r^2} \tag{3.7}$$

$$\sigma_{YL}(T_L) = \sigma_{YL0} exp(-E_2 T_L) \tag{3.8}$$

Where r is the radius of the lead core, h_L is the height of the lead core, t_s is the total steel height of the steel layers, c_L is specific heat of the lead, σ_{YL0} is the yield stress of lead at the initial temperature, ρ_L is desity of lead, α_s is thermal diffusion of steel, t^+ is the dimensionless time, E_2 is the constant that deal with temperature and yield stress. The typical properties given by Kalpakidis and Constantinou are as follows ρ_L= 11.200 kg/m³, c_L= 130J/(kg°C), k_s= 50W/(kg°C), α_s= 1.41x10⁻⁵ m²/s, E_2=0.0069/°C.

The temperature dependent hysteretic model developed by Kalpakidis and Constantinou [20] gives closer results to the actual behavior than bounding analyses. These features will probably make the strength deteriorating model as the most commonly used material model for lead rubber bearings in the next years. The force displacement relationship of temperature dependent material

model which was obtained from the results of the analyses which were conducted for this study was given in Figure 3.3.

Figure 3.3. Force displacement relationship of temperature dependent material model

4. MODELING OF STRUCTURES AND ISOLATION DEVICES

In this section, mathematical models and design approaches of superstructures and isolators are introduced in detail. Two different superstructure models were examined in this study. One is 23-story reinforced concrete structure and the other is 3-story steel structure. By selecting two different structural systems enable us to include the structural system as a variable in addition to the isolator properties (T and Q/W) and the PGV of ground motion on the superstructure response.

4.1. 23-Story Reinforced Concrete Structure

4.1.1 Design of superstructure

Considered 23-story reinforced concrete building structure was adopted from study of Calugaru and Panagiotou [40]. The structural model has 4 axes in X and Y directions. Lengths of each axis are 9.1m. 50cm thick core wall is stated in the middle of the structure and the elevator shaft was located in that core wall. 12 columns are placed at the intersection of the axes as shown in the Figure 4.1.b. Dimensions of columns are 100cm in both directions from the base slab to top. The building is symmetrical in plan and has flat slabs at the floor levels. The thickness of the base and typical floor slabs are 22cm. There are no beams that were connected to the columns and walls. The structure has 23-story. First three stories are the rigid basement stories and the others are typical stories. The story height of the basement floors and typical floors are 3.35m and 3m, respectively. So that the total height of the building is 70.05 m. Columns of the basement floors attached to each other with 50cm thick basement wall as shown in the Figure 4.1.a.

The floor masses are 11760kN for each basement floor and 8440kN for each typical floor. The floor masses were equally distributed to each node at the floor level.

Rigid floor assumption was made for all story levels with the help of elastic elements that were placed between master node and slave nodes as shown in the

Figure 4.2. All horizontal components (rigid fictive beams and rigid diaphragm beams) and columns were attached to each other with full rigid connection.
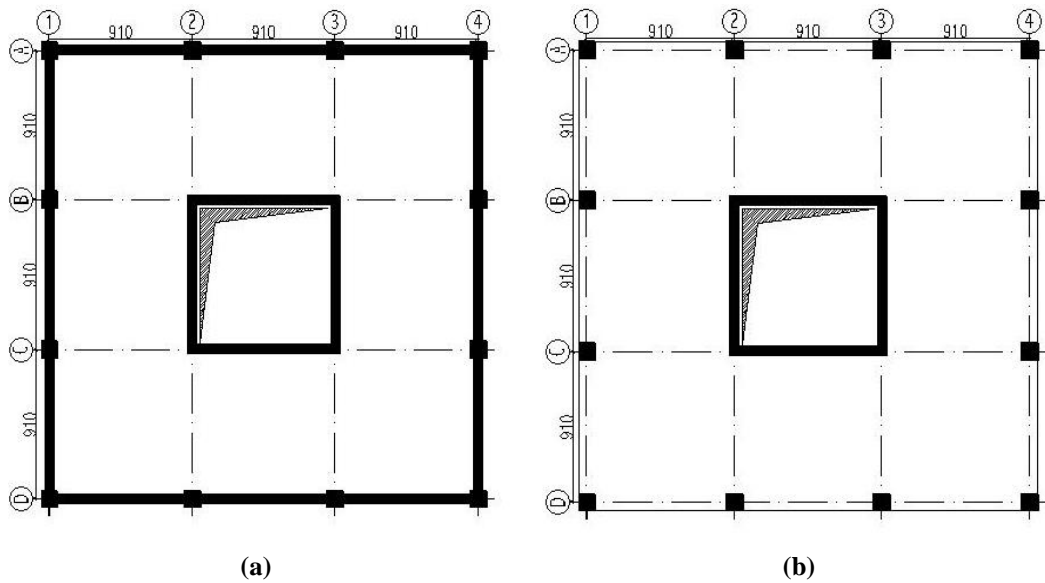

(a)   (b)

Figure 4.1. Considered reinforced concrete structure a) plan view of the rigid basement floors, b) plan view of the typical floors
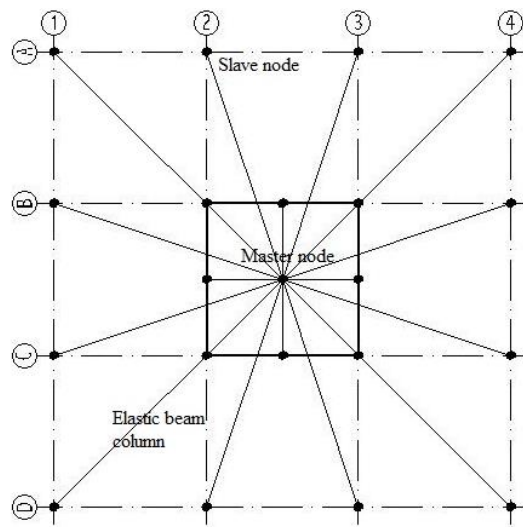

Figure 4.2. Rigid floor diaphragm model

The structural model was developed with Open System for Earthquake Engineering Simulation (OpenSees) software that is capable for temperature dependent analyses [42].

Columns and shear walls are modeled with elastic beam column element since the superstructure of the seismically isolated structure behaves like a rigid block that lies in the elastic range. Shear walls modeled with frame element so that rigid fictive beams attached to the columns as shown in Figure 4.3.b. The mathematical models of the column were given in Figure 4.4.

(a)	**(b)**

Figure 4.3. Shear wall model a) 3-D view, b) mathematical model

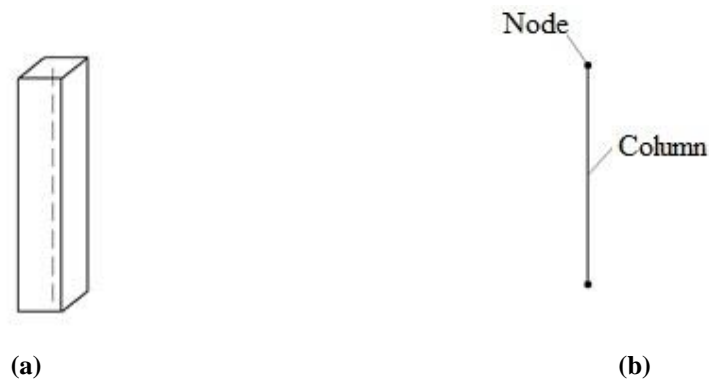|	
(a)	**(b)**

Figure 4.4. Column model a) 3-D view, b) mathematical model

4.1.2 Design of isolation devices

In this study three different material models were used for conducting nonlinear time history analyses. One of them was the temperature dependent material model which considers strength deterioration and the others were the material models of bounding analyses (upper and lower bound analyses) which do not consider strength deterioration in the calculations. The force deformation relationship of bounding analyses can be constructed with characteristic strength, yield displacement and post elastic stiffness.

The yield stress value of the lead core was chosen as 10 Mpa for lower bound analyses and 13.5 Mpa for upper bound analyses according to Constantinou et al. [28]. The yield stress value for upper bound analyses is the initial yield stress of the temperature dependent analyses.

The design of isolation devices starts with assumption for isolation period and accordingly isolator displacement and Q/W ratio. The selected target spectrum is modified with calculated damping reduction factor. Then the assumed displacement for isolator and obtained displacement value from the spectrum is compared. If the results are close enough the assumed displacement value is used as the maximum displacement value otherwise the iterative calculation starts.

The 16 lead rubber bearings having different properties were applied to the 23-story reinforced concrete structure separately. They were illustrated in Figure 4.5 and their properties were given in Table 4.1. The isolators were classified with their Q/W ratios and T. Where; Q is the strength of the lead core, W is the weight supported by the isolator, T is the isolation period, r is the radius of the lead core, h is the height of the isolator, t_s is the total thickness of the steel shim plates.

T and Q/W are the two important isolator properties influencing the seismic response of the base isolated building considerably. The results of the analyses are highly dependent on these two parameters.

Figure 4.5. Considered isolators for the 23-story RC structure

Table 4.1. Properties of isolators used for 23-story reinforced concrete structure

Q/W ratio	T	F_y (N)		E (N/mm^2)		b (k_d/k_e)		r	h	t_s	Yield disp.
	(s)	Lower	Upper	Lower	Upper	Lower	Upper	(mm)	(mm)	(mm)	(mm)
0.090	3.25	1006083	1324758	40243	52990	0.096	0.073	170	333	125	25
0.090	3.50	991860	1310534	39674	52421	0.083	0.063	170	398	150	25
0.090	3.75	981954	1300629	39278	52025	0.074	0.055	170	450	170	25
0.090	4.00	973127	1291801	38925	51672	0.065	0.049	170	515	195	25
0.105	3.25	1157678	1529465	46307	61178	0.083	0.063	184	333	125	25
0.105	3.50	1143455	1515241	45738	60610	0.072	0.054	184	398	150	25
0.105	3.75	1133549	1505336	44988	60213	0.056	0.048	184	450	170	25
0.105	4.00	1124722	1496508	44988	59860	0.056	0.042	184	515	195	25
0.120	3.25	1309273	1734172	52371	69367	0.074	0.055	197	333	125	25
0.120	3.50	1295049	1719948	51802	68798	0.063	0.048	197	398	150	25
0.120	3.75	1285144	1710043	51406	68402	0.056	0.042	197	450	170	25
0.120	4.00	1276316	1701215	51052	68049	0.05	0.037	197	515	195	25
0.135	3.25	1460867	1938879	58435	77555	0.066	0.05	208	333	125	25
0.135	3.50	1446644	1924656	57866	76986	0.057	0.043	208	398	150	25
0.135	3.75	1436739	1914750	57470	76590	0.05	0.038	208	450	170	25
0.135	4.00	1427911	1905922	57116	76237	0.044	0.033	208	515	195	25

20 lead rubber bearings were used under 23-story reinforced concrete building. They placed under columns and walls. The location of these bearings was shown in Figure 4.6. All the bearings were modelled with zero length element objects in OpenSees. The zero length elements composed of two nodes at the same point which are attached by uniaxial material object to construct the force deformation relation for seismic isolator.
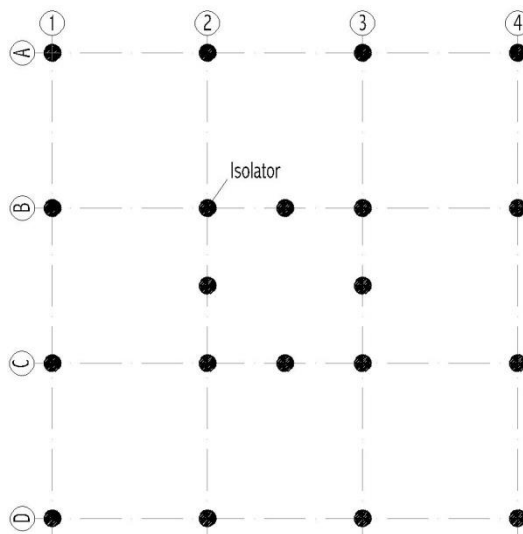

Figure 4.6. Location of lead rubber bearings for 23-story reinforced concrete building

4.2. 3-Story Steel Structure

4.2.1 Design of superstructure

The plan view of considered 3-story steel structure is schematically shown in the Figure 4.7. It was adopted from study of Dr. Charles Kircher [41]. The structural model has 7 axes in long direction and 5 axes in short direction and the distance between each axes are 9m. 35 columns were used as a vertical supporting member. These columns attached with elastic beams and girders. The building is regular both plan and elevation. The total height of the structure is 9m. It composed of 3 stories.

Total weight of the structure is 73000kN. The floor masses were equally distributed to each node at the floor level.

Rigid floor assumption was made for all story levels with the help of elastic elements that were placed between master node and slave nodes. All beams and columns were attached to each other with fully rigid connection. The plan view and the three dimensional view of three story superstructure were given in Figure 4.7 and Figure 4.8. Also, sections of the structure from long and short directions were presented in Figure 4.9.
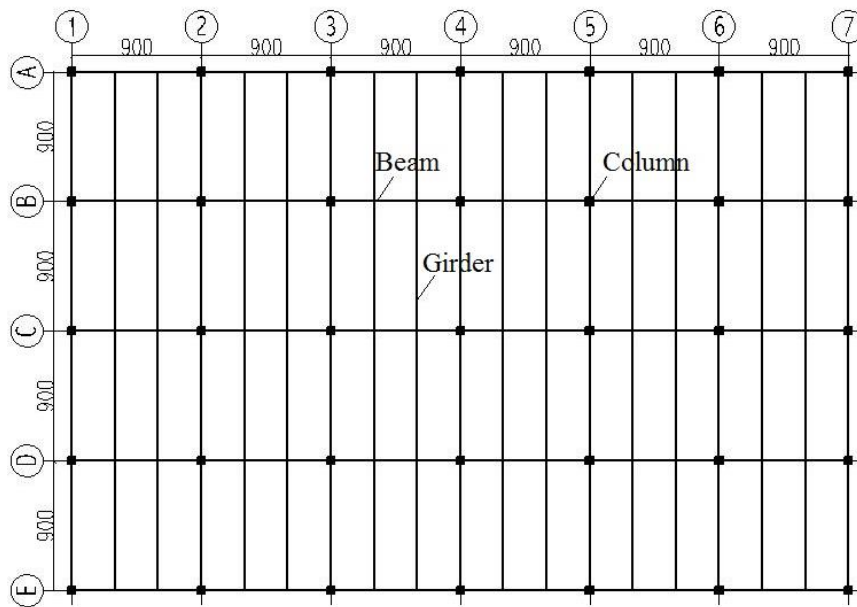
Figure 4.7. Plan view of the 3-story steel structure
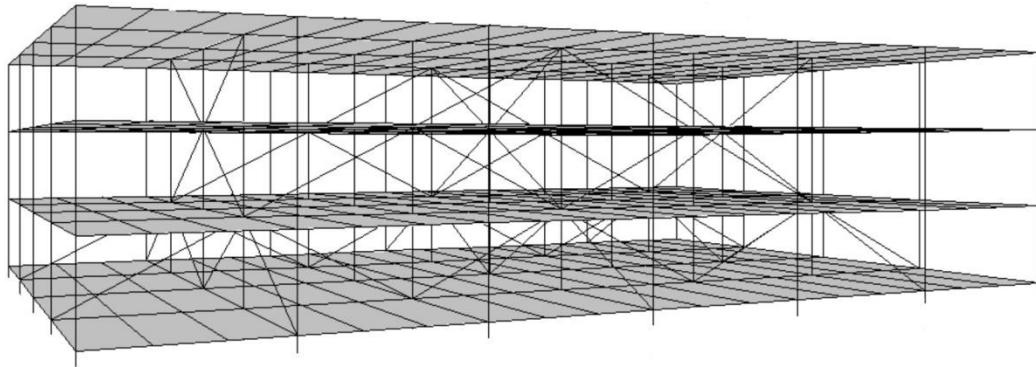
Figure 4.8. 3D view of the 3-story steel structure
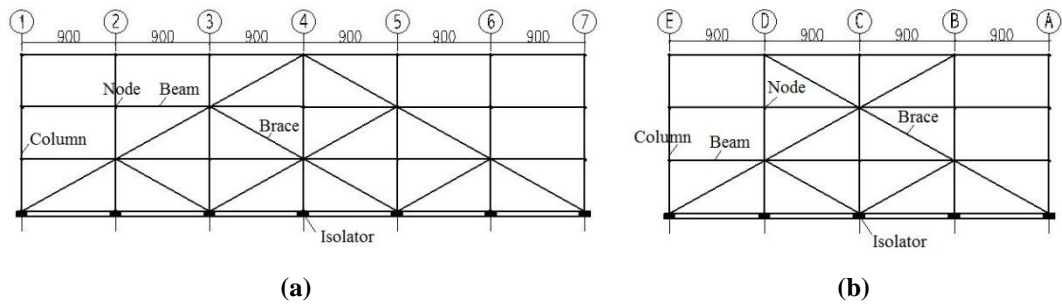
Figure 4.9. Section of the 3-story steel structure a) B and D axis b) 2 and 6 axis

The structural model was developed with OpenSees and the columns and beams of the superstructure were modeled with elastic beam column element as in the 23-story reinforced concrete structure.

4.2.2   Design of isolation devices

The 16 lead rubber bearings having different properties were applied to the 3-story steel structure separately. They were illustrated in Figure 4.10 and their properties were given in Table 4.2.

40

Figure 4.10. Considered isolators for the 3-story steel structure

Table 4.2 Properties of isolators used for 3-story steel structure

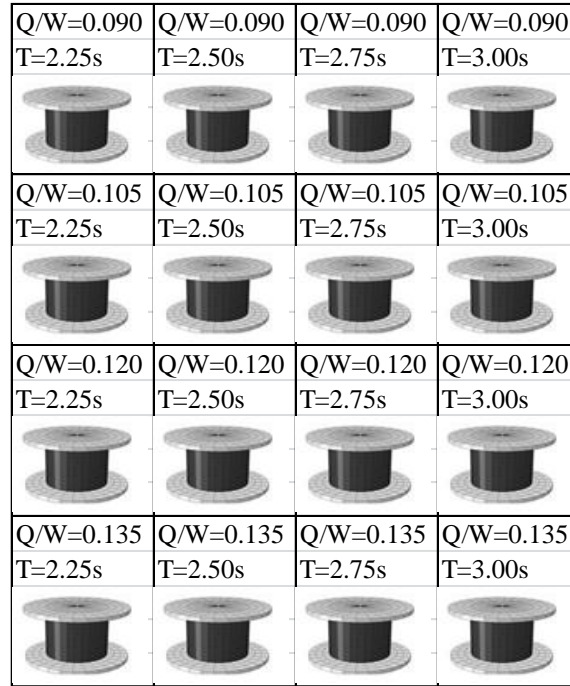| Q/W ratio	T	F_y (N)		E (N/mm^2)		b (k_d/k_e)		r	h	t_s	Yield disp.
	(s)	Lower	Upper	Lower	Upper	Lower	Upper	(mm)	(mm)	(mm)	(mm)
0.090	2.25	230100	296676	9204	11867	0.182	0.141	77.5	229	66	25
0.090	2.50	221712	288287	8868	11531	0.151	0.116	77.5	290	84	25
0.090	2.75	216120	282695	8645	11308	0.129	0.099	77.5	341	99	25
0.090	3.00	211500	278076	8460	11123	0.110	0.084	77.5	411	120	25
0.105	2.25	261460	337645	10458	13506	0.160	0.124	83.5	229	66	25
0.105	2.50	253072	329257	10123	13170	0.133	0.102	83.5	290	84	25
0.105	2.75	247480	323665	9899	12947	0.113	0.086	83.5	341	99	25
0.105	3.00	242860	319045	9714	12762	0.096	0.073	83.5	411	120	25
0.120	2.25	292820	381668	11713	15267	0.143	0.110	89.5	229	66	25
0.120	2.50	284432	373280	11377	14931	0.118	0.090	89.5	290	84	25
0.120	2.75	278840	367688	11153	14708	0.100	0.076	89.5	341	99	25
0.120	3.00	274220	363068	10969	14523	0.085	0.064	89.5	411	120	25
0.135	2.25	324180	424705	12967	16988	0.129	0.099	95.0	229	66	25
0.135	2.50	315792	416317	12632	16653	0.106	0.080	95.0	290	84	25
0.135	2.75	310199	410725	12408	16429	0.090	0.068	95.0	341	99	25
0.135	3.00	305580	406105	12223	16244	0.076	0.057	95.0	411	120	25

35 lead rubber bearings were used under 3-story steel structure. They were placed under each column. The location of these bearings was shown in Figure 4.11. All the bearings were constructed with zero length element objects in OpenSees.
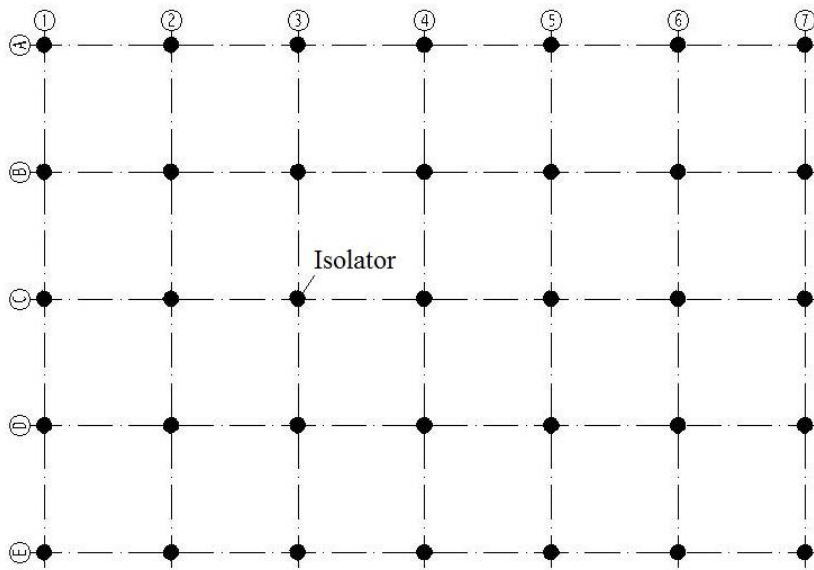
Figure 4.11. Location of lead rubber bearings for 3 story steel structure

5. GROUND MOTION SELECTION

The properties of layers of the earth are very important to understand the seismic activities and their physical results. The seismic activities that make the continents move are originated by radioactivity within the core. Radioactive events increase the heat in the internal structure of the earth and the change in temperature generates heat flow towards the surface from the outer core of the earth as shown in Figure 3.1. The movement produced by heat convection affects the tectonic plates. They diverge or converge over each other as a result of these movements.
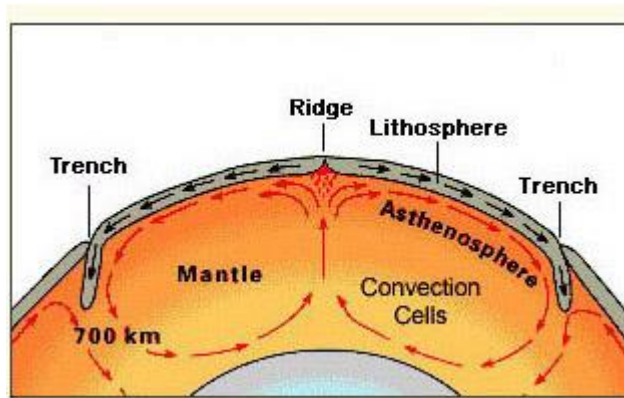

Figure 5.1. Heat convection within the internal structure of the Earth [43]

The formation of the earthquakes mainly originated from interaction of tectonic plates. Therefore, numerous earthquakes occur at the boundaries of tectonic plates. They are called inter-plate earthquakes which were used to conduct the analyses in this study. Besides, the other earthquakes occurred far from the boundaries of tectonic plates are called intra-plate earthquakes. They are usually very small compared to inter-plate earthquakes and they are out of the scope of this study.

The mechanism of inter-plate earthquakes is explained by the elastic rebound theory. According to elastic rebound theory, the parts located at the two sides of the fault resist against driving forces exerted by tectonic movements up to the point of internal strength. While the strain energy is accumulated at plate

boundaries, sides of the fault start to deform slowly. After the internal strength is exceeded, the sudden rupture occurs and accumulated large amount of strain energy is released. Accordingly, the strong ground shaking is developed around the fault. Finally, the sides of the fault snap back to original undeformed shape. The mentioned elastic rebound theory is schematically illustrated in Figure 5.2.
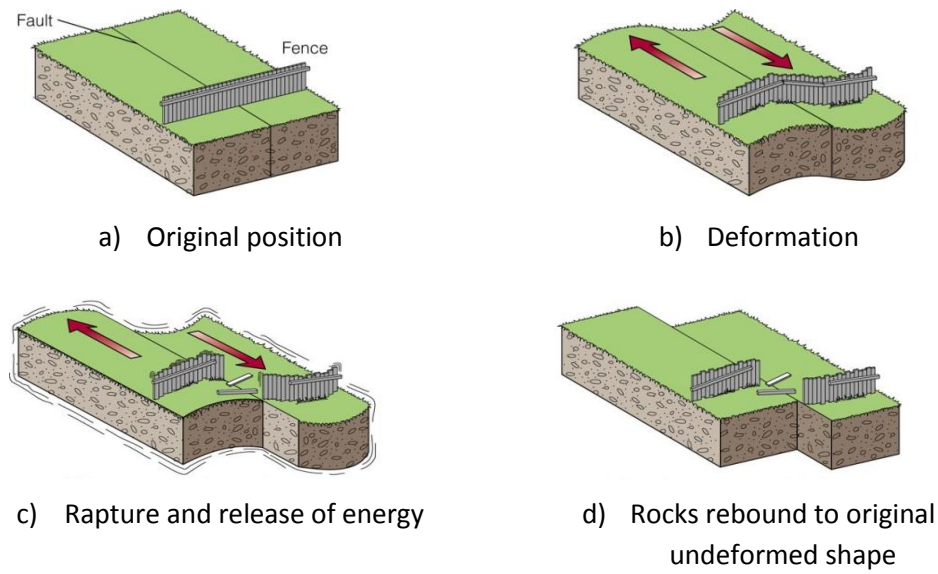

a) Original position

b) Deformation

c) Rapture and release of energy

d) Rocks rebound to original undeformed shape

Figure 5.2. Schematic illustration of elastic rebound theory [44]

Earthquake induced forces which act the superstructure during the strong ground shaking is needed for structural calculations. The forces that exerted by earthquakes are subjected to the mass of the structures according to Newton's 2nd law of motion. The mass of the structure is already known so that the earthquake engineers require the acceleration time histories of earthquakes in order to conduct the analyses. The devices are called accelerograph, which records the acceleration of the particles on the surface of the earth as a function of time during the earthquake. These strong motion records also give information about the nature and the characteristic of earthquakes.

Acceleration time histories which are recorded at distance less than 20km between site and source (epicentral distance illustrated in the Figure 5.3) are called near fault ground motions in the study of Somerville et al. [45]. In contrast, the ground motion records which are recorded at 20km away from the source are

called far fault ground motions. The near fault and far fault ground motions have different characteristics from each other. Strong ground motions recorded at near fault regions cause the structure to deform beyond its elastic limit and result destructive damage during the earthquake. Their seismic demands are very large compared to far fault motions [45-47].

In this study, the near fault ground motions were selected to perform the time history analyses in order to force the structure to its limits for understanding the changes in their response clearly. While the earthquake records were being selected, the exact distance were not specified, only the earthquakes occurred within 20km site to source distance were taken into consideration.
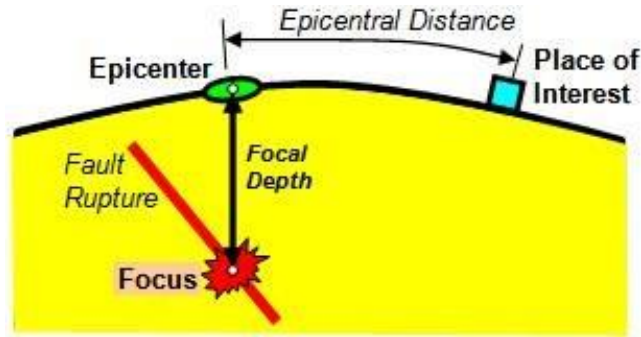

Figure 5.3. Epicenteral distance is the distance between site and epicenter

Magnitude measurement is the most widely used quantitative measurement of the earthquake energy. Total amount of seismic energy released during an earthquake is measured with magnitude measurement. The importance of an earthquake magnitude is mentioned in the studies of Stewart et al. [48] and Bommer and Acevedo [47]. In this study the moment magnitude was used as a magnitude scale which does not subjected to saturation and works under wider range of earthquake sizes. The moment magnitude (M_w) is directly related to the seismic moment (M_0) given in the (3.1). The moment magnitudes of the earthquakes were used in this study were selected between 6.0 and 8.0 which are called high moment magnitude earthquakes.

$$M_w = \frac{2}{3}\log(M_0) - 6.0 \tag{5.1}$$

As indicated in the previous sections, the peak velocity of ground motion (PGV) has considerable influence on the seismic response of the base isolated structures [49]. Therefore, PGV affects the temperature change in the lead core of

isolator. One of the objectives of this study is to investigate the effect of peak ground velocity (PGV) values of earthquake records on the superstructure response of seismically isolated buildings with lead rubber bearings. Therefore, the earthquake records were also selected according to their PGV values. The selected records were clustered in three groups (PGV=30-50 cm/s, PGV=50-70 cm/s, PGV>70 cm/s) in order to observe the effect of PGV values on the behavior of superstructure.

In this study, all selected strong ground motion records possessing the features mentioned above had been searched and taken from PEER Strong Motion Database (http://peer.berkeley.edu/smcat/). The website serves numerous earthquake records from tectonically active regions with their magnitude, distance to fault site conditions, peak ground acceleration (PGA), peak ground velocity (PGV) and peak ground displacement (PGD). 60 strong ground motion records were selected according to their PGV values, magnitudes and site to source distances. The response spectrum of 60 selected earthquake ground motions and the mean spectrum and their standard deviation of classified earthquakes according to their PGV values were given in Figure 5.4 and Figure 5.5 respectively. Also, PGA and PGV distributions of these selected earthquake records and PGV/PGA ratios were presented in Figure 5.6.
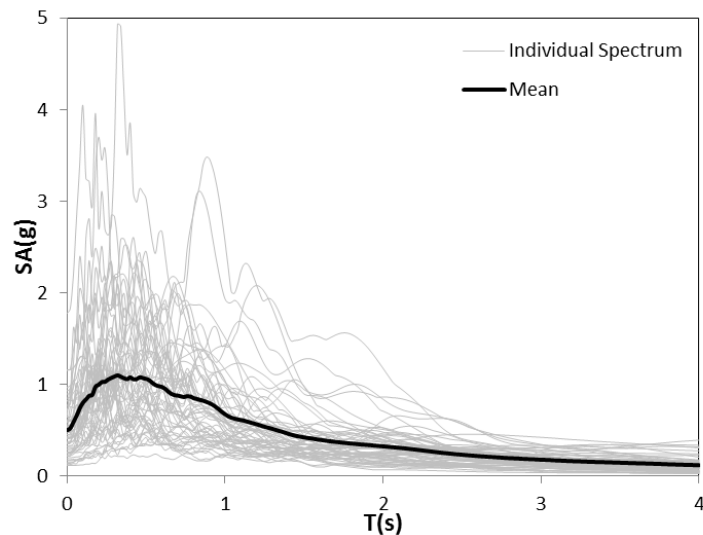

Figure 5.4. %5 damped acceleration response spectrum of 60 selected earthquake ground motions
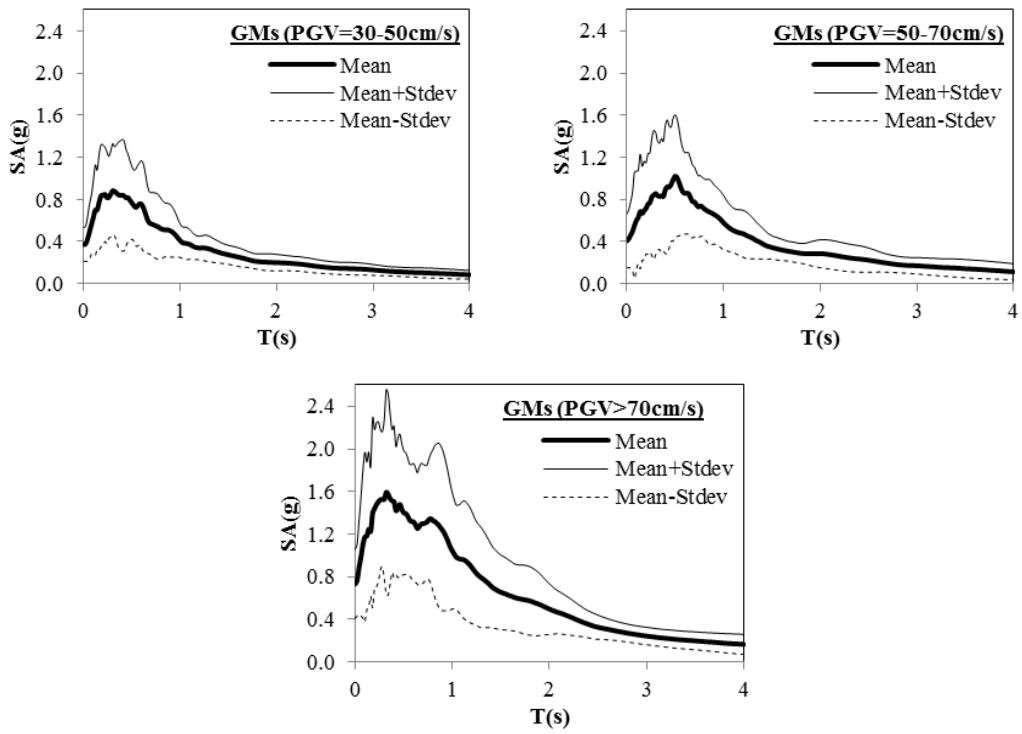
Figure 5.5. Comparison of mean and ±1 SD of response spectra
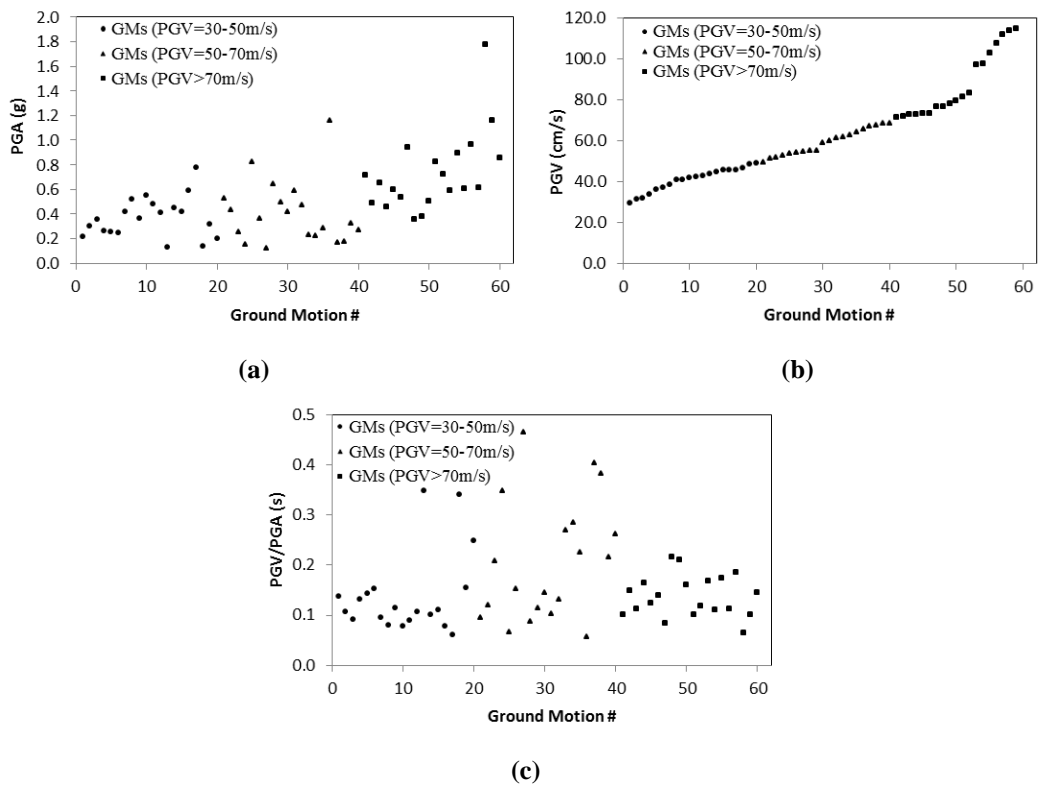

(a)

(b)

(c)

Figure 5.6. a)PGA, b) PGV, c)PGV/PGA ratios of the considered ground motions

The selected earthquake records and their properties were given in Table 5.1 with the increasing PGV values.

Table 5.1. Selected earthquake ground motions

Earthquake	Station	M_w	Epicentral d (km)	Comp.	PGA (g)	PGV (cm/s)	PGD (cm)
Kocaeli, Turkey	Izmit	7.4	4.80	90	0.220	29.8	17.12
Northridge	Pacoima Kagel C.	6.7	8.20	90	0.301	31.4	10.87
Northridge	Canoga Park – T. Can	6.7	15.80	106	0.356	32.1	9.13
Chi-Chi, Taiwan	TCU122	7.6	9.03	N	0.261	34.0	36.08
Superstitn Hills(B)	El Centro Imp. Co.	6.7	13.90	90	0.258	36.3	20.20
Chi-Chi, Taiwan	CHY035	7.6	18.12	W	0.250	37.4	12
Loma Prieta	Gilroy Array #4	6.9	16.10	0	0.417	38.8	7.09
Imperial Valley	El Centro Array #5	6.5	1.00	140	0.52	40.9	35.4
Loma Prieta	Gilroy Array #3	7.1	14.40	90	0.367	41.1	19.25
Cape Mendocino	Rio Dell Overpass-FF	7.1	18.50	360	0.549	42.1	18.62
Imperial Valley	El Centro Array #4	6.5	4.20	140	0.485	42.6	20.23
Northridge	C. Country-W L.Cany	6.7	13.00	0	0.410	43.0	11.75
Chi-Chi, Taiwan	TCU106	7.6	15.22	N	0.128	43.7	35.83
Imperial Valley	El Centro Array #8	6.5	3.80	230	0.454	44.7	35.59
Chi-Chi, Taiwan	TCU084	7.6	10.39	N	0.417	45.6	21.27
Cape Mendocino	Petrolia	7.1	9.50	0	0.590	45.6	21.74
Imperial Valley	Bonds Corner	6.5	2.50	230	0.775	45.9	14.89
Chi-Chi, Taiwan	TCU053	7.6	6.69	N	0.140	46.9	48.05
Loma Prieta	Saratoga - Aloha Ave	7.1	13.00	90	0.32	48.4	27.5
Chi-Chi, Taiwan	TCU060	7.6	9.46	W	0.201	49.1	51.89
Loma Prieta	Bran	6.93	9.01	0	0.526	49.7	10.53
Northridge	Pacoima Kagel C.	6.7	8.20	360	0.433	51.5	7.21
Chi-Chi, Taiwan	TCU070	7.6	19.10	W	0.255	52.1	48.09
Chi-Chi, Taiwan	TCU109	7.6	13.09	N	0.155	53.1	34.74
Duzce, Turkey	Bolu	7.1	17.60	90	0.822	54	13.55
Chi-Chi, Taiwan	CHY006	7.6	14.93	E	0.364	54.3	25.59
Chi-Chi, Taiwan	TCU064	7.6	15.07	N	0.12	54.8	59
Loma Prieta	Corralitos	7.1	5.10	0	0.644	55.2	10.88
Erzincan, Turkey	Erzincan	6.9	2.00	W	0.496	55.4	22.78
Northridge	Beverly Hills - 14145 M.	6.7	19.60	9	0.416	59.0	13.14
Coalinga	Pleasant Valley P.P.	6.4	8.50	45	0.592	60.2	8.77

Table 5.1. (Continue) Selected earthquake ground motions

Northridge	Northridge - 17645 S.	6.7	13.30	180	0.477	61.5	22.06
Imperial Valley	EC County Center FF	6.5	7.50	92	0.235	62.1	39.35
Chi-Chi, Taiwan	TCU120	7.6	8.10	W	0.225	63.1	54.09
Kobe	Kobe University	6.9	0.90	0	0.29	64.3	13.5
San Fernando	Pacoima Dam	6.6	2.80	254	1.160	65.7	11.73
Chi-Chi, Taiwan	TCU128	7.6	9.70	N	0.170	67.4	41.87
Chi-Chi, Taiwan	TCU110	7.6	12.56	W	0.180	67.5	40.97
Northridge	Newhall - W. Pico C. Rd.	6.7	7.10	316	0.325	68.8	16.11
Kocaeli, Turkey	Yarimca	7.4	2.60	60	0.268	68.8	57.01
Gazli	Karakyr	6.8	12.82	90	0.718	71.6	23.71
Chi-Chi, Taiwan	TCU072	7.6	7.36	W	0.489	71.7	38.64
Chi-Chi, Taiwan	CHY028	7.6	7.31	W	0.653	72.8	14.68
Superstition Hills(B)	Parachute Test Site	6.7	0.70	225	0.455	73.1	52.80
Chi-Chi, Taiwan	TCU074	7.6	13.67	W	0.597	73.3	20.44
Duzce, Turkey	Duzce	7.1	8.20	270	0.535	73.3	51.59
Northridge	Sepulveda VA	6.69	8.48	360	0.939	76.6	14.95
Imperial Valley	El Centro Array #4	6.5	4.20	230	0.360	76.6	59.02
Imperial Valley	El Centro Array #5	6.5	1.00	230	0.379	78.2	63.03
Chi-Chi, Taiwan	TCU067	7.6	0.33	W	0.503	79.5	93.09
Kobe	KJMA	6.9	0.60	0	0.821	81.3	17.68
Landers	Lucerne	7.3	1.10	275	0.721	83.5	70.31
Northridge	Newhall - Fire Sta	6.7	7.10	360	0.590	97.2	38.05
Northridge	Sylmar - Converter	6.7	6.20	142	0.897	97.6	46.99
Northridge	Sylmar - Olive View	6.7	6.40	90	0.604	102.8	16.05
Chi-Chi, Taiwan	CHY080	7.6	6.95	W	0.968	107.5	18.60
Kobe	0 Takatori	6.9	0.30	90	0.616	112.0	32.72
Northridge	Tarzana, Cedar Hill	6.7	17.50	90	1.779	113.6	33.22
Chi-Chi, Taiwan	TCU084	7.6	10.39	W	1.157	114.7	31.43
Tabas, Iran	Tabas	7.4	2.10	TR	0.852	121.4	94.58

6. RESULTS

In this study the response of superstructure of isolated buildings was investigated with the material model considering strength deterioration during the motion. Also, the upper and lower bound analyses were conducted for comparison purposes. Therefore, 3 material models were used for performing the analyses.

23-story reinforced concrete superstructure and 3-story steel superstructure were chosen as a high-rise and low-rise superstructure respectively. All the isolated structure models were developed with these 2 superstructure models.

In order to investigate the effect of isolation properties on the response of superstructure, 16 different LRBs were applied to the analytical model of the concrete and steel structures separately. Thus, 32 isolated buildings were designed to conduct the analyses.

The heat increase in the lead core and the related strength deterioration of isolator during the motion is directly related with the velocity of the motion. Thus, to examine the importance of ground motion characteristics on the response 60 earthquake ground motion with varying PGV values were selected for this study.

In total 5760 nonlinear time history analyses were conducted with 3 material models, 32 isolated structures, 60 earthquake ground motions. All the analyses were performed with OpenSees structural analyses software that is capable of calculating the strength reduction of LRB during motion. The results of these analyses were given in the Figure 6.1-Figure 6.48.

The analyses results are presented in terms of two engineering demand parameters, which are absolute floor accelerations and the inter-story drift ratios for each story. Absolute floor acceleration is considered the indication for the safety of the equipment at the story level. While the inter-story drift ratio is related with the structural damage in the superstructure components. Instead of presenting the results of each individual ground motions, average values for each PGV cluster is given in Figure 6.1-Figure 6.48.
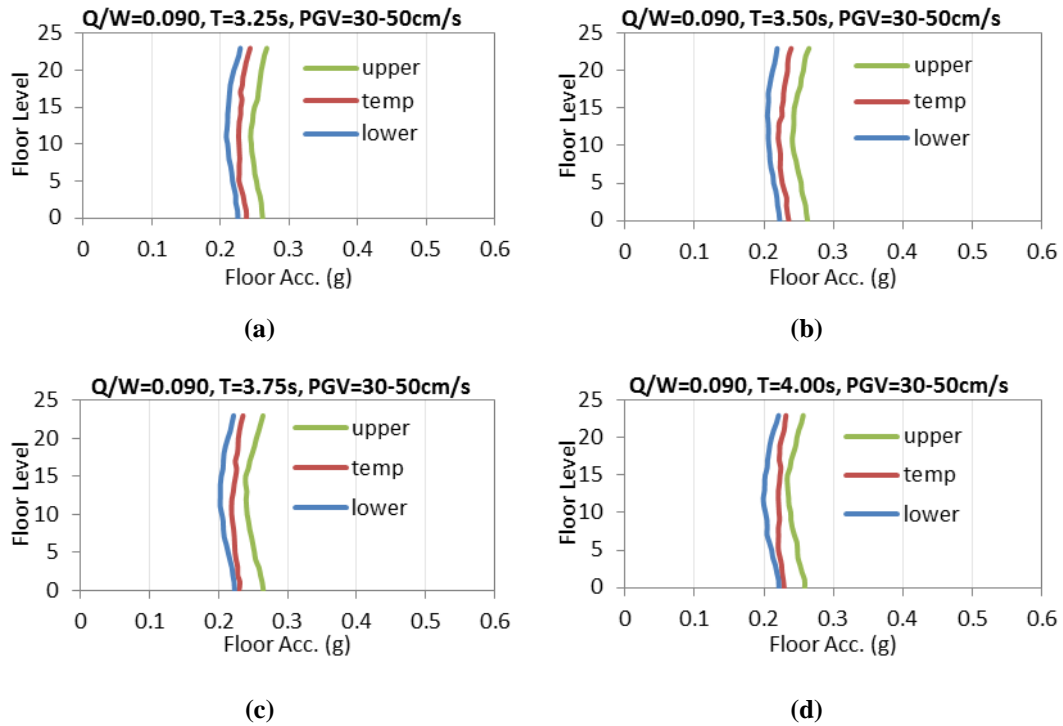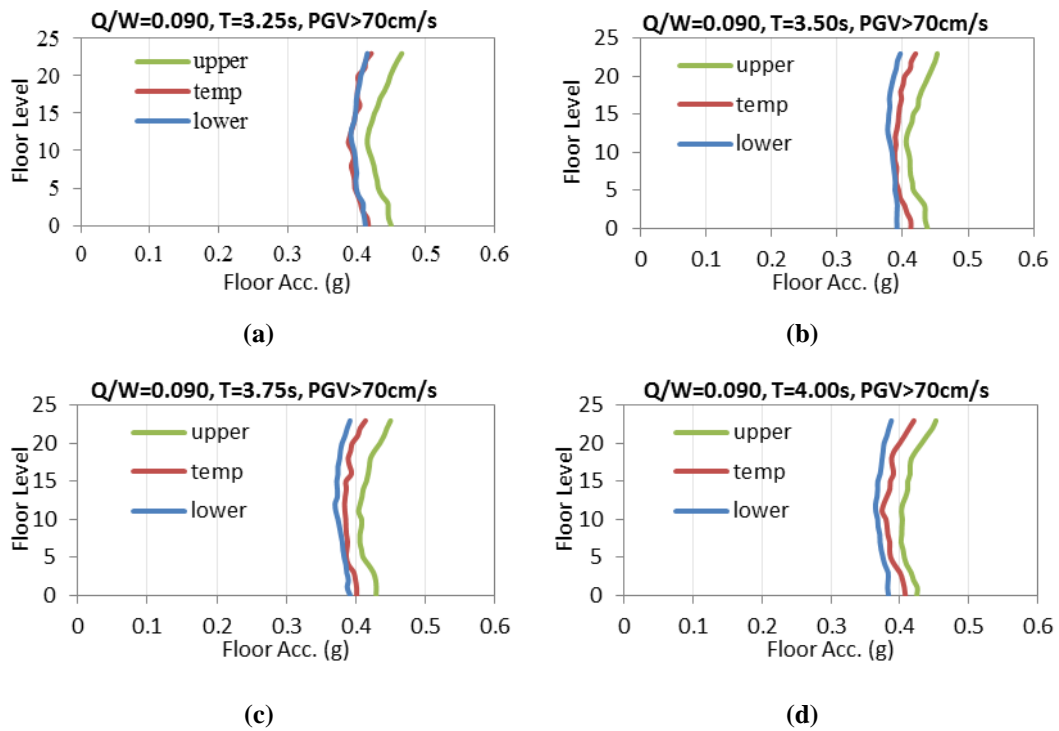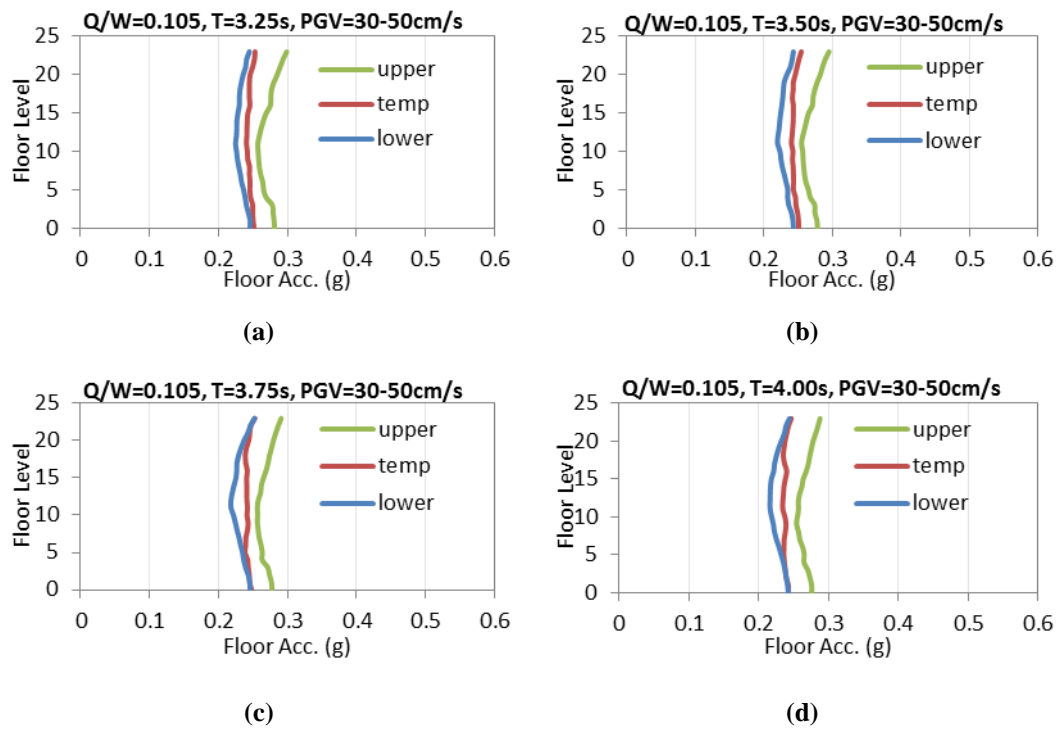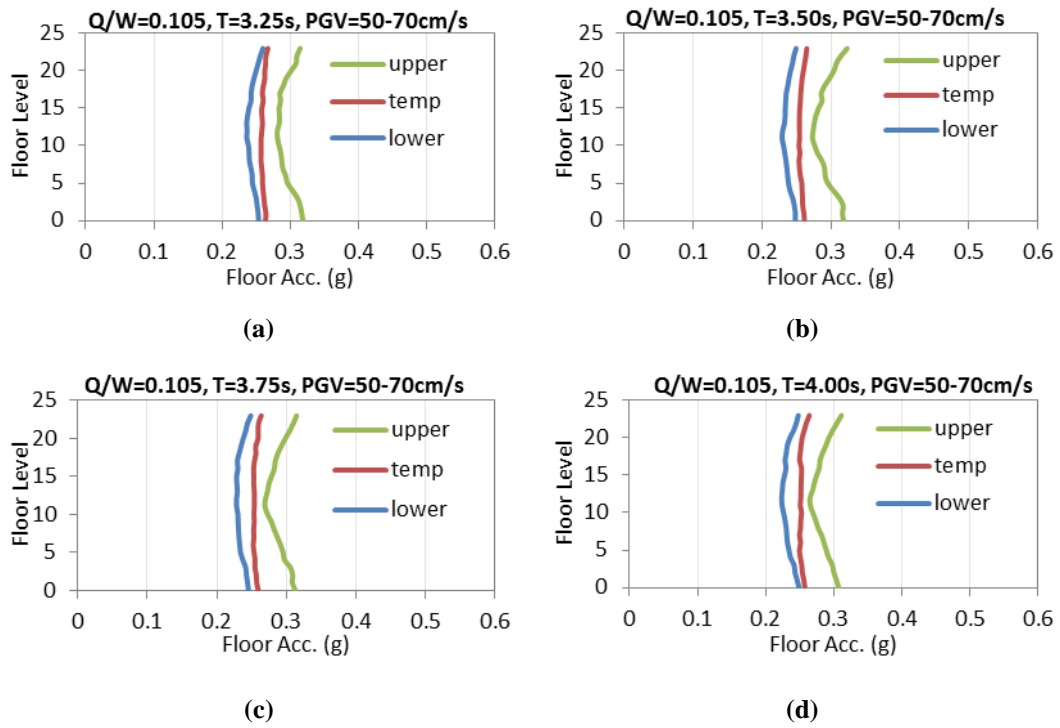
Figure 6.1 Average peak floor accelerations of 23 story reinforced concrete structures with same Q/W=0.090, PGV=30-50cm/s and different T: a)T=3.25s, b)T=3.50s, c)T=3.75s, d)T=4.00s
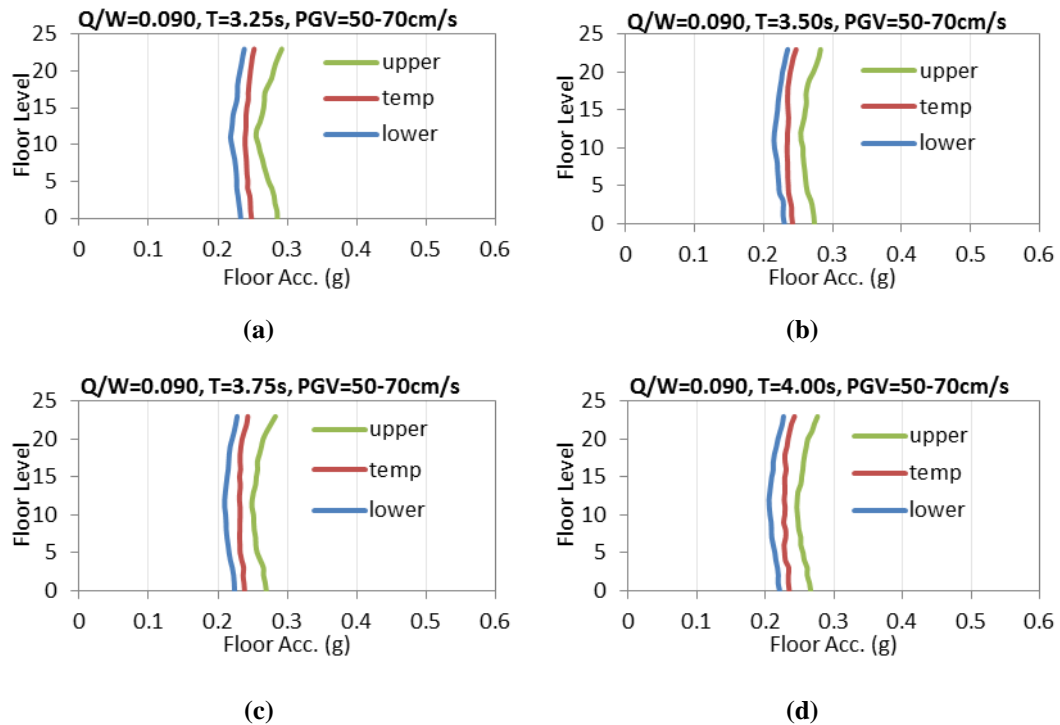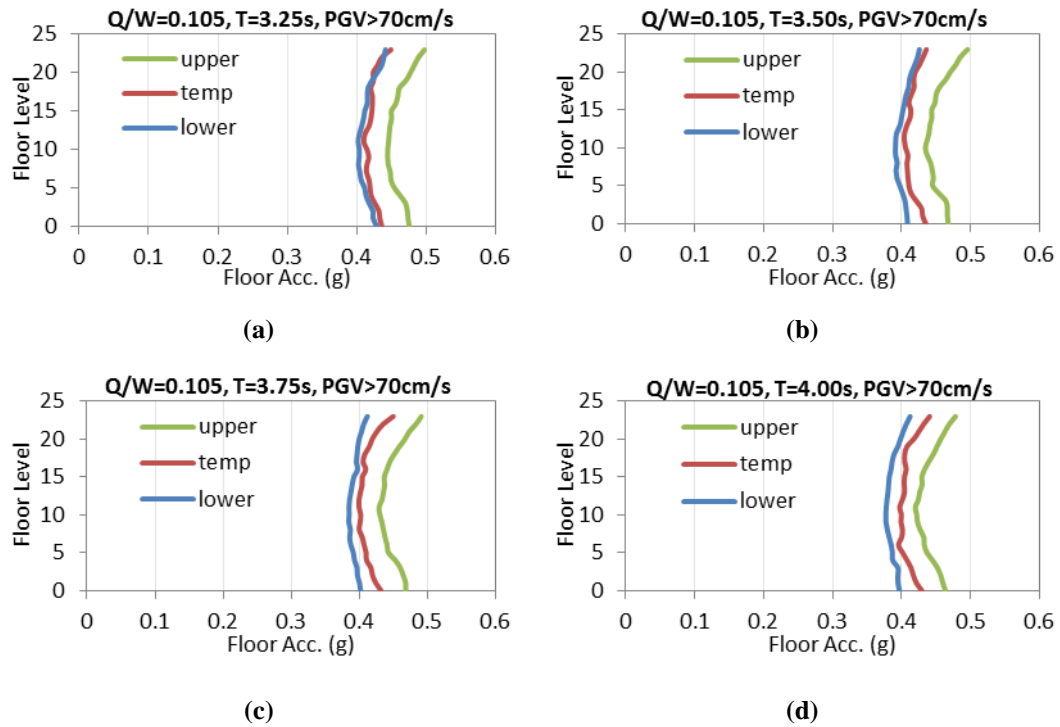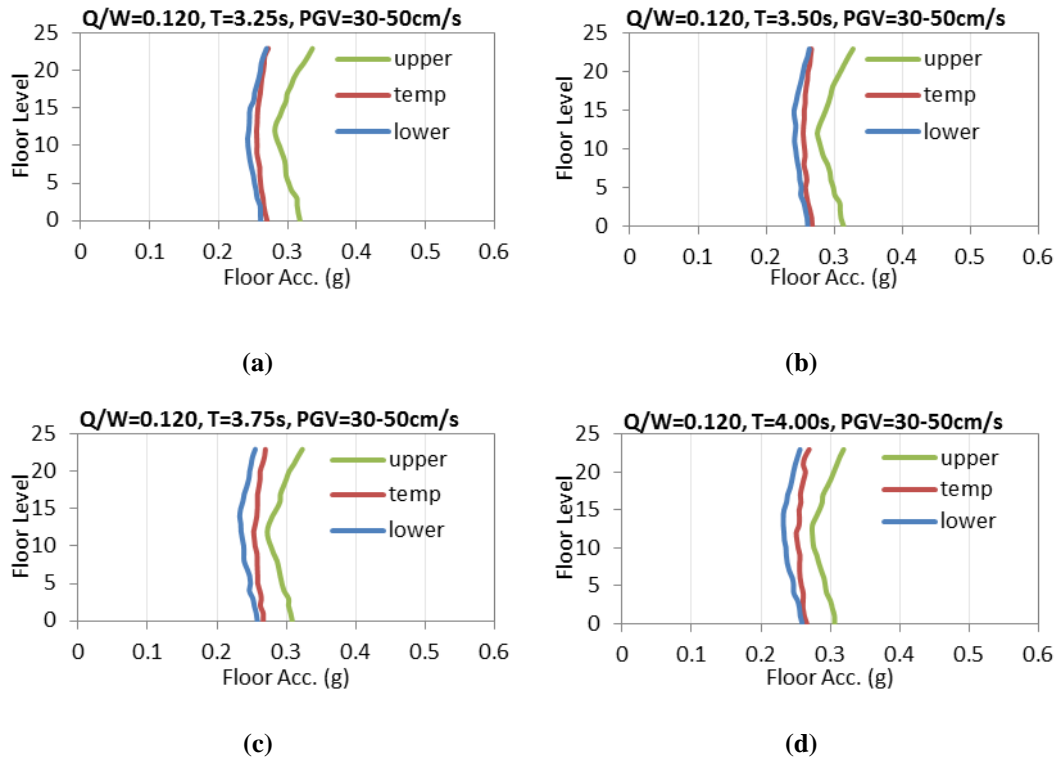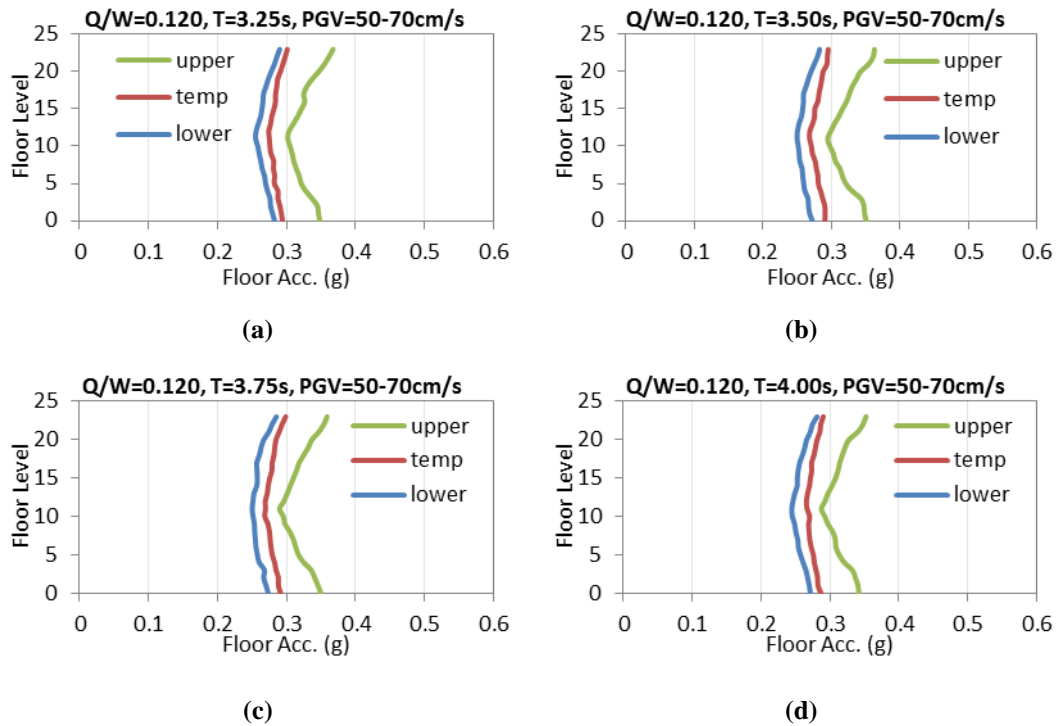

Figure 6.2 Average peak floor accelerations of 23 story reinforced concrete structures with same Q/W=0.090, PGV=50-70cm/s and different T: a)T=3.25s, b)T=3.50s, c)T=3.75s, d)T=4.00s

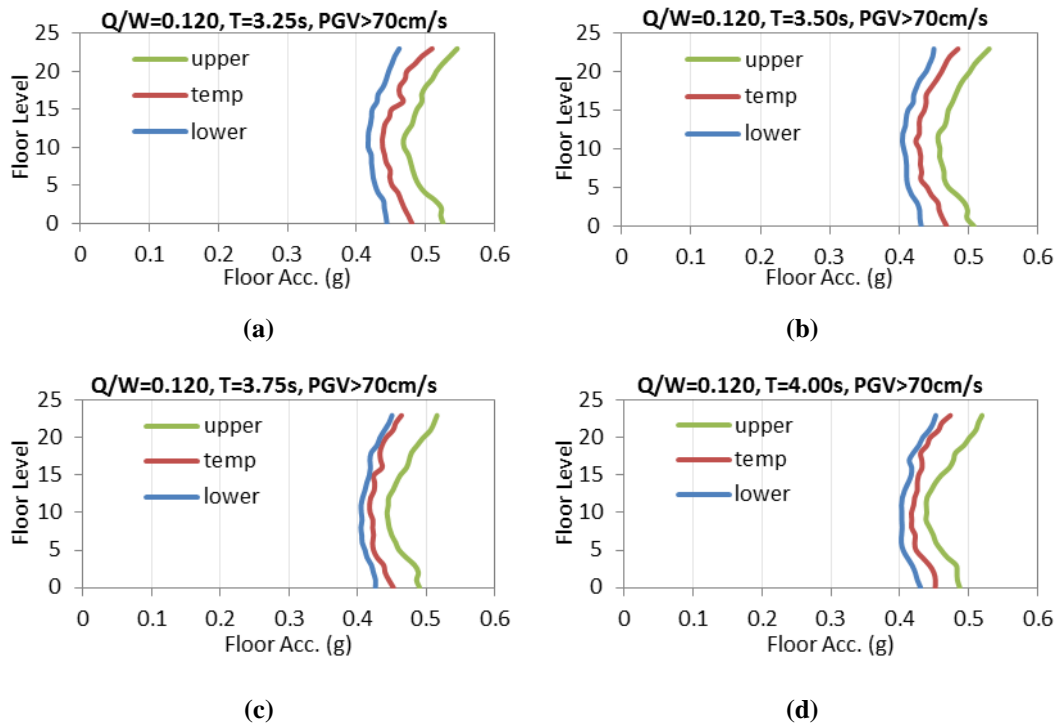**Figure 6.3** Average peak floor accelerations of 23 story reinforced concrete structures with same Q/W=0.090, PGV>70cm/s and different T: a)T=3.25s, b)T=3.50s, c)T=3.75s, d)T=4.00s
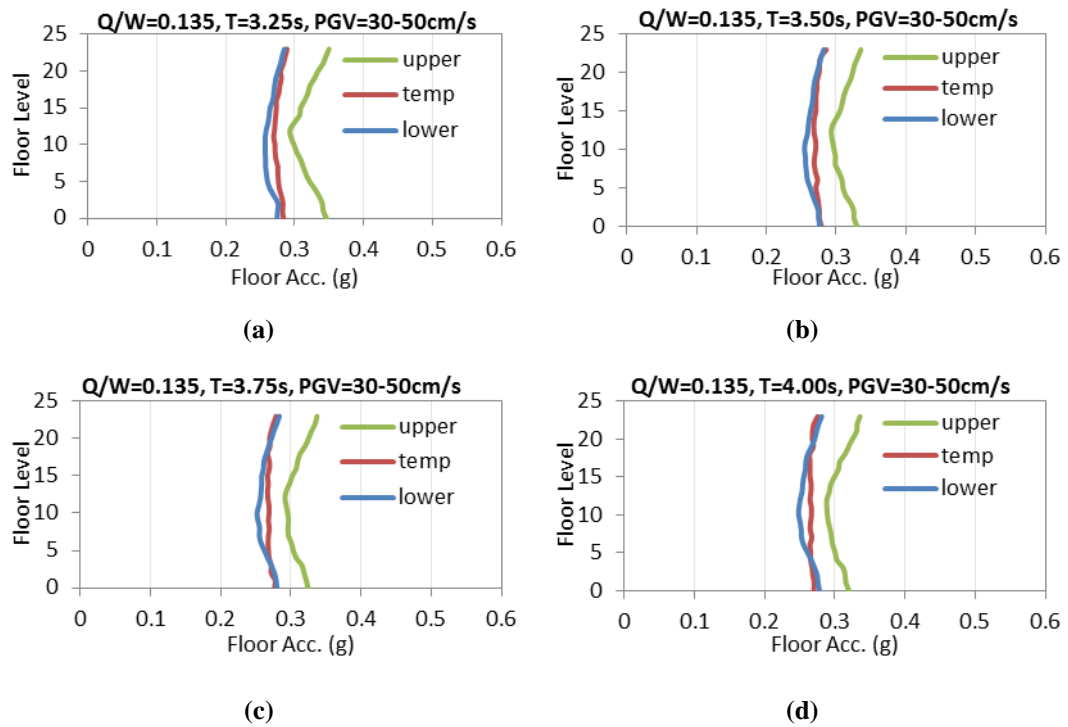

Figure 6.4 Average peak floor accelerations of 23 story reinforced concrete structures with same Q/W=0.105, PGV=30-50cm/s and different T: a)T=3.25s, b)T=3.50s, c)T=3.75s, d)T=4.00s
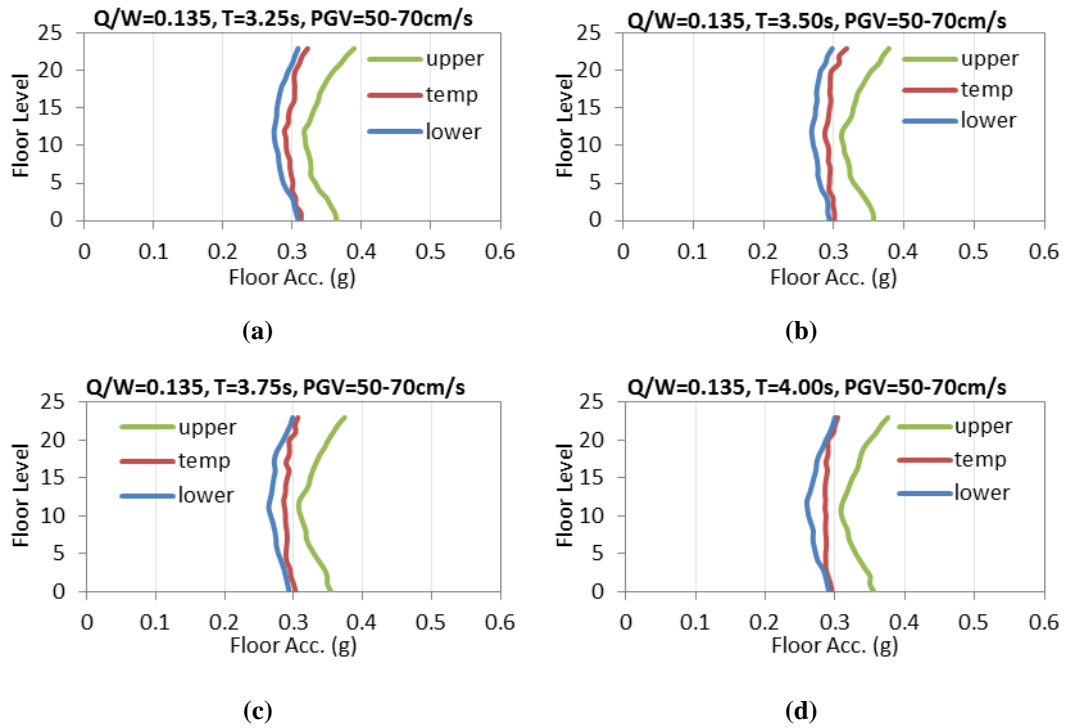
Figure 6.5 Average peak floor accelerations of 23 story reinforced concrete structures with same Q/W=0.105, PGV=50-70cm/s and different T: a)T=3.25s, b)T=3.50s, c)T=3.75s, d)T=4.00s

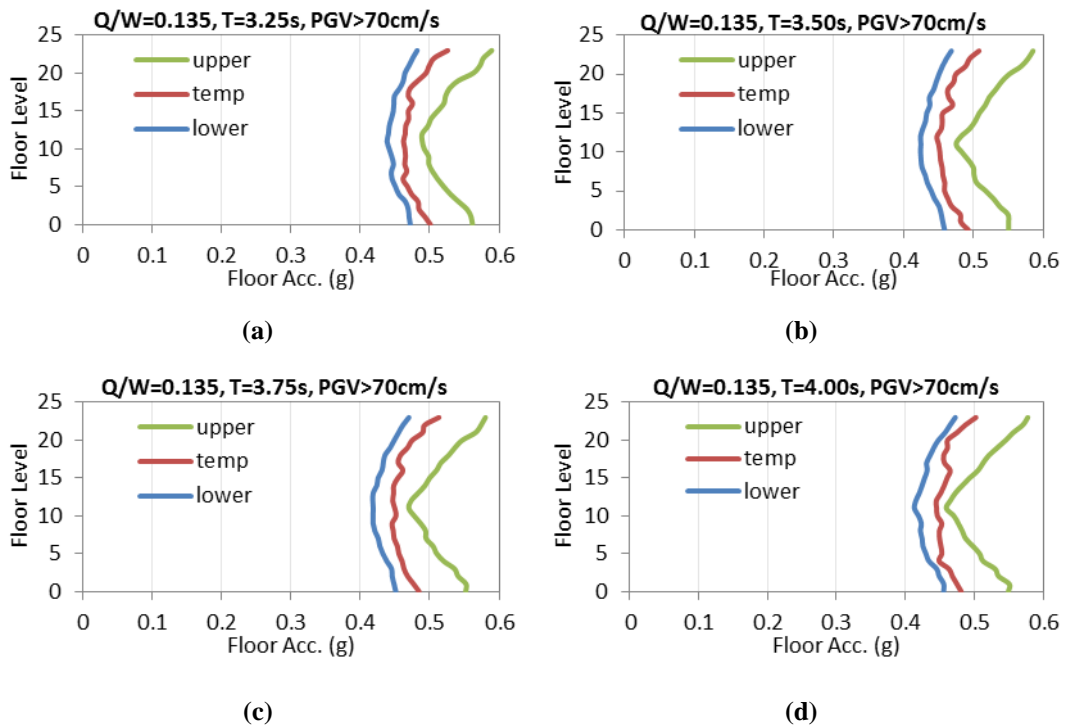**Figure 6.6** Average peak floor accelerations of 23 story reinforced concrete structures with same Q/W=0.105, PGV>70cm/s and different T: a)T=3.25s, b)T=3.50s, c)T=3.75s, d)T=4.00s

Figure 6.7 Average peak floor accelerations of 23 story reinforced concrete structures with same Q/W=0.120, PGV=30-50cm/s and different T: a)T=3.25s, b)T=3.50s, c)T=3.75s, d)T=4.00s

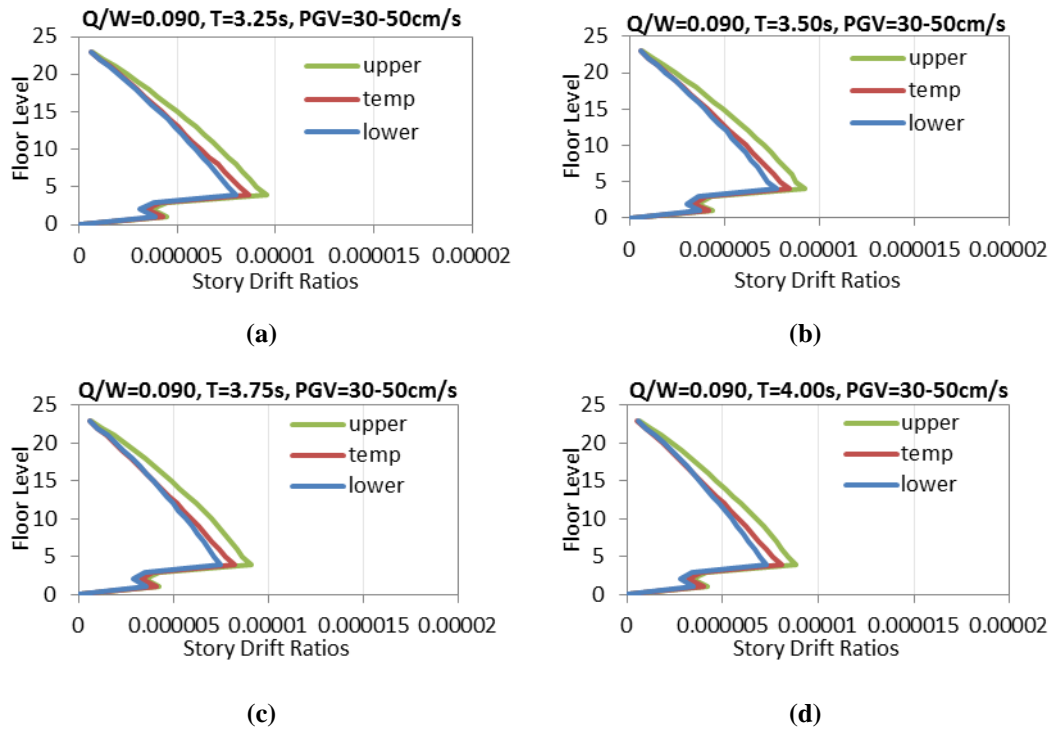**Figure 6.8** Average peak floor accelerations of 23 story reinforced concrete structures with same Q/W=0.120, PGV=50-70cm/s and different T: a)T=3.25s, b)T=3.50s, c)T=3.75s, d)T=4.00s

Figure 6.9 Average peak floor accelerations of 23 story reinforced concrete structures with same Q/W=0.120, PGV>70cm/s and different T: a)T=3.25s, b)T=3.50s, c)T=3.75s, d)T=4.00s

Figure 6.10 Average peak floor accelerations of 23 story reinforced concrete structures with same Q/W=0.135, PGV=30-50cm/s and different T: a)T=3.25s, b)T=3.50s, c)T=3.75s, d)T=4.00s
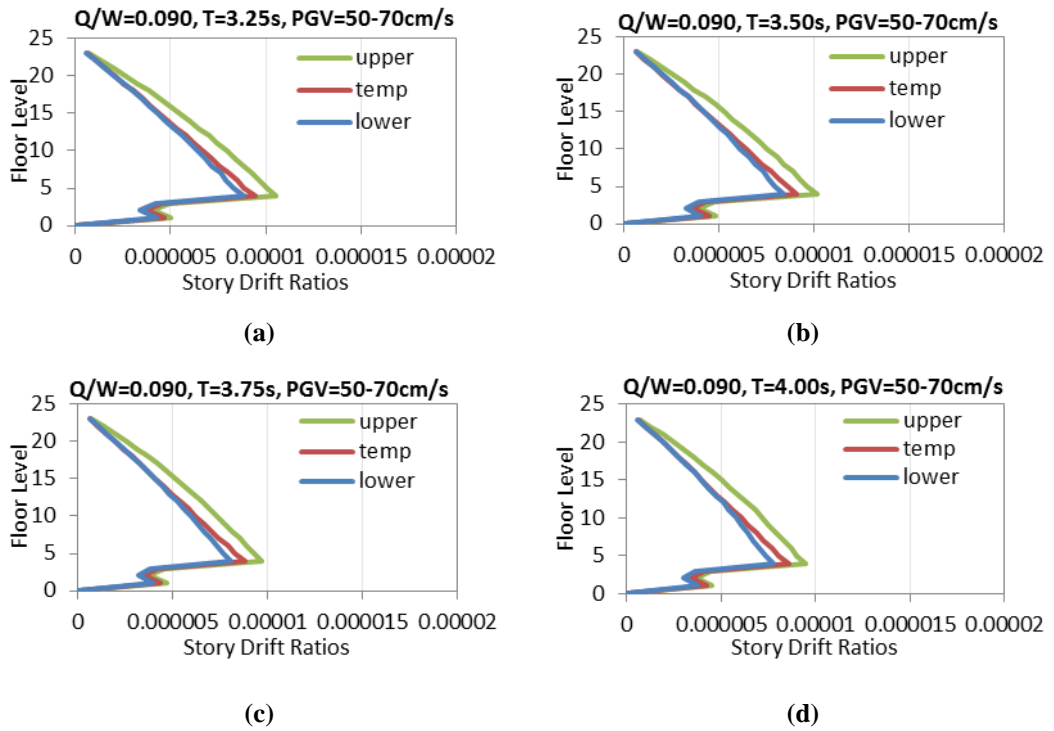
Figure 6.11 Average peak floor accelerations of 23 story reinforced concrete structures with same Q/W=0.135, PGV=50-70cm/s and different T: a)T=3.25s, b)T=3.50s, c)T=3.75s, d) T=4.00s

Figure 6.12 Average peak floor accelerations of 23 story reinforced concrete structures with same Q/W=0.135, PGV>70cm/s and different T: a)T=3.25s, b)T=3.50s, c)T=3.75s, d)T=4.00s

Figure 6.13 Average peak drift ratios of 23 story reinforced concrete structures with same Q/W=0.090, PGV=30-50cm/s and different T: a) T=3.25s, b) T=3.50s, c) T=3.75s, d) T=4.00s

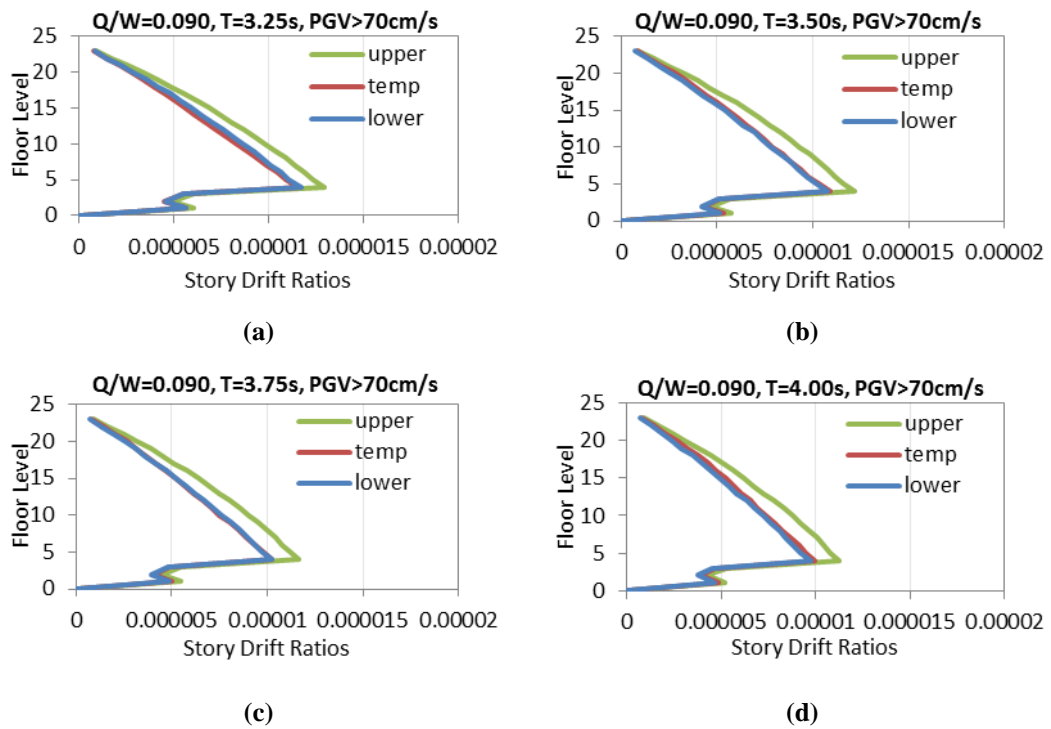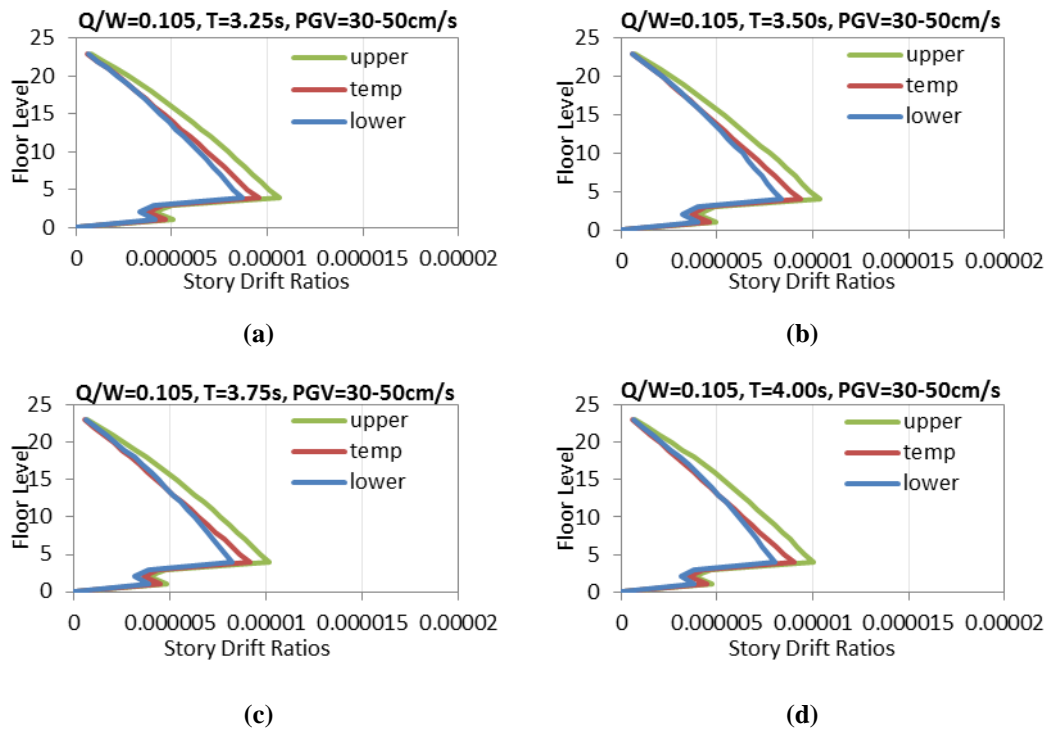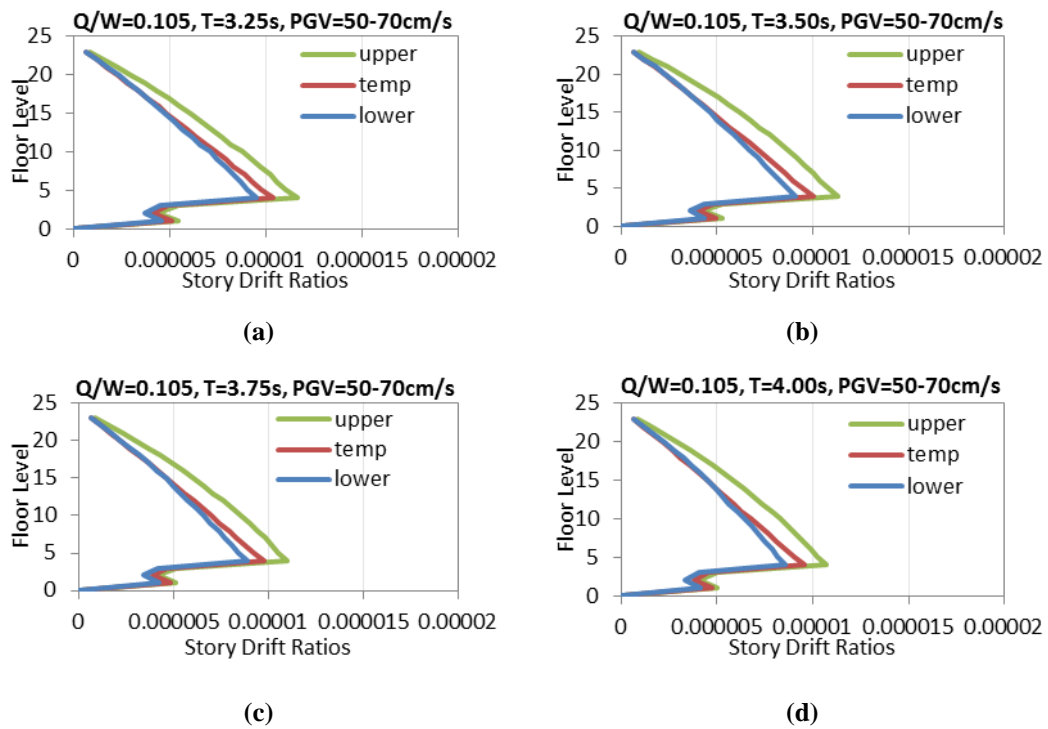**Figure 6.14** Average peak drift ratios of 23 story reinforced concrete structures with same Q/W=0.090, PGV=50-70cm/s and different T: a) T=3.25s, b) T=3.50s, c) T=3.75s, d) T=4.00s

Figure 6.15 Average peak drift ratios of 23 story reinforced concrete structures with same Q/W=0.090, PGV>70cm/s and different T: a) T=3.25s, b) T=3.50s, c) T=3.75s, d) T=4.00s

Figure 6.16 Average peak drift ratios of 23 story reinforced concrete structures with same Q/W=0.105, PGV=30-50cm/s and different T: a) T=3.25s, b) T=3.50s, c) T=3.75s, d) T=4.00s

Figure 6.17 Average peak drift ratios of 23 story reinforced concrete structures with same Q/W=0.105, PGV=50-70cm/s and different T: a) T=3.25s, b) T=3.50s, c) T=3.75s, d) T=4.00s
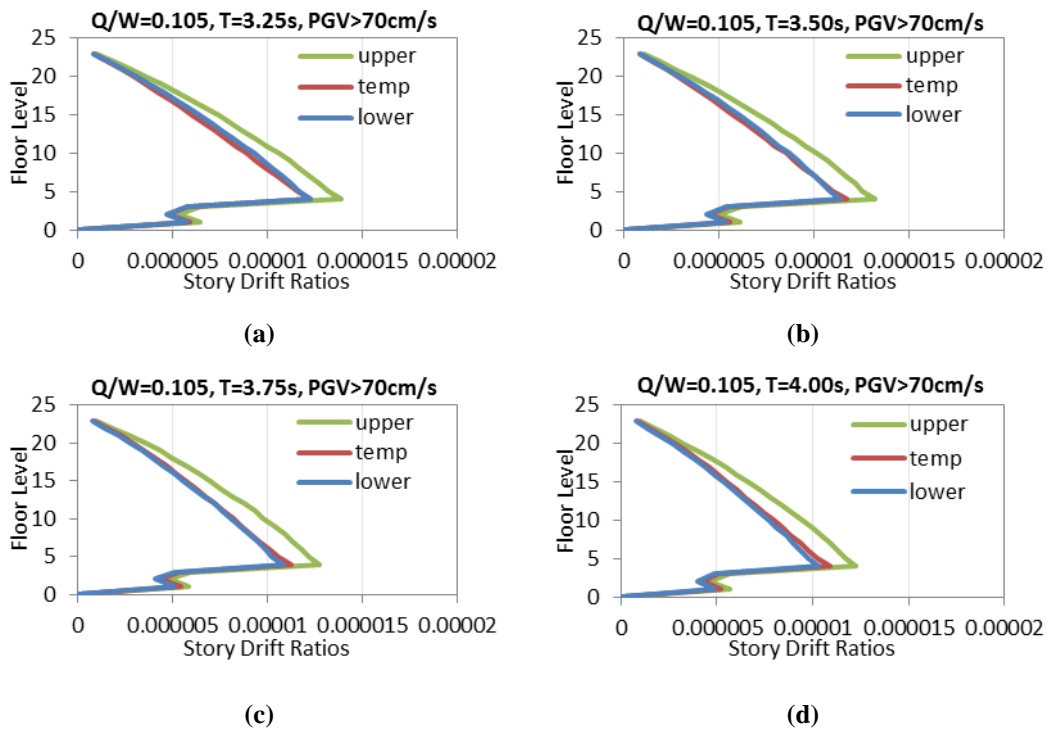

Figure 6.18 Average peak drift ratios of 23 story reinforced concrete structures with same Q/W=0.105, PGV>70cm/s and different T: a) T=3.25s, b) T=3.50s, c) T=3.75s, d) T=4.00s

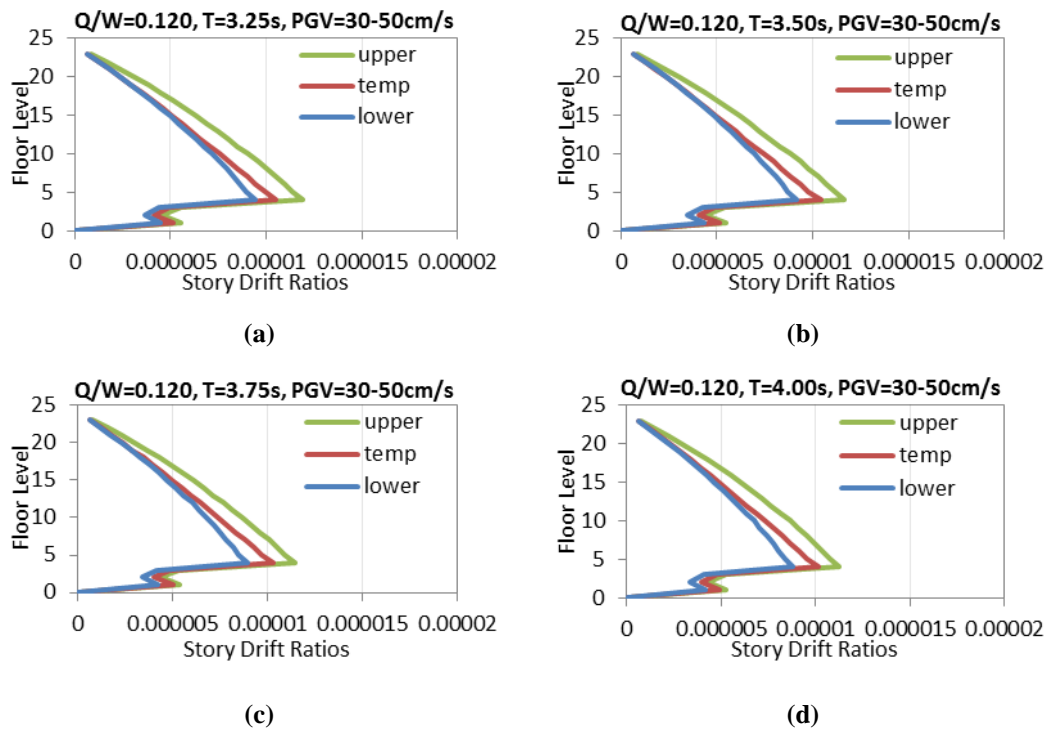**Figure 6.19** Average peak drift ratios of 23 story reinforced concrete structures with same Q/W=0.120, PGV=30-50cm/s and different T: a) T=3.25s, b) T=3.50s, c) T=3.75s, d) T=4.00s
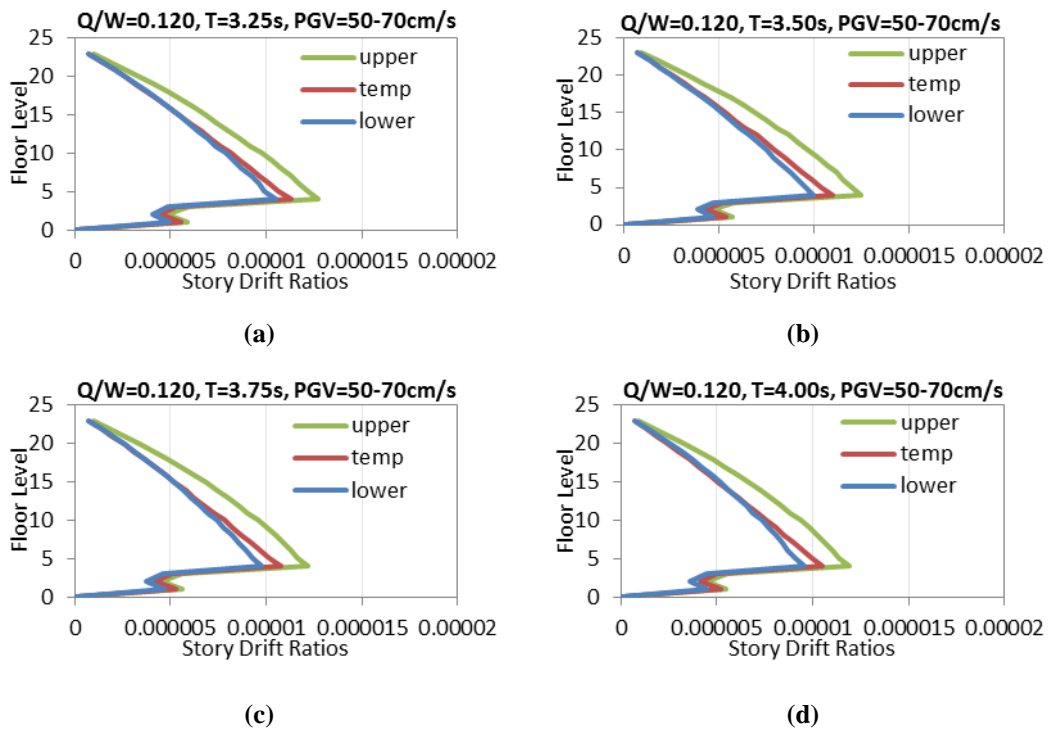

Figure 6.20 Average peak drift ratios of 23 story reinforced concrete structures with same Q/W=0.120, PGV=50-70cm/s and different T: a) T=3.25s, b) T=3.50s, c) T=3.75s, d) T=4.00s
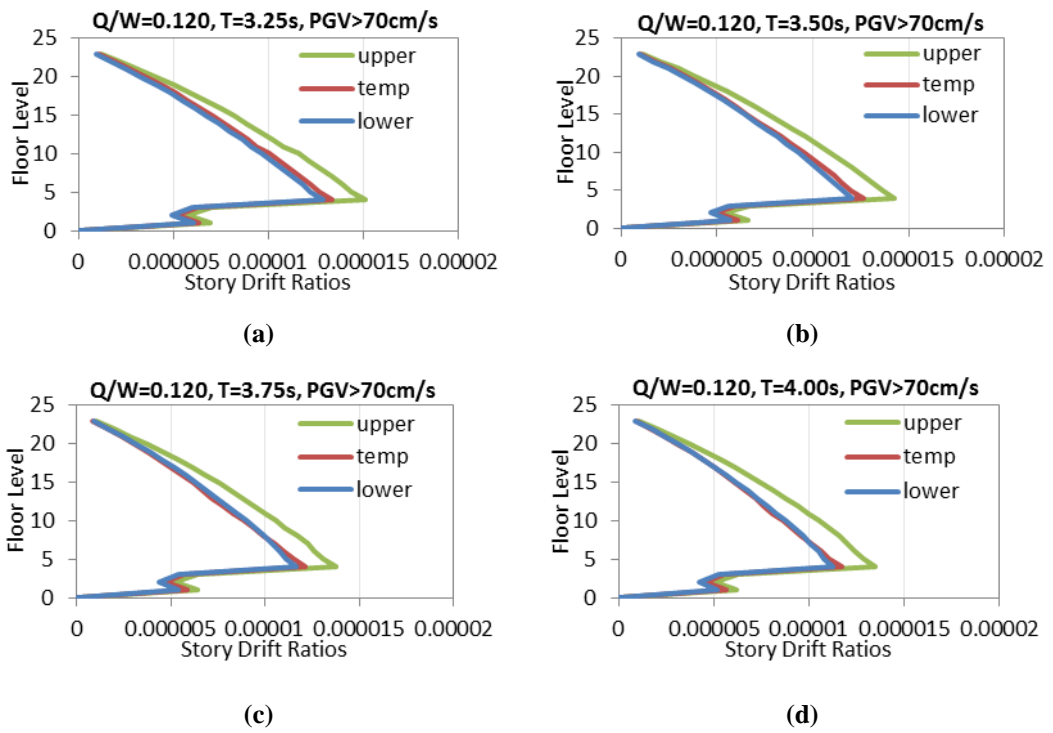
Figure 6.21 Average peak drift ratios of 23 story reinforced concrete structures with same Q/W=0.120, PGV>70cm/s and different T: a) T=3.25s, b) T=3.50s, c) T=3.75s, d) T=4.00s

Figure 6.22 Average peak drift ratios of 23 story reinforced concrete structures with same Q/W=0.135, PGV=30-50cm/s and different T: a) T=3.25s, b) T=3.50s, c) T=3.75s, d) T=4.00s

Figure 6.23 Average peak drift ratios of 23 story reinforced concrete structures with same Q/W=0.135, PGV=50-70cm/s and different T: a) T=3.25s, b) T=3.50s, c) T=3.75s, d) T=4.00s
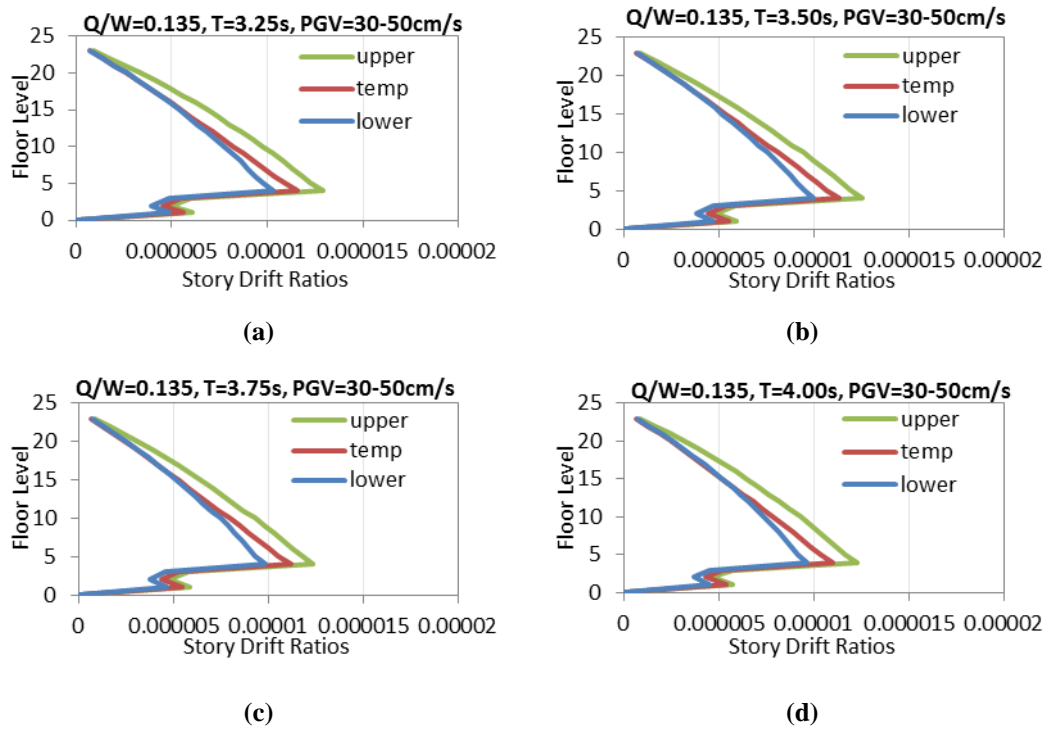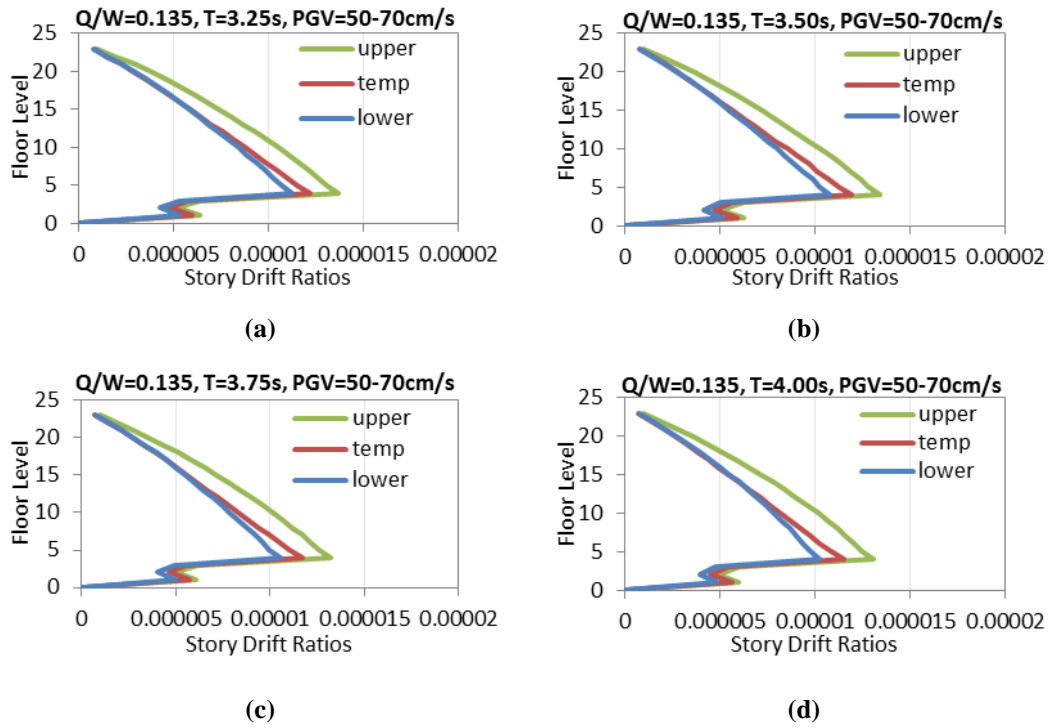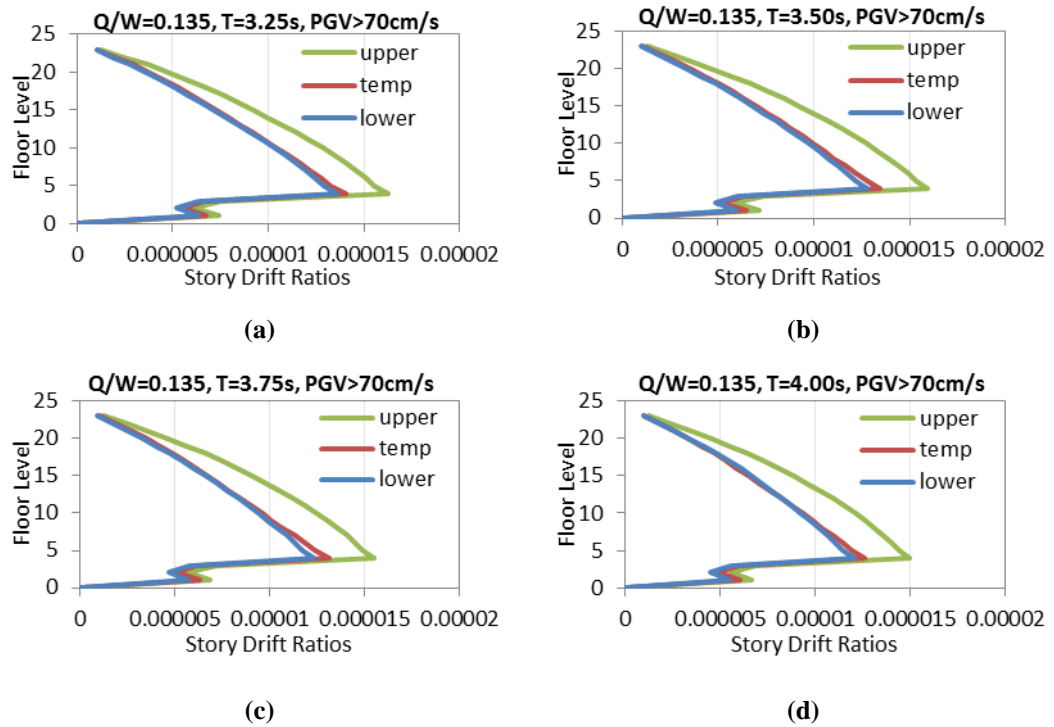

Figure 6.24 Average peak drift ratios of 23 story reinforced concrete structures with same Q/W=0.135, PGV>70cm/s and different T: a) T=3.25s, b) T=3.50s, c) T=3.75s, d) T=4.00s

Figure 6.25 Average peak floor accelerations of 3 story steel structures with same Q/W=0.090, PGV=30-50cm/s and different T: a)T=2.25s, b)T=2.50s, c)T=2.75s, d) T=3.00s

Figure 6.26 Average peak floor accelerations of 3 story steel structures with same Q/W=0.090, PGV=50-70cm/s and different T: a)T=2.25s, b)T=2.50s, c)T=2.75s, d) T=3.00s

Figure 6.27 Average peak floor accelerations of 3 story steel structures with same Q/W=0.090, PGV>70cm/s and different T: a)T=2.25s, b)T=2.50s, c)T=2.75s, d) T=3.00s

Figure 6.28 Average peak floor accelerations of 3 story steel structures with same Q/W=0.105, PGV=30-50cm/s and different T: a)T=2.25s, b)T=2.50s, c)T=2.75s, d) T=3.00s

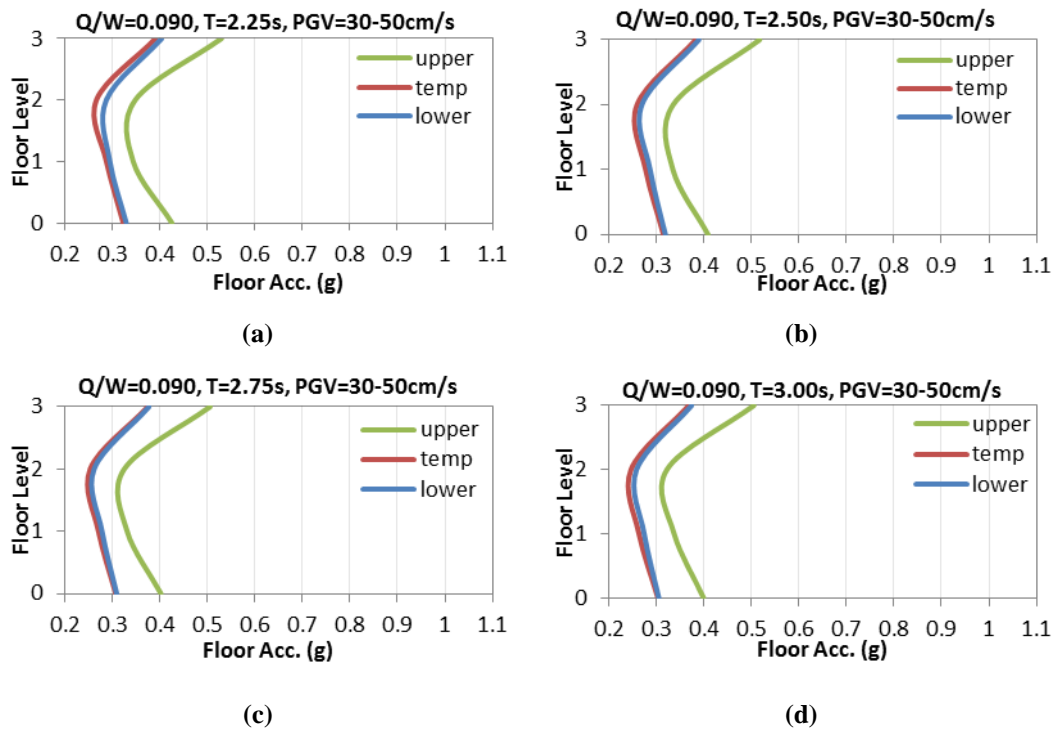**Figure 6.29** Average peak floor accelerations of 3 story steel structures with same Q/W=0.105, PGV=50-70cm/s and different T: a)T=2.25s, b)T=2.50s, c)T=2.75s, d) T=3.00s

Figure 6.30 Average peak floor accelerations of 3 story steel structures with same Q/W=0.105, PGV>70cm/s and different T: a)T=2.25s, b)T=2.50s, c)T=2.75s, d) T=3.00s
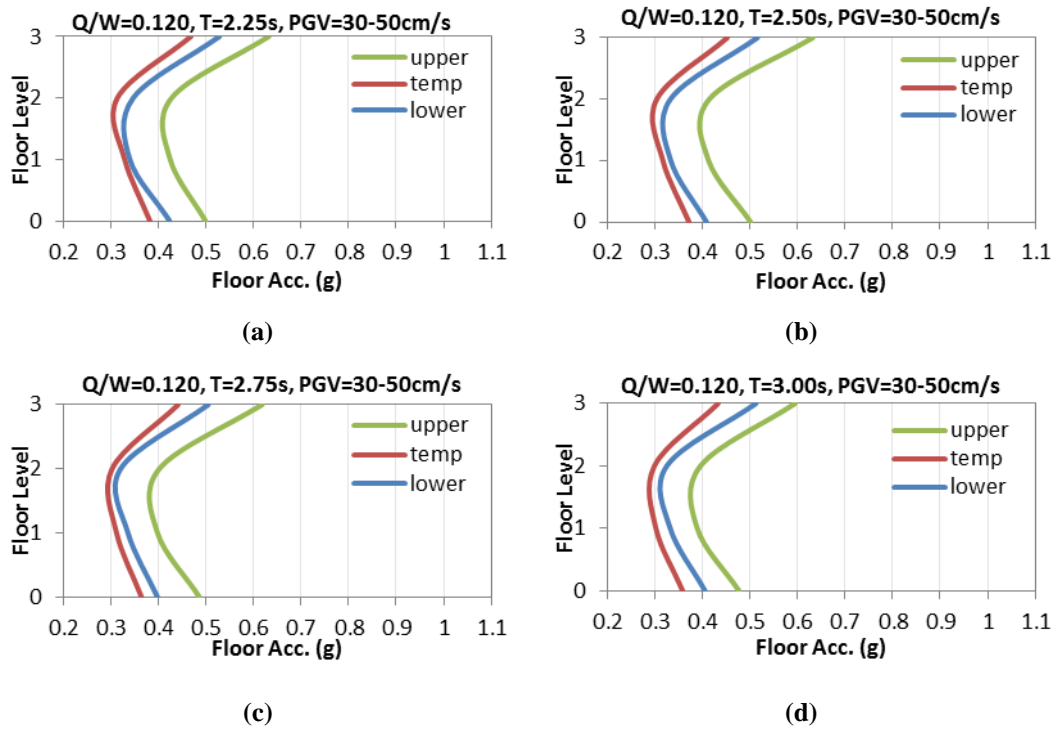
Figure 6.31 Average peak floor accelerations of 3 story steel structures with same Q/W=0.120, PGV=30-50cm/s and different T: a)T=2.25s, b)T=2.50s, c)T=2.75s, d) T=3.00s
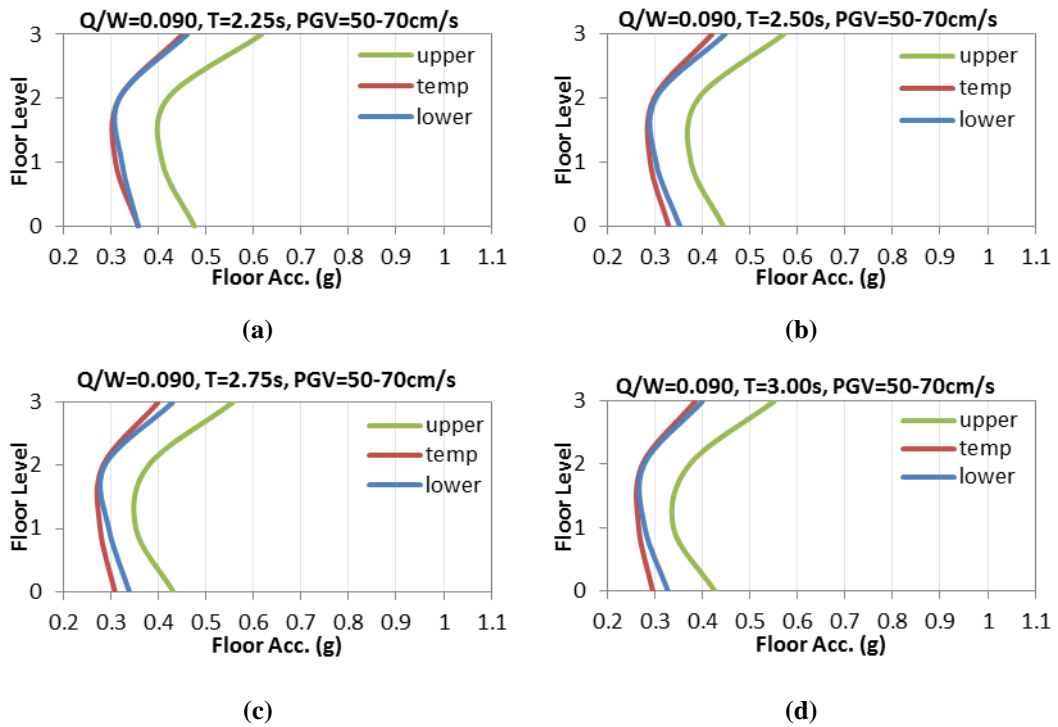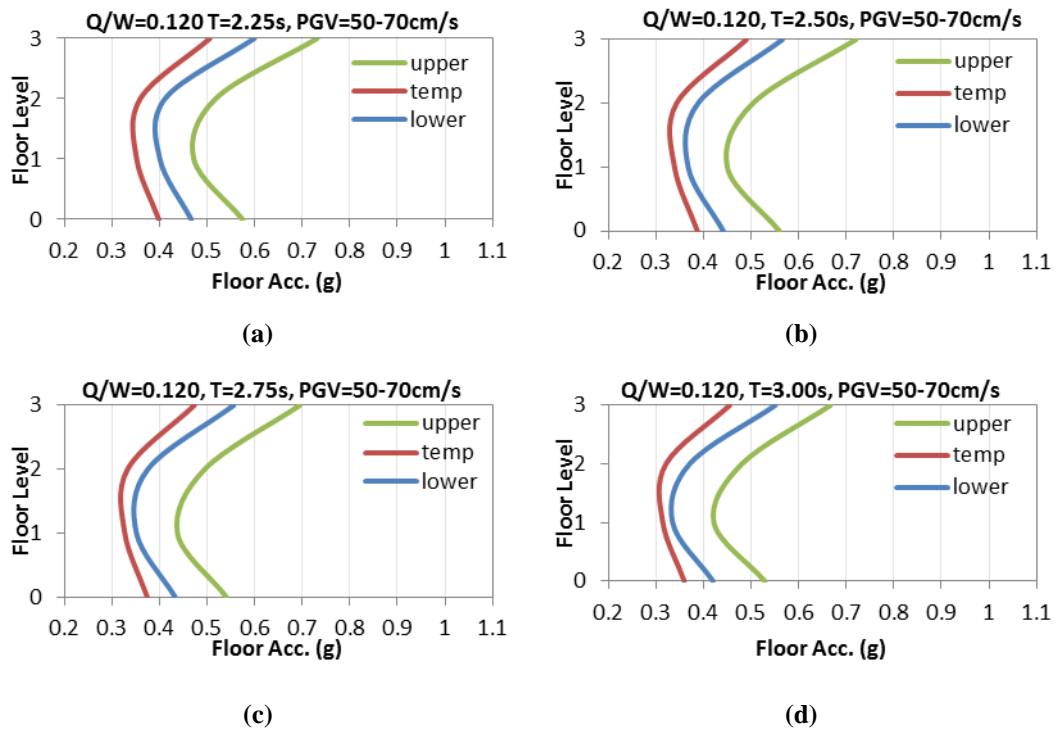

Figure 6.32 Average peak floor accelerations of 3 story steel structures with same Q/W=0.120, PGV=50-70cm/s and different T: a)T=2.25s, b)T=2.50s, c)T=2.75s, d) T=3.00s
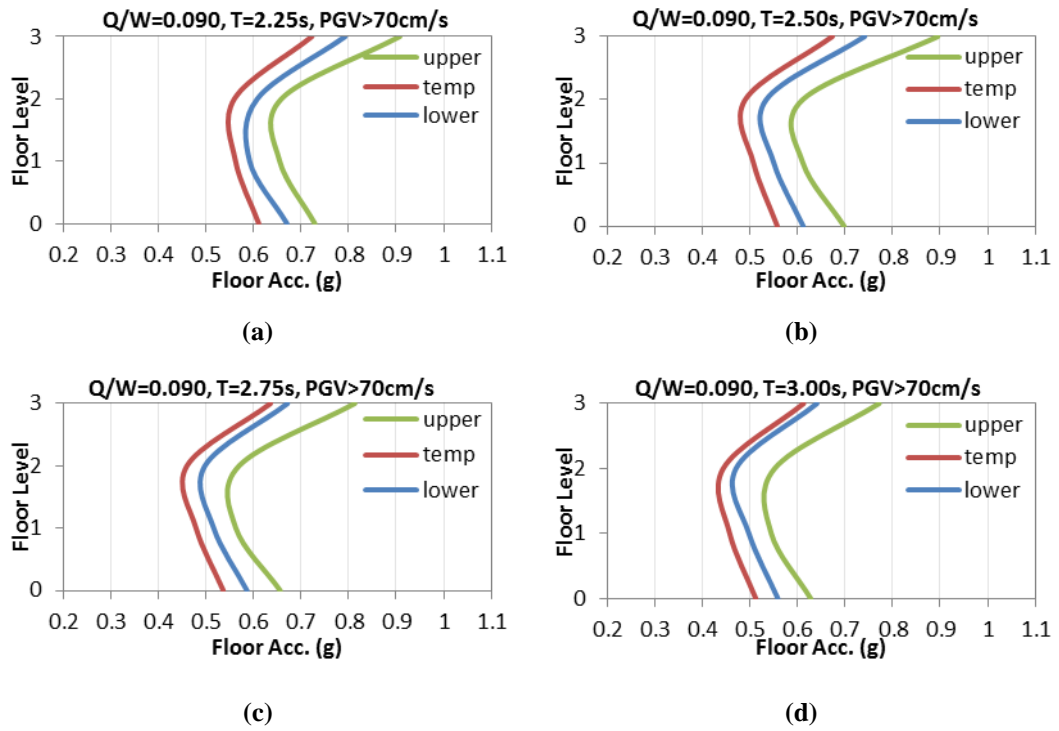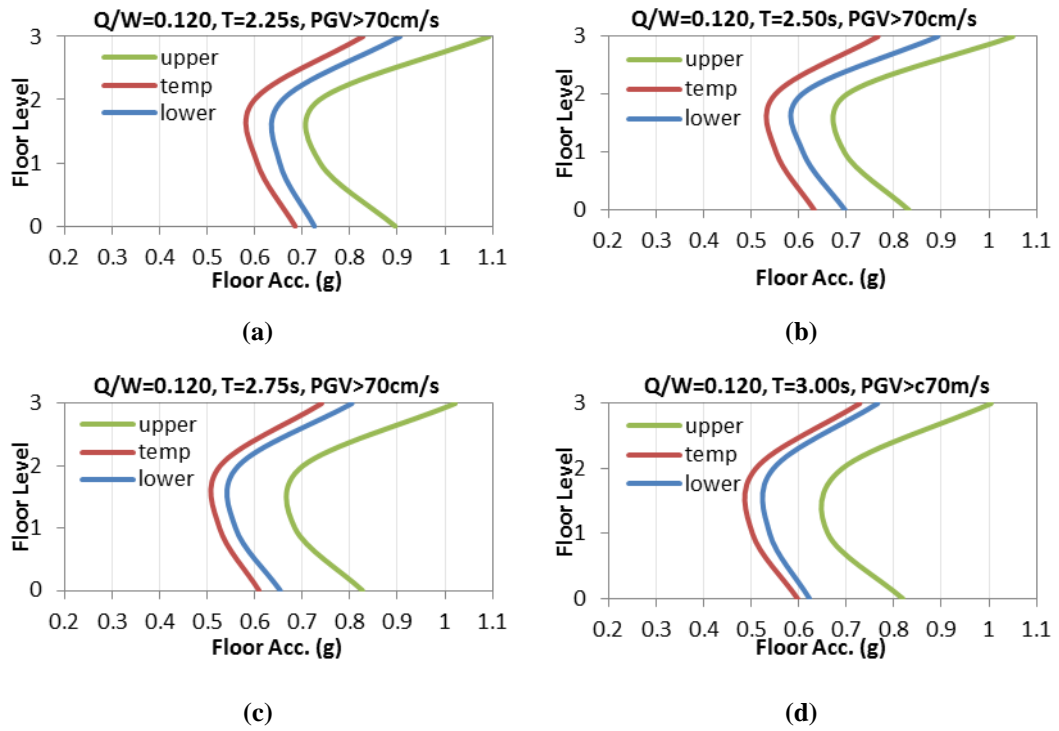
Figure 6.33 Average peak floor accelerations of 3 story steel structures with same Q/W=0.120, PGV>70cm/s and different T: a)T=2.25s, b)T=2.50s, c)T=2.75s, d) T=3.00s

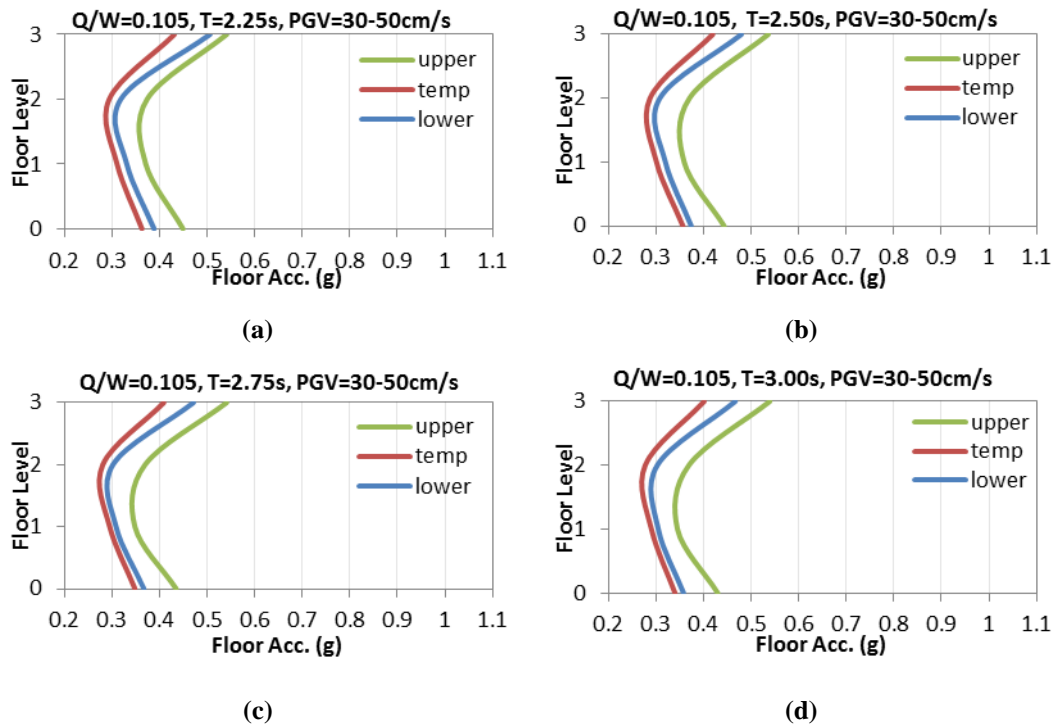**Figure 6.34** Average peak floor accelerations of 3 story steel structures with same Q/W=0.135, PGV=30-50cm/s and different T: a)T=2.25s, b)T=2.50s, c)T=2.75s, d) T=3.00s
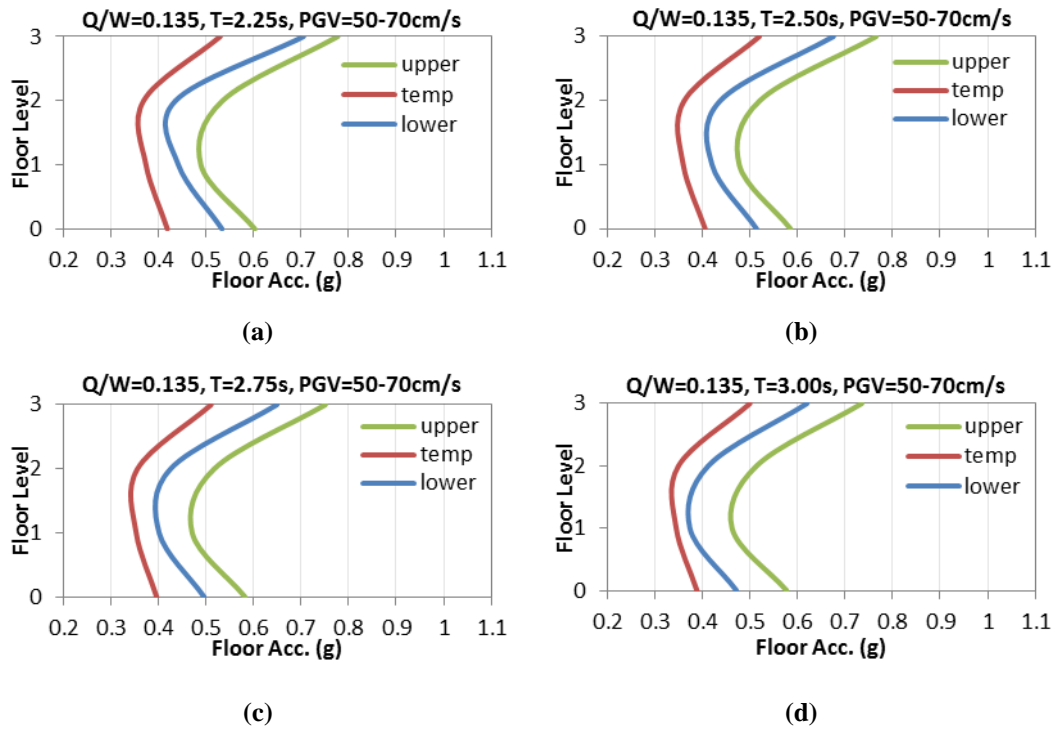
Figure 6.35 Average peak floor accelerations of 3 story steel structures with same Q/W=0.135, PGV=50-70cm/s and different T: a)T=2.25s, b)T=2.50s, c)T=2.75s, d) T=3.00s
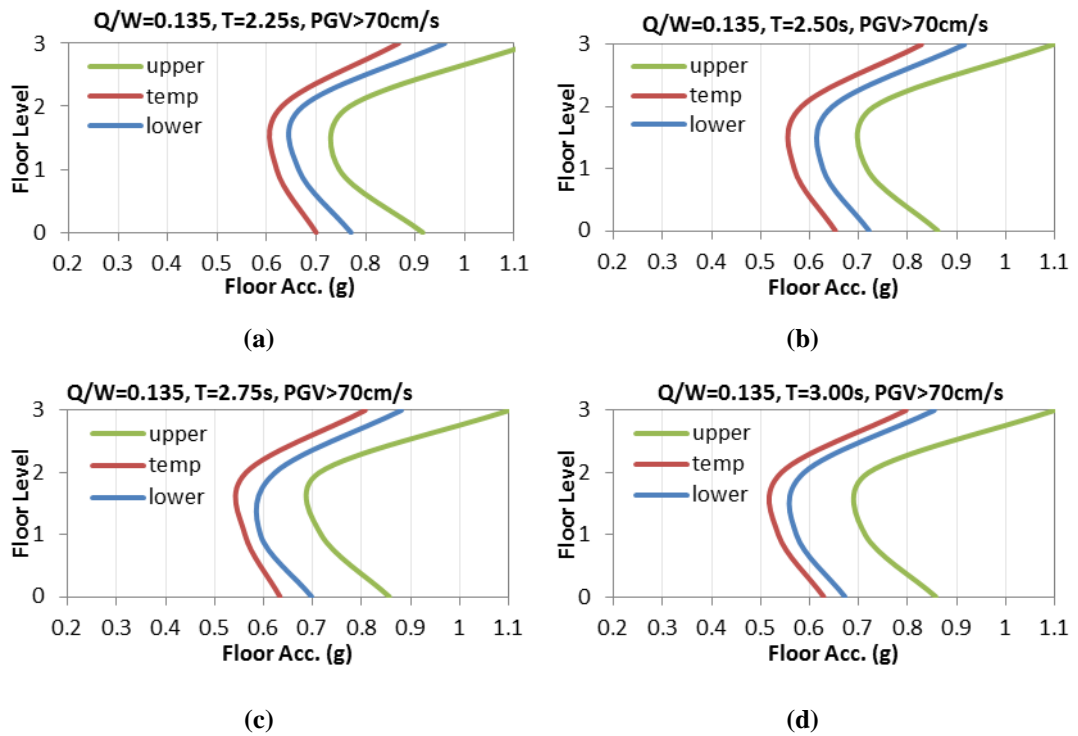
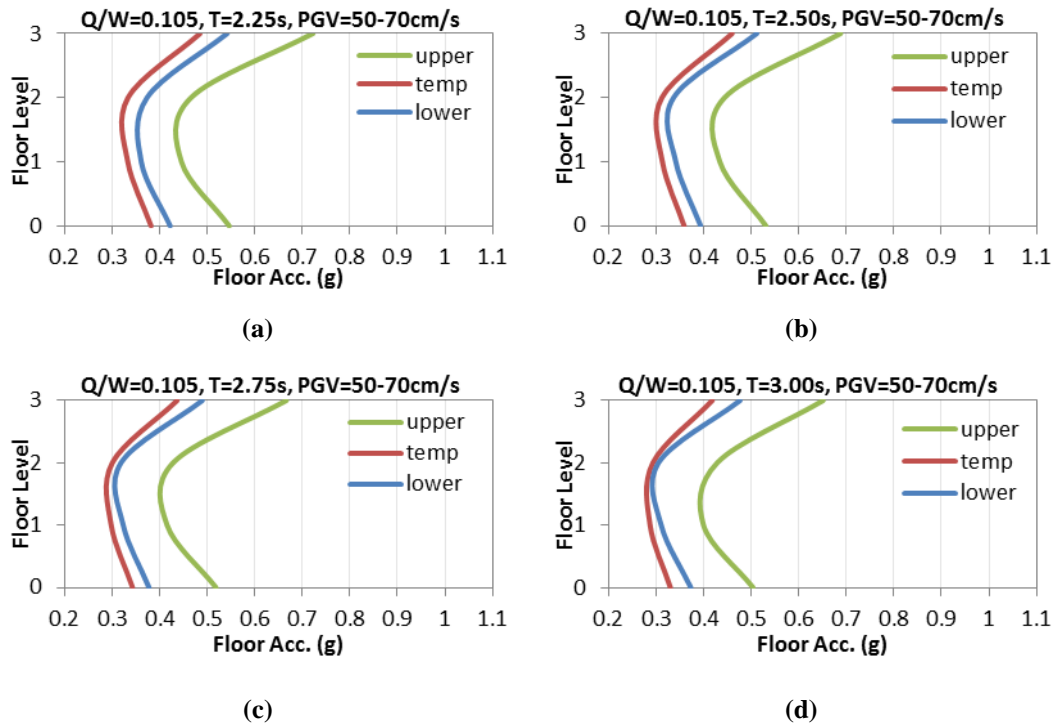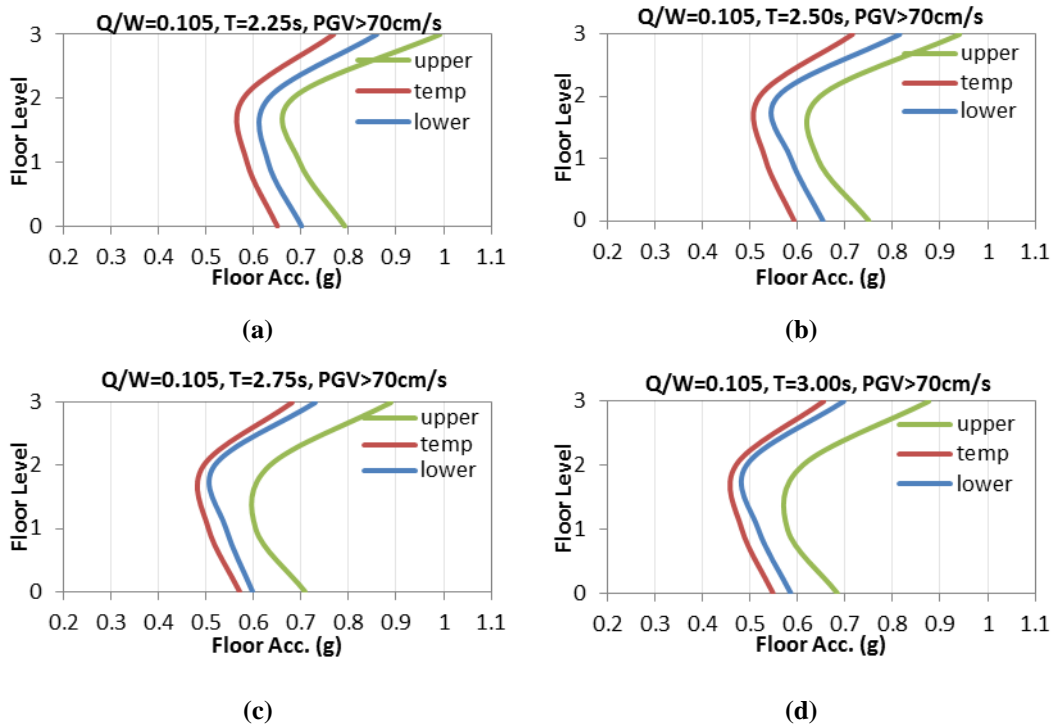**Figure 6.36** Average peak floor accelerations of 3 story steel structures with same Q/W=0.135, PGV>70cm/s and different T: a)T=2.25s, b)T=2.50s, c)T=2.75s, d) T=3.00s

Figure 6.37 Average peak story drift ratios of 3 story steel structures with same Q/W=0.090, PGV=30-50cm/s and different T: a)T=2.25s, b)T=2.50s, c)T=2.75s, d) T=3.00s

Figure 6.38 Average peak story drift ratios of 3 story steel structures with same Q/W=0.090, PGV=50-70cm/s and different T: a)T=2.25s, b)T=2.50s, c)T=2.75s, d) T=3.00s

Figure 6.39 Average peak story drift ratios of 3 story steel structures with same Q/W=0.090, PGV>70cm/s and different T: a)T=2.25s, b)T=2.50s, c)T=2.75s, d) T=3.00s

Figure 6.40 Average peak story drift ratios of 3 story steel structures with same Q/W=0.105, PGV=30-50cm/s and different T: a)T=2.25s, b)T=2.50s, c)T=2.75s, d) T=3.00s

Figure 6.41 Average peak story drift ratios of 3 story steel structures with same Q/W=0.105, PGV=50-70cm/s and different T: a)T=2.25s, b)T=2.50s, c)T=2.75s, d) T=3.00s

Figure 6.42 Average peak story drift ratios of 3 story steel structures with same Q/W=0.105, PGV>70cm/s and different T: a)T=2.25s, b)T=2.50s, c)T=2.75s, d) T=3.00s

Figure 6.43 Average peak story drift ratios of 3 story steel structures with same Q/W=0.120, PGV=30-50cm/s and different T: a)T=2.25s, b)T=2.50s, c)T=2.75s, d) T=3.00s
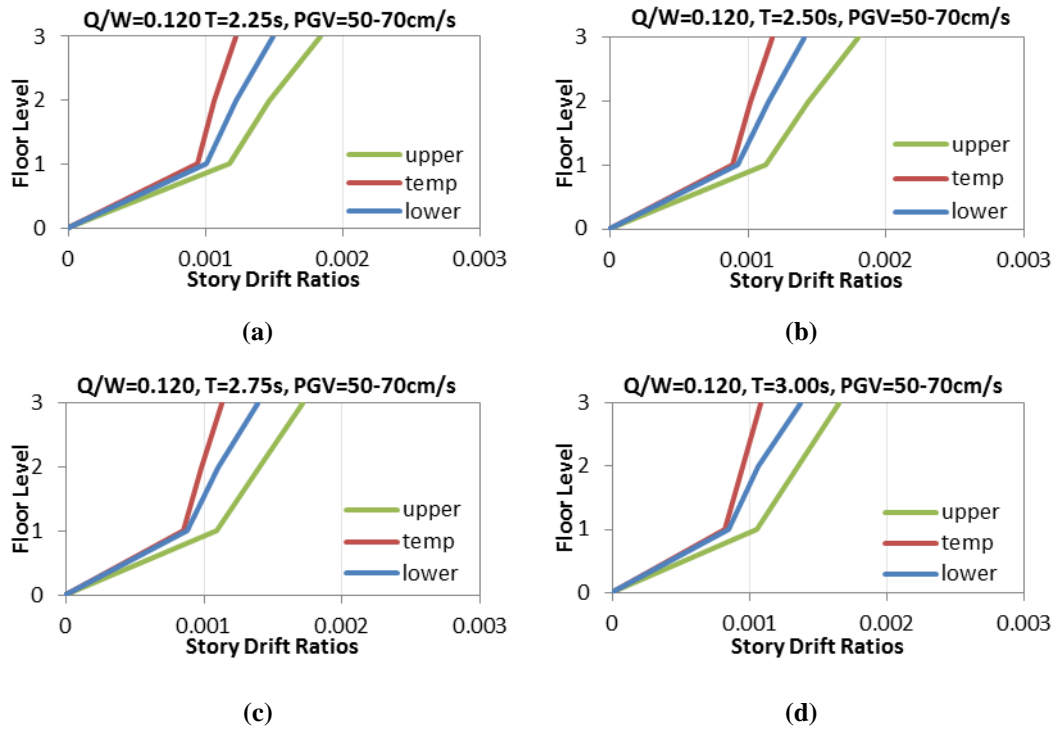
Figure 6.44 Average peak story drift ratios of 3 story steel structures with same Q/W=0.120, PGV=50-70cm/s and different T: a)T=2.25s, b)T=2.50s, c)T=2.75s, d) T=3.00s
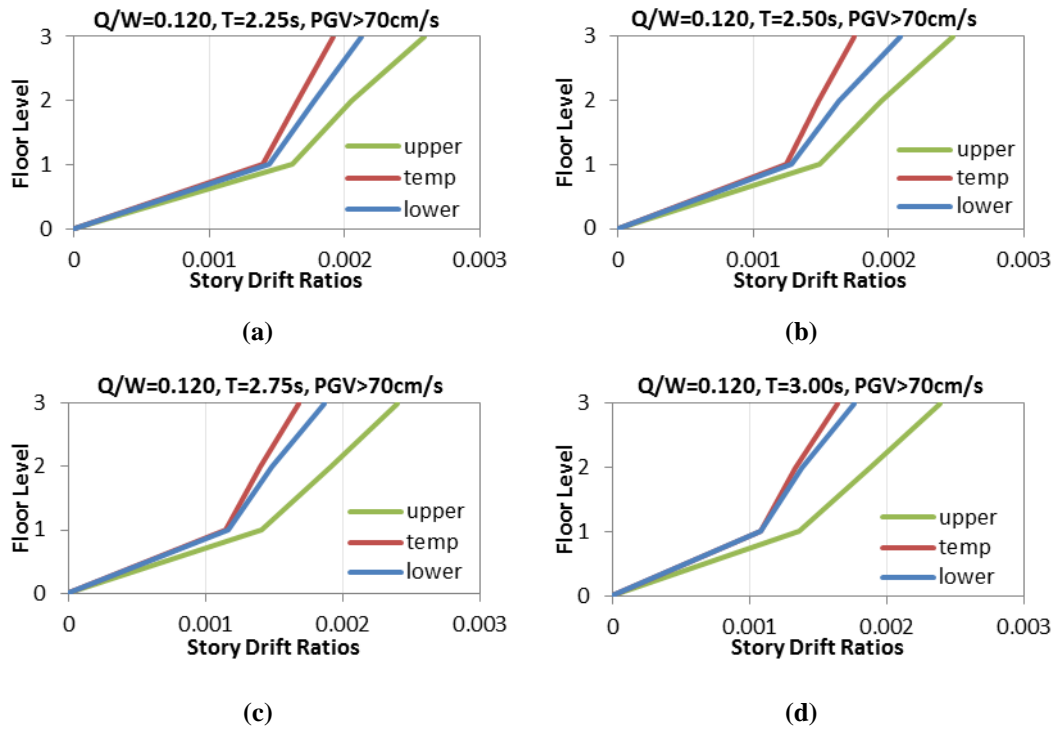
Figure 6.45 Average peak story drift ratios of 3 story steel structures with same Q/W=0.120, PGV>70cm/s and different T: a)T=2.25s, b)T=2.50s, c)T=2.75s, d) T=3.00s
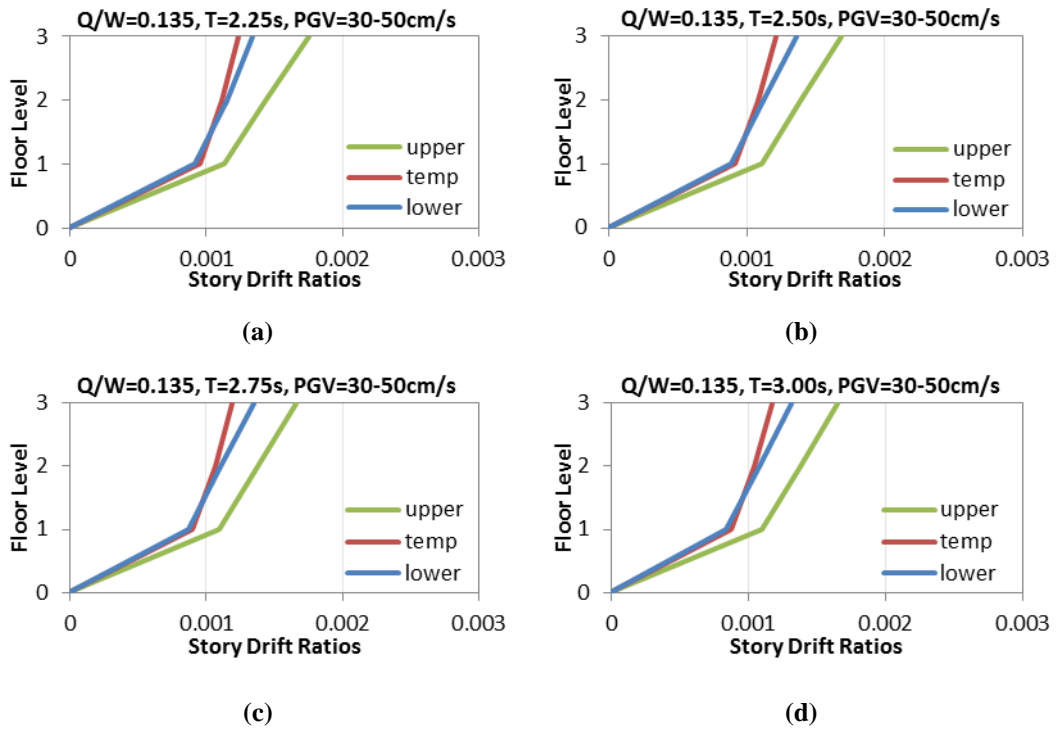
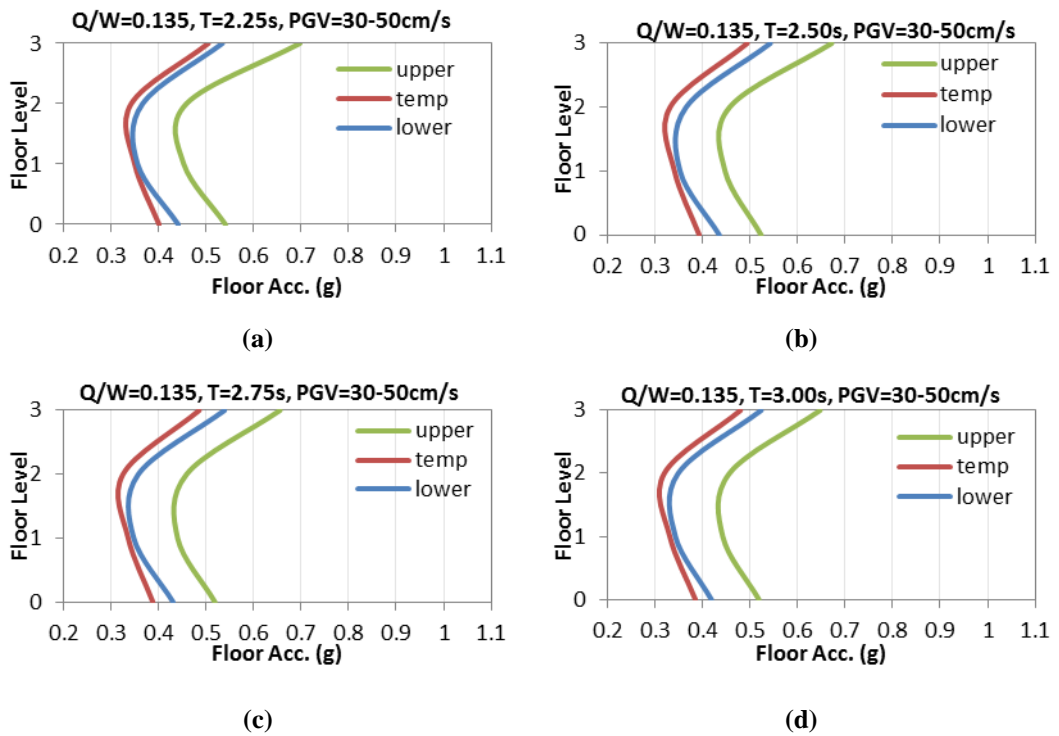**Figure 6.46** Average peak story drift ratios of 3 story steel structures with same Q/W=0.135, PGV=30-50cm/s and different T: a)T=2.25s, b)T=2.50s, c)T=2.75s, d) T=3.00s
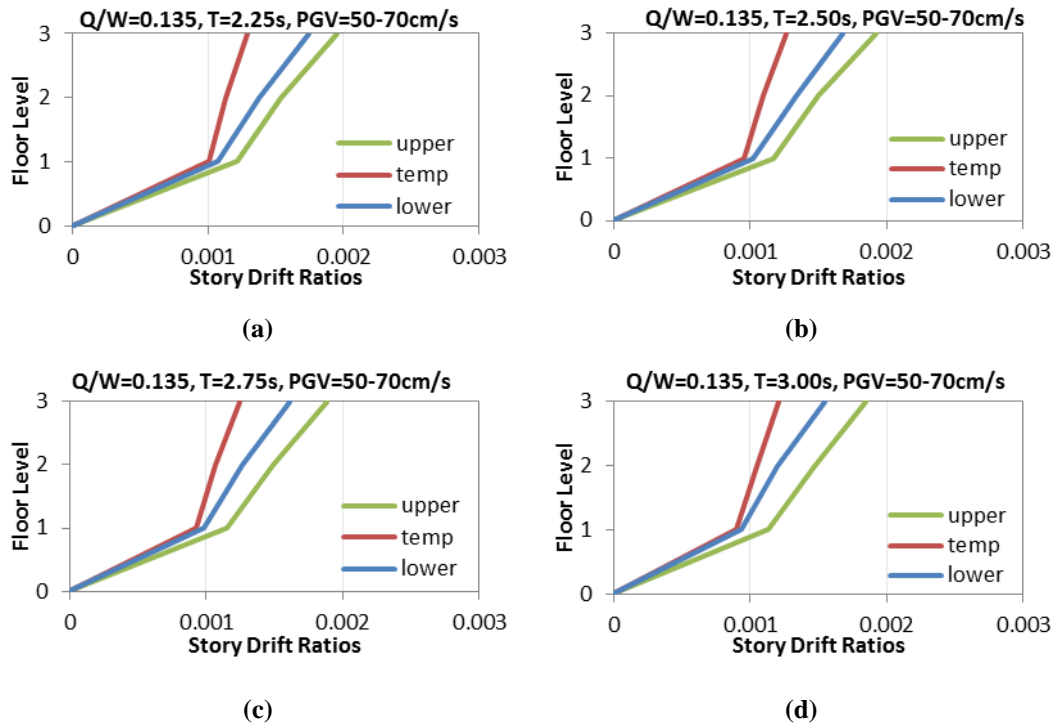
Figure 6.47 Average peak story drift ratios of 3 story steel structures with same Q/W=0.135, PGV=50-70cm/s and different T: a)T=2.25s, b)T=2.50s, c)T=2.75s, d) T=3.00s

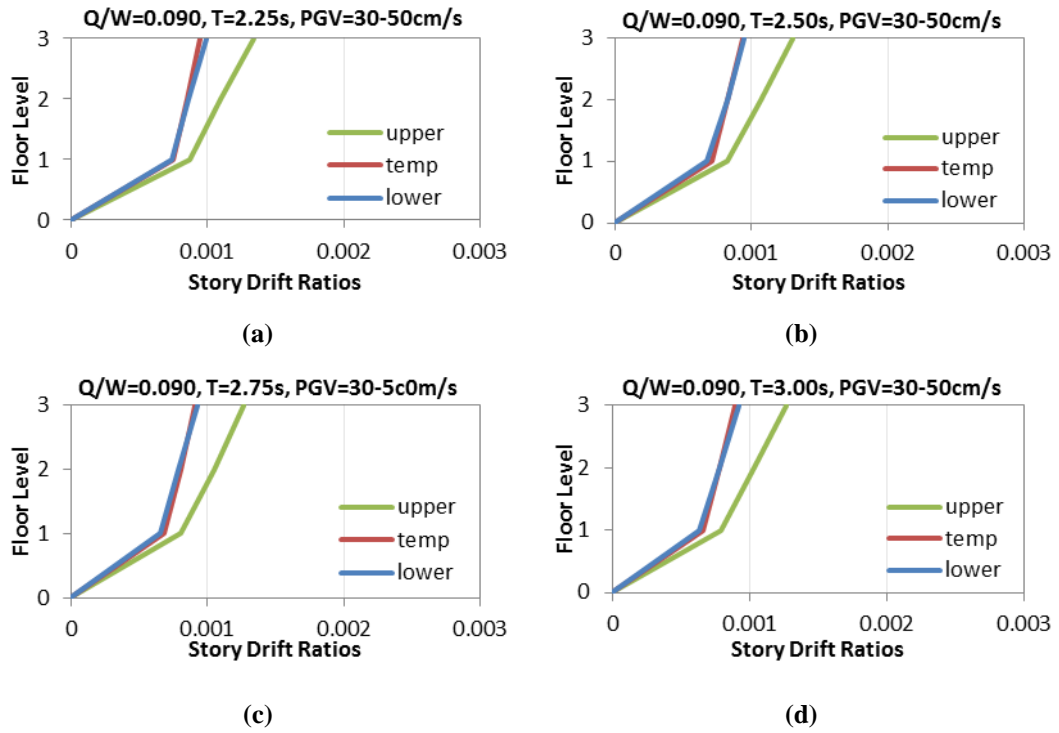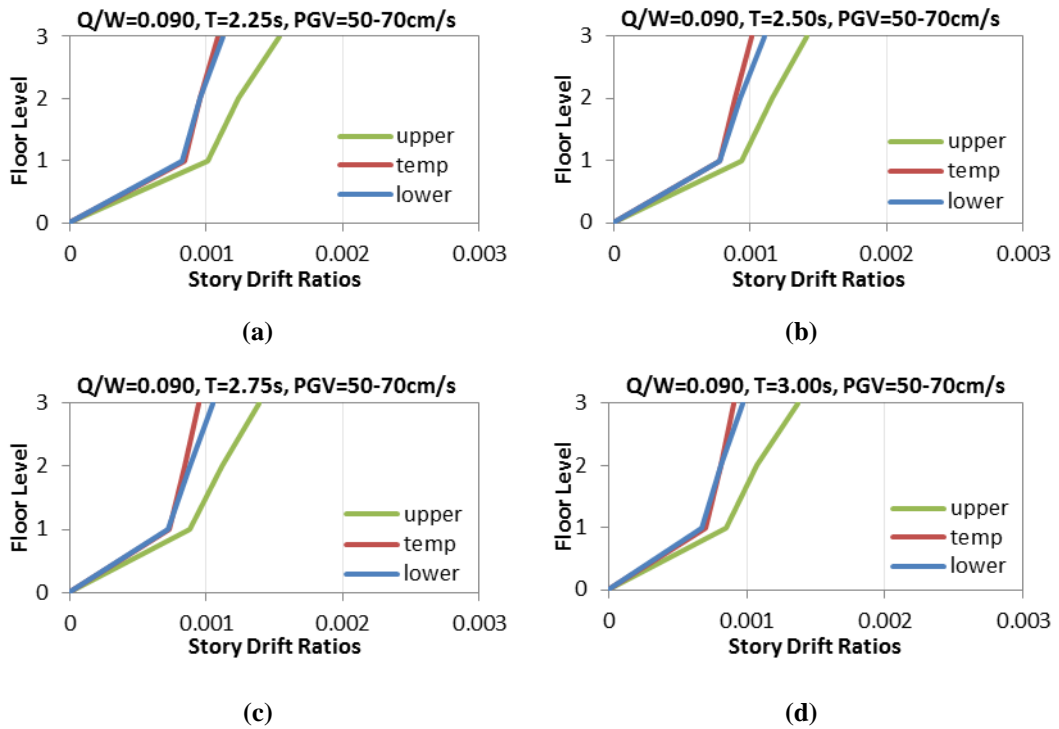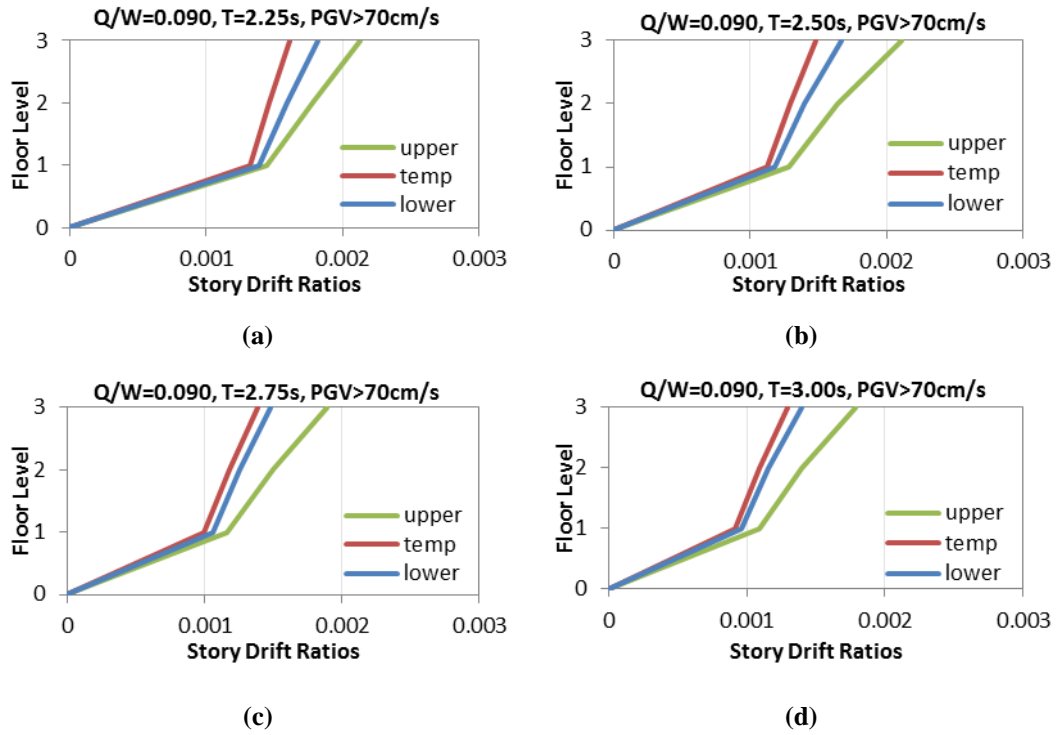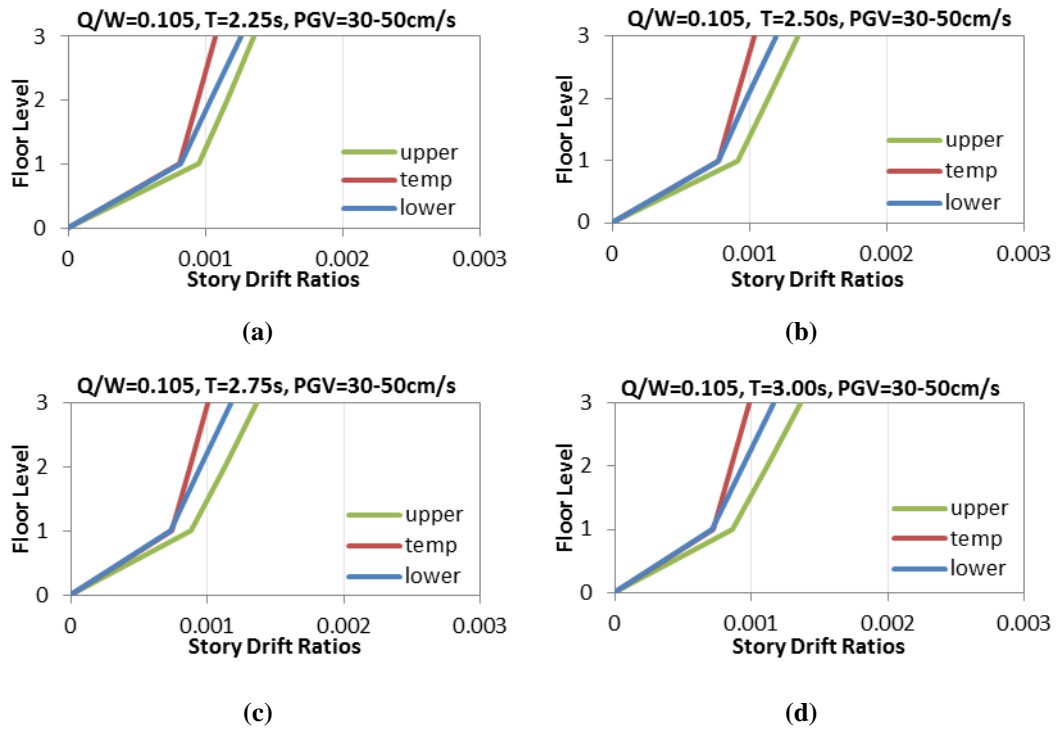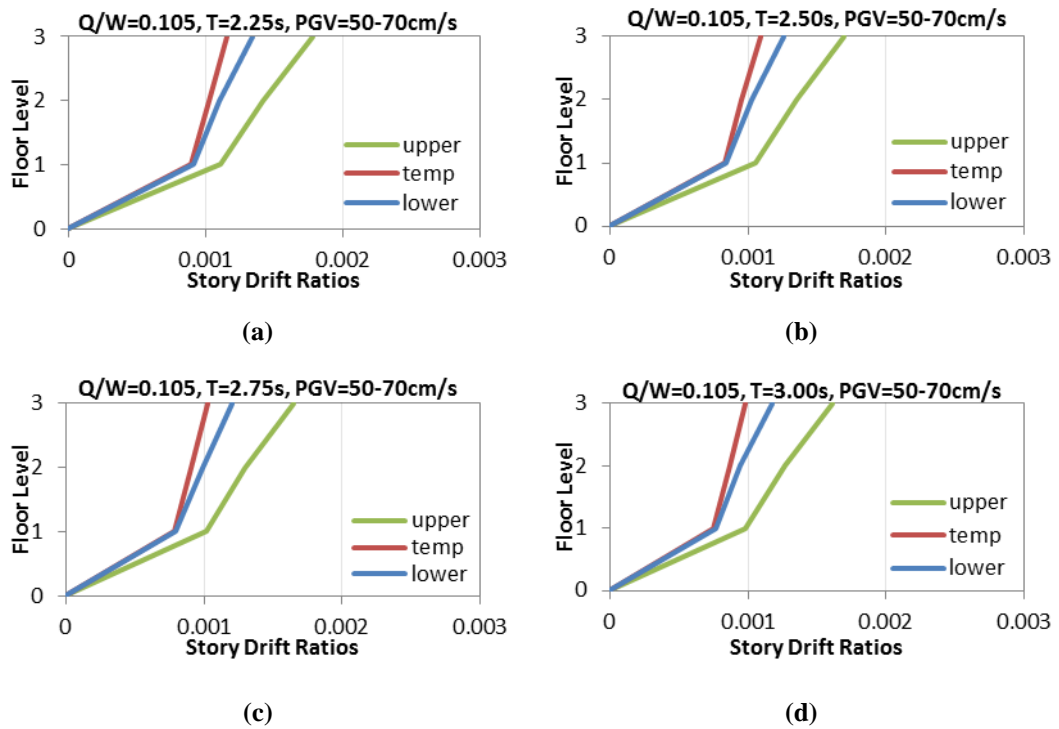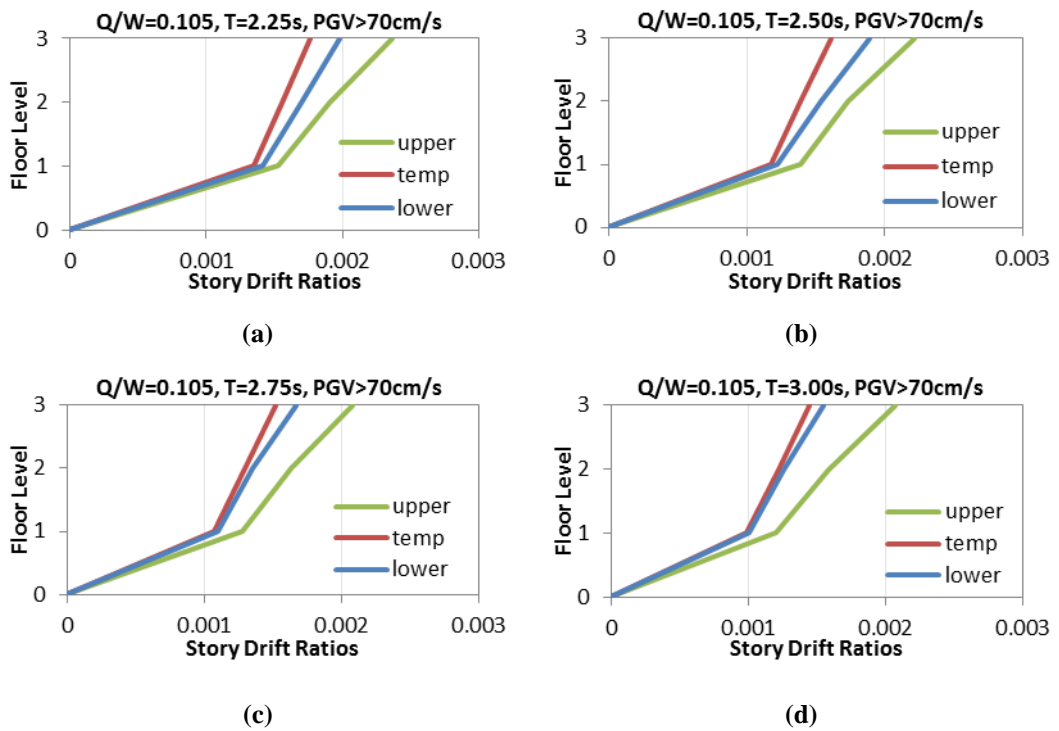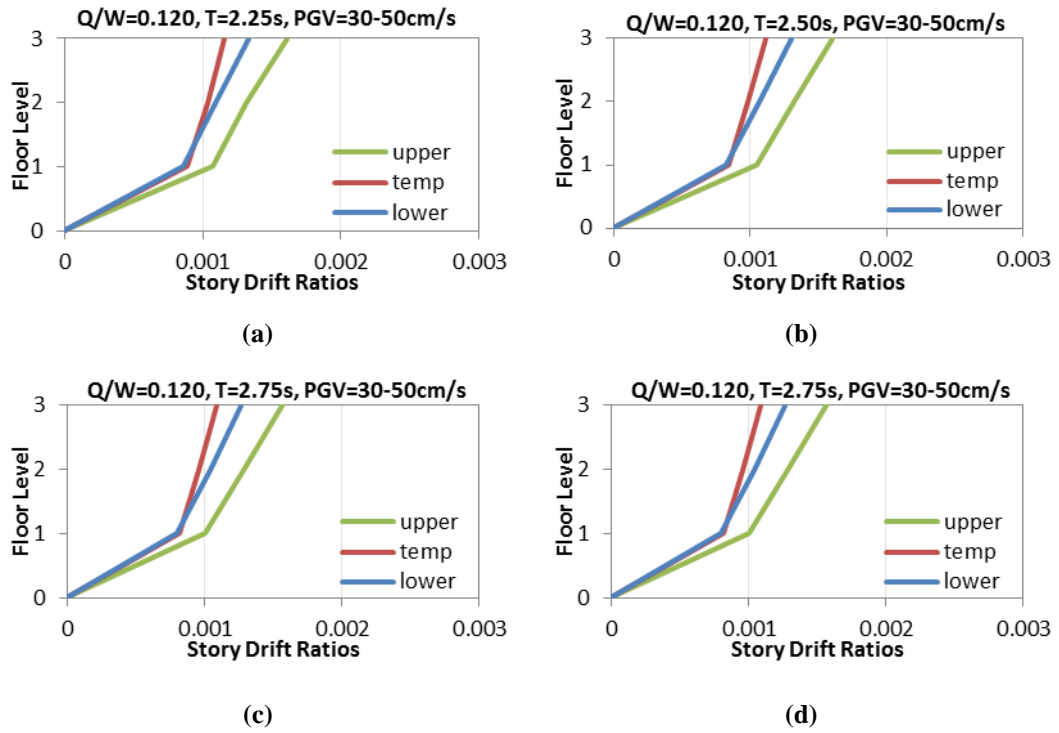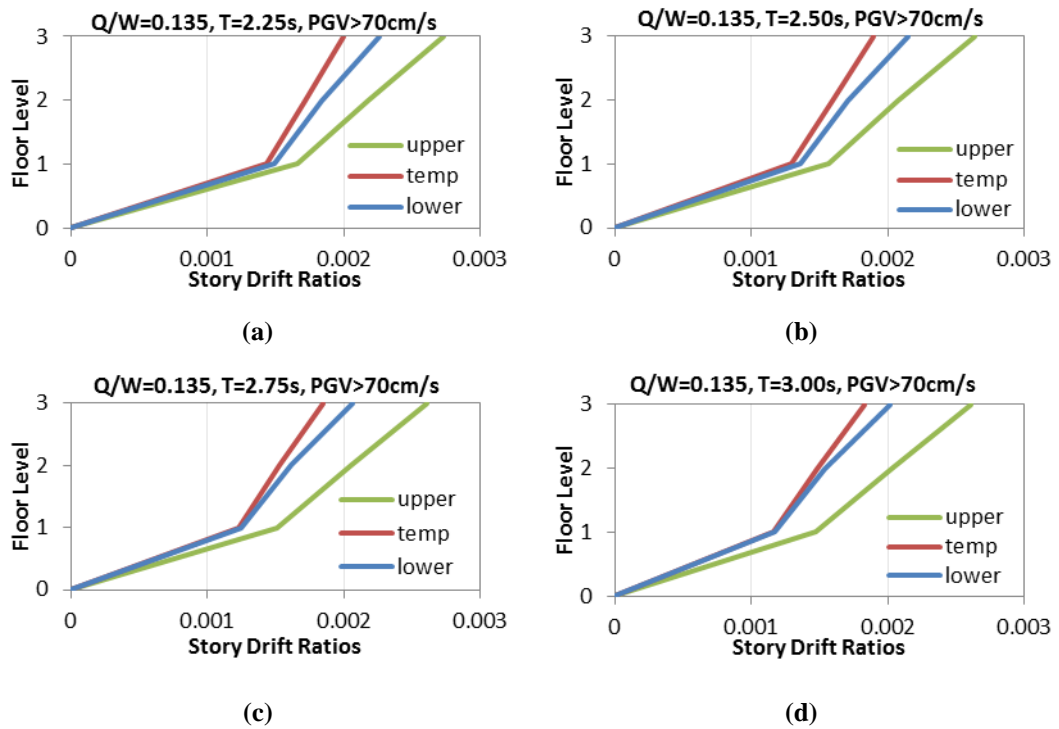**Figure 6.48** Average peak story drift ratios of 3 story steel structures with same Q/W=0.135, PGV>70cm/s and different T: a)T=2.25s, b)T=2.50s, c)T=2.75s, d) T=3.00s

7. DISCUSSION OF THE RESULTS

In this study the response of superstructure of isolated buildings was investigated with the material model considers strength deterioration during the motion. Also, the upper and lower bound analyses were conducted for comparison purposes. Therefore, 3 material models were used for performing the analyses of base isolated buildings.

23-story reinforced concrete superstructure and 3-story steel superstructure were chosen as a high-rise and low-rise superstructure respectively. All the isolated structure models were developed with these 2 superstructure models. In order to investigate the effect of isolation properties on the response of superstructure 16 different LRBs were applied to considered concrete and steel structure separately. Thus, 32 isolated buildings were designed to conduct the analyses. The heat increase in the lead core and the related strength deterioration of isolator during the motion is directly related with the velocity of the motion. Thus, to examine the importance of ground motion characteristics on the superstructure response 60 earthquake ground motions were selected for this study. In total 5760 nonlinear time history analyses were conducted with 3 material models, 32 isolated structures, 60 earthquake ground motions. All the analyses were performed with OpenSees structural analyses software that is capable of calculating strength reduction of LRB during motion. The results of these analyses were given in the Figure 4.1 6.1- 6.48.

The graphs of peak floor accelerations of 23-story reinforced concrete structure clearly showed that the results of temperature dependent analyses are in-between the results of bounding analyses. But in some cases the results of temperature dependent analyses were very close to results of lower bound analyses. Therefore, the results of temperature dependent analyses can expected to be below the results of lower bound analyses when different types of isolators, superstructures of ground motion data is of concern. When the results examined in more detail it was seen that the results of temperature dependent analyses obtained with structures having low Q/W were closer to the results of lower bound analyses. Besides, with the increasing PGV values the results of temperature

dependent analyses become closer to the results of lower bound analyses in general for the 23-story building. This can be explained by the temperature rise in the lead core due to the more severe strength deterioration for the ground motions with higher PGV values. Thus, the acceleration values reduce at the story levels. The results of the temperature dependent analyses tend to approach the results of the lower bound analyses as a result of heating of the lead core. As far as it can be seen from the results, isolation period has no significant effect on the response.

There is no limit exceed for the results of temperature dependent analyses in terms of peak drift ratios when 23-story reinforced concrete structure is of concern. The results are very close to lower bound values. The most significant variation of results of temperature dependent analyses has occurred with the variation in PGV. The results obtained with structures subjected to high PGV values showed that the results of temperature dependent analyses were almost equal to lower bound results for all type of isolators. Besides, the peak drift ratios obtained with temperature dependent analyses come closer to the lower bound with the decreasing isolation period and Q/W. This behavior denoted that the temperature of the lead core increases depending on the properties of the isolator and the ground motion and accordingly the relative story displacements reduces.

The results of temperature dependent analyses of 3-story steel structure were below the results of lower bound analyses in terms of both peak floor accelerations and relative story displacements without any exception. These results showed that the actual response of the base isolated low rise superstructure is out of the range specified by the bounding analyses with non-deteriorating model. The Q/W ratio of the isolators and PGV values affect the superstructure response in the 3-story steel structure.. The difference between the temperature dependent analyses and the lower bound analyses becomes obvious for larger Q/W ratio and higher PGV values. Increasing PGV values speed up the heat increase in the lead core and accordingly results of floor accelerations and relative story displacements decreases. Also the variation of isolation period does not have any significant effect on the response of superstructure according to the comparison of temperature dependent analyses and bounding analyses. For the

low-rise building, the superstructure response parameters (floor accelerations and relative story displacements) decrease with the increasing Q/W ratio.

Especially for the low-rise building, temperature dependent analyses resulted in lower seismic demands compared to the bounding analyses method. This can lead to more cost-effective designs for the superstructure of the base isolated buildings. Therefore, it is suggested to support the bounding analyses results with the temperature dependent analyses in the design of base isolated structures.

8. CONCLUSION

In this dissertation temperature dependent analysis, which is recently developed and gives acceptably closer results to the actual behavior, and the bounding analyses, which is widely used method and give approximate results to estimating the response of isolated structures, were compared to each other. This comparison is important for the analyses method used for years (bounding analyses) whether their response prediction are acceptable or not. Second, the effect of the isolation period, Q/W ratio of an isolator and PGV of an earthquake ground motion on the variation of the results was investigated. The aim is to examine the parameters that may affect the temperature rise in the lead core. The investigation of the effect of the PGV has a particular importance in this study because it has good correlation with seismic response of the base isolated structures..

Two types of superstructure models were used in this study. These are 23-story reinforced concrete structure and 3-story steel structure representing the high-rise and low-rise structures respectively. 16 LRBs having different isolation period and Q/W were applied both for 23-story and 3-story superstructures separately. All the analyses were conducted with 3 material models that represent the behavior of temperature dependent analyses and bounding analyses. Each designed isolated structures analyzed under 60 different near source earthquake ground motions with varying PGV values. Consequently, 5760 nonlinear time history analyses were conducted for this study.

The following conclusions are derived based on the comparisons in terms of maximum average absolute floor accelerations and inter-story drift ratios for various isolator, superstructure and ground motion properties.

1) The bounding analyses predict the response of superstructure for 23-story reinforced concrete structure reasonably with upper and lower bound analyses compared to temperature dependent (more realistic) analyses. But, in some cases the results of temperature dependent analyses were very close to lower bound analyses. It means bounding analyses has remained on the safe side. On the other hand, the results of temperature dependent analyses exceeded the limits of

bounding analyses without any exception when 3-story steel structure is of concern. The results of temperature dependent analyses were determined to be lower than the results of lower bound analyses. The results showed that the bounding analyses could not predict the results with sufficient approximation. Economic limits were exceeded with this method compared to the actual behavior obtained by the temperature dependent model. Therefore, the bounding analyses can result in non-economic solutions for such base isolated buildings.

2) This study showed that PGV value of an earthquake record has a direct relationship with the temperature rise in the lead core. The temperature of the lead core increases and accordingly the strength of the isolator decreases with the increasing PGV values. Therefore high PGV values leads reduction in the response parameters (floor acceleration and relative drift ratio) of the superstructure because an isolator with reduced strength transmit less energy to the superstructure relatively.

3) The isolation period has no significant effect on the results of the temperature dependent analyses compared to the upper and lower bound limits for both building types.

4) The Q/W ratio of the isolator has considerable amount of influence on the superstructure response especially for higher PGV values. As the Q/W ratio increases the difference between the temperature dependent analyses results becomes obvious compared to the lower bound analyses results. Therefore, it can be concluded that the temperature dependent analyses method, which is considered to be the actual response, can result in cost-effective solutions for low-rise base isolated buildings especially for higher Q/W ratios.

In conclusion, the bounding analyses give conservative results compared to temperature dependent analyses with upper bound limit. The temperature dependent analyses results for superstructure response are mostly close result to the lower bound or exceeded the lower bound limits. This indicates that the bounding analyses can give non-economical results for certain cases. Therefore, the isolated structures that will be analyzed with bounding analyses must be controlled and supported with the temperature dependent analyses, which can represent the actual behavior of the base isolated buildings effectively.

REFERENCES

[1]   Anonymous, *Earthquake response of buildings*, 2015. http://seismicdesign-
       zone.com/-designing-around-base-isolation/

[2]   Anonymous, *Erechtheion Temple, Greece*, 2015. http://theredlist.com/wiki-
       2-19-878-1075-1084-view-greece-profile-erechtheion-5c-bc-athenianacrop-
       olisgreece.-html

[3]   Naderzadeh, A., *Historical structure, Medina*, 2015. http://www.cibw114-
       .net/symposium-2009/pdf/OS09

[4]   Anonymous, *Parthenon, Greece*, 2015. http://fineartamerica.com/featured/-
       parthenongreececonstantinosiliopoulos.html

[5]   Naderzadeh, A., ''Application of seismic base isolation technology in Iran''

[6]   Constantinou, M.C., ''Lecture Notes of Aseismic Base Isolation'', State
       University of New York at Buffalo

[7]   Anonymous, *Foothill Communities Law & Justice Center, San Bernardino,
       California*, 2015. http://www.pbs.org/wgbh/nova/next/tech/rubber-bearings-
       seismic-protection/

[8]   Anonymous, *Los Angeles County Fire Command & Control Facility,
       California*,   2015.   http://www.fireengineering.com/articles/print/volume-
       164/issue   10/features-/usar-response-to-japan-earthquake-and-tsunamis-
       part-1.html

[9]   Anonymous, *Los Angeles County Fire Command & Control Facility,
       California*, 2015. http://www.fireengineering.com/articles/print/volume164
       /issue10/features/usar-response-to-japan-earthquake-and-tsunamis-part
       1.html

[10]   Anonymous, *Caltrans Traffic Management Center, Kearney Mesa,
       California*,   2015.   http://mceer.buffalo.edu/infoservice/reference_services/
       baseIsolation1.asp

[11] Anonymous, Drew Diagnostics Trauma Center, California, 2015. http://www.kdg-architects.com/kdmc.htm

[12] Anonymous, *Flight simulator manufacturing facility,* 2015. http://helihub.com/2011/08/21/flightsafetyopenssimulatordesignmanufacturing-and-support-facility/

[13] Anonymous, *Erzurum health campus,* 2015. http://www.saglikyatirimlari.gov.tr/-Default.aspx?tabid=92&ArtMID=857&ArticleID=34

[14] *Gümüşdoğrayan, S., Van maternity hospital*, 2015. http://www.seldagumus-dograyan.com /- projeler/500-yatakli-van-kadindogum-ve-kvc-hastanesi

[15] Anonymous, *Oakland City Hall was established in Oakland, California,* 2015. http://www.planestrainsandrunning.com/2010_12_01_archive.html

[16] Anonymous, *San Francisco City Hall, San Francisco, California*, 2015. http://en.wikipedia.org/wiki/San_Francisco_City_Hall

[17] Anonymous, Los Angles City Hall, 2015. http://www.7thdistrict.net/staff

[18] Skinner, R.I., Robinson, W.H., McVerry, G.H., ''An Introduction to Seismic Isolation'', John Willey & Sons, Inc., 1993.

[19] Robinson, W. H. 1982. "Lead-rubber hysteretic bearings suitable for protecting structures during earthquakes", Earthquake Engineering and Structural Dynamics, 10, 593-604.

[20] Kalpakidis, I. V., Constantinou, M. C. 2009a. "Effects of heating on the behavior of lead-rubber bearing. I:Theory", Journal of Structural Engineering (ASCE), 135, 1440-1449.

[21] Kalpakidis, I. V., Constantinou, M. C. 2009b. "Effects of heating on the behavior of lead-rubber bearing. II:Verification of theory", Journal of Structural Engineering (ASCE), 135,1450-1461.

[22] Kelly, J.M., ''Earthquake resistant design with rubber'', Springer-Verlag London Limited,1997.

[23] Naeim, F., Kelly, J.M., ''Design of Seismic Isolated Structures'', John Wiley & Sons, Inc.,1999.

[24] American Association of State Highway and Transportation Officials (AASHTO). 2010. "AASHTO LRFD bridge design specifications", 5th Ed., Washington, DC.

[25] American Society of Civil Engineers, Structural Engineering Institute (ASCE/SEI). 2010. "Minimum design loads for buildings and other structures." ASCE 7-10.

[26] Constantinou, M. C., Whittaker, A. S., Kalpakidis, I. V., Fenz, D. M., Warn, G. P. 2007. "Performance of seismic isolation hardware under service and seismic loading", Technical Report MCEER-07-0012, Multidisciplinary Center for Earthquake Engineering Research, Department of Civil, Structural and Environmental Engineering, State University of New York at Buffalo.

[27] Kalpakidis, I. V., Constantinou, M. C. 2008. "Effects of heating and load history on the behavior of lead-rubber bearings", Technical Report MCEER-08-0027, Multidisciplinary Center for Earthquake Engineering Research, Department of Civil, Structural and Environmental Engineering, State University of New York at Buffalo.

[28] Constantinou MC, Whittaker AS, Fenz DM, Apostolakis G. Seismic Isolation of Bridges. Department of Civil,Structural and Environmental Engineering: State University of New York at Buffalo, 2007.

[29] Kalpakidis, I. V., Constantinou, M. C., Whittaker, A. S. 2010. "Modeling strength degradation in lead-rubber bearings under earthquake shaking", Earthquake Engineering and Structural Dynamics, 39, 1533-1549.

[30] Özdemir, G., Avşar, Ö., Bayhan, B. 2011. "Change in Response of Bridges Isolated with LRBs due to Lead Core Heating", Soil Dynamics and Earthquake Engineering, 31, 921-929.

[31] Özdemir, G., Dicleli, M. 2012. "Effect of Lead Core Heating on the Seismic Performance of Bridges Isolated with LRB in Near Fault Zones", Earthquake Engineering and Structural Dynamics, 41, 1989-2007.

[32] Özdemir, G. 2013. "Formulations for Equivalent Linearization of LRBs in order to Incorporate Effect of Lead Core Heating", Earthquake Spectra, DOI: 10.1193/041913EQS107M.

[33] Benzoni, G., Casarotti, C. 2009. "Effects of vertical load, strain rate and cycling on the response of lead-rubber seismic isolators", Journal of Earthquake Engineering, 13, 293-312.

[34] Matsagar, V. A., Jangid, R. S. 2004. ''Influence of isolator characteristics on the response of base-isolated structures'', Engineering Structures, 26, 1735-1749.

[35] Alhan, C., Gavin, H. P. 2005. "Reliability of base isolation for the protection of critical equipment from earthquake hazards", Engineering Structures, 27, 1435-1449.

[36] Kelly, M., Tsai, H. 2006. ''Seismic response of light internal equipment in base-isolated structures'', Earthquake Engineering and Structural Dynamics, 13, 711-732.

[37] Providakis, C. P. 2008. "Effect of LRB isolators and supplemental viscous dampers on seismic isolated buildings under near-fault excitations", Engineering Structures, 30, 1187-1198.

[38] Providakis, C. P. 2009. "Effect of supplemental damping on LRB and FPS seismic isolators under near-fault ground motions", Soil Dynamics and Earthquake Engineering, 29, 80-90.

[39] Yang, T. Y., Konstantinidis, D., Kelly, J. M. 2010. "The influence of isolator hysteresis on equipment performance in seismic isolated buildings", Earthquake Spectra, 26, 275-293.

[40] Calugaru V, Panagiotou M (2013) ''Seismic response of 20-story base-isolated and fixed-base reinforced concrete structural wall buildings at a near-fault site'' *Earthquake Engineering and Structural Dynamics*, 10, 1002-2381

[41] FEMA 451. NEHRP Recommended Provisions: Design Examples. Building Seismic Safety Council. National Institute of Building Sciences, Washington, 2006.

[42] OpenSees (2009). Open system for earthquake engineering simulation, OpenSees version: 2.4.4. University of California, Pacific Earthquake Engineering Research Center, Berkeley, California.

[43] Anonymous, *Heat convection within the internal structure of the Earth*, 2015. http://www.earthhistory.org.uk/key-concepts/plate-tectonics-1.

[44] Anonymous, *Schematic illustration of elastic rebound theory*, 2015. http://earthquakesplates.blogspot.com.tr/2011/08/elastic-rebound.html.

[45] Somerville, P. G., Smith, N. F., Graves, R. W., Abrahamson, N. A. 1997. "Modification of empirical strong ground motion attenuation relations to include the amplitude and duration effects of rupture directivity", Seismological Research Letters, 68, 199-222.

[46] Shome N., Cornell C.A., Bazzurro P. and Carballo J.E., 1998, "Earthquakes, Records and Nonlinear Responses", Earthquake Spectra, 14(3), pp. 469-500.

[47] Bommer J.J. and Acevedo A.B., 2004, "The Use of Real Earthquake Accelerograms as Input to Dynamic Analysis", Journal of Earthquake Engineering, Volume 8, Special Issue 1, pp. 43-92.

[48] Stewart J.P., Chiou S.-J., Bray J.D., Graves R.W., Somerville P.G. and Abrahamson N.A., 2001, "Ground Motion Evaluation Procedures for Performance-Based Design", PEER Report 2001/09, Pacific Earthquake Engineering Research Center, University of California, Berkeley.

[49] Avsar O., and Ozdemir G. 2013. "Response of Seismic-Isolated Bridges in Relation with Intensity Measures of Ordinary and Pulse-Like Ground Motions", ASCE Journal of Bridge Engineering, Vol. 18, No. 3, pp. 250-260.